GENETIC ANALYSIS OF GLANDULAR TRICHOME DEVELOPMENT AND METABOLISM IN CULTIVATED TOMATO

By

Brian St. Aubin

A DISSERTATION

Submitted to
Michigan State University
in partial fulfillment of the requirements
for the degree of

Plant Biology—Doctor of Philosophy

2019

PUBLIC ABSTRACT

GENETIC ANALYSIS OF GLANDULAR TRICHOME DEVELOPMENT AND METABOLISM IN CULTIVATED TOMATO

By

Brian St. Aubin

Plants protect themselves from being eaten by producing physical and chemical barriers. Some plants, such as cultivated tomato, are covered in cellular hairs known as trichomes that produce and store chemicals to ward off attacks. While it is known how the chemicals are produced, it is unclear how the plants restrict the production and storage of these chemicals to these special hair cells. Several mutants have been found that fail to produce the hairs or the chemicals. By analyzing the genes that have been mutated in these plants we can identify key aspects to the development of these barriers to attack.

In this work I identified a gene involved in the production of a class of molecules that are important for cellular membrane function. Restoration of this gene just in the hair cells of plants lacking this activity restored chemicals important for protection of the plant from predation. The results of this and similar experiments, with other mutants included here, provide a clearer picture of hair cell development and on how plants rely on other metabolic pathways for the development of hairs and the production of chemicals necessary to defend against attack.

ABSTRACT

GENETIC ANALYSIS OF GLANDULAR TRICHOME DEVELOPMENT AND METABOLISM IN CULTIVATED TOMATO

By

Brian St. Aubin

Morphological structures and associated chemical compounds serve important functions during the life cycle of plants, including deterrence of herbivores. Terpenoids represent a major class of compounds involved in defending plants from herbivores. Their differential accumulation in specific tissues and cell types is at present not well understood. In cultivated tomato (*Solanum lycopersicum*), terpenoids and flavonoids accumulate in type VI glandular trichomes that are found on most above ground plant organs. Due to our ability to isolate them, these glandular trichomes of tomato are an attractive model system that can help us better understand how plants regulate the biosynthesis of terpenoids. The mutations in the *odorless-2* (*od-2*) and the *anthocyanin free* (*af*) genes produce defective type VI glandular trichomes that fail to accumulate flavonoids and volatile terpenoids. Accordingly, these mutants provide useful genetic tools to study the relationship between the development and metabolic capacity of glandular trichomes.

In this work, I determined the molecular basis of the *od-2* mutation and showed that the wild-type *Od-2* gene encodes an enzyme (designated LCB1A for long chain base 1A) involved in the biosynthesis of long-chain base precursors of sphingolipids. A functional *LCB1A* gene is necessary for type VI trichomes to produce high levels of volatile terpenoids. Transgenic expression of the wild-type LCB1A cDNA from the *Cauliflower Mosaic Virus* 35S promoter complemented both the leaf developmental and sphingolipid content phenotypes of the leaflets of the mutant but failed to rescue the terpenoid deficiency. Conversely, expression of LCB1A from a trichome-specific promoter restored terpenoid production in type VI trichomes of *od-2* but did

not complement the foliar sphingolipid profile or other leaf developmental defects. These results provide new insights into the tissue- and cell type-specific function of sphingolipid biosynthesis in tomato and establish an essential role for sphingolipids in trichome-borne specialized metabolism.

In a similar fashion, I used the chalcone isomerase 1 (CHI1)-deficient *af* mutant to study the tissue and cell-type specific role of flavonoids. Specifically, I constructed transgenic lines in which *CHI1* was expressed in the *af* mutant background from either the 35S or a trichome-specific promoter. Detailed biochemical and physiological characterization of these lines showed that CHI1 activity in type VI glandular trichomes, but not in other cell types of the leaf, is required for abundant production of volatile terpenoids. Expression of CHI1 in type VI trichomes was also required to restore resistance of *af* leaves to feeding by the two-spotted spider mite *Tetranychus urticae*. In summary, the results described in this thesis advance knowledge of how various metabolic pathways, including sphingolipid and flavonoid biosynthesis, operate to promote normal development and function of glandular trichomes.

ACKNOWLEDGEMENTS

I would like to thank Edward Cahoon for the extraction and measurements of sphingolipids which were conducted in his lab at the University of Nebraska, Lincoln. Tom Sharkey and Alan McClain were essential for helping me to set up for measurement of and understanding of photosynthetic parameters of *odorless-2*. A significant amount of work was done by Jin-Ho Kang which allowed the finding of the causal mutation in *odorless-2*, and in developing the *pCHI* and *p35S* lines in *anthocyanin free*. Thanks are also due to Koichi Sugimoto for the identification of the tomato mutant *anthocyanin free* being susceptible to the two-spotted spider mite. Metabolic analysis were conducted primarily at the Michigan State University Mass Spectrometry – Research Technology Support Facility and the time and teaching provided by the staff (especially Tony Schilmiller and Arthur Jones) were a major help in all sections of this work. Working with Guo-qing Song to perform the tomato transformations taught me so much and they could not have gone better.

Computational work in support of this research was performed at Michigan State University High Performance Computing Center. This publication was made possible by a predoctoral training award to Brian St. Aubin from Grant Number T32-GM110523 from National Institute of General Medical Sciences of the National Institutes of Health, and a Michigan State University College of Natural Sciences dissertation completion fellowship. This study was supported by a National Science Foundation grant (award 1456864).

I would like to thank my dissertation committee that supported and guided this research from the beginning to the end. I would especially like to acknowledge Gregg Howe for all the time he has spent in helping me bring the story of this research into clear view.

TABLE OF CONTENTS

LIST OF TABLES

LIST OF FIGURES

KEY TO ABBREVIATIONS

Af	Anthocyanin free
CHI1	Chalcone isomerase 1
GIPC	Glycosyl inositol phospho-ceramides
GTs	Glandular trichomes
LCB1A	Long chain base 1A
MEP	Methyl erythritol phosphate
MKS	Methyl ketone synthase
MVA	Mevalonate
Od-2	Odorless-2
SNP	Single nucleotide polymorphism
WT	Wild-type

CHAPTER 1 INTRODUCTION

DEVELOPMENTAL SPECIALIZATION OF EPIDERMAL CELLS

The epidermis mediates the plant interactions with the environment. Plant protodermal cells differentiate into a variety of shapes and sizes, each with different impacts on environmental interactions. Mature pavement cells, for example, have a flat exterior surface, reticulated-interlocking edges, and are often transparent. Stomata contain a pair of guard cells that form an epidermal pore for facilitating gas exchange. Trichomes are single- or multi-celled epidermal projections. Each of these epidermal cell types are characterized by unique developmental, signaling, and metabolic activities. This diversity of cell types arises through cell division and differentiation of protodermal cells. The formation of pavement cells occurs through the expansion and anticlinal division of protodermal cells. A key characteristic of pavement cells is the cuticle, which is a complex low-permeability wax-containing layer on the outer surface of the cell (Ingram and Nawrath 2017). Guard cells develop through a series of unequal anticlinal divisions of pavement cells (Shpak et al. 2005). Guard cells have the unique ability to allow gas exchange across the epidermis through the stoma, control transpiration, and limit intrusion of pathogens. The opening and closing of guard cells is controlled by turgor pressure and actin dynamics (Yi et al. 2019). Trichomes are formed from an outgrowth perpendicular to the surface of the epidermis. This process often involves at least one periclinal division and can result in a trichome consisting of many cells. The projection of these cells away from the epidermal surface requires additional mechanical support as a freestanding structure. Such physical support typically involves the cytoskeleton, as well as the cell wall, and turgor pressure (El-Assal et al. 2004; Folkers et al. 2002). Another unique attribute of trichomes, and glandular trichomes in particular is the production and storage specialized metabolites (Werker 2000). Storage or secretion of metabolites from trichomes

can have a profound impact on plant biotic interactions (Glas et al. 2012; Sánchez-Hernández et al. 2006).

BIOLOGICAL FUNCTION OF TRICHOMES

The unique functions that trichomes provide are often based on their shape. Long, sharp, or densely growing trichomes provide physical deterrence against herbivory (Agrawal 1999; Agren and Schemske 1993). Dense, wispy trichomes or large umbrella-shaped trichomes can provide protection from excessive light exposure, or may limit water loss (Liakoura et al. 1997). Some trichomes have physical characteristics that help maintain leaf dryness (Barthlott et al. 2009). Bulbus trichomes often store specific compounds. Within these basic classes of trichome shape there is yet more diversity. Long and sharp trichomes, for example, may be straight, curved, twisted, or hooked. They can be as large as a raspberry prickle or as small as a single cell. Bulbus trichomes, typically referred to as glandular, can be single- or multi-celled structures, and can be extended away from the surface on a stalk, held close to the surface, or even sunk in a cavity within the epidermis. Glandular trichomes store or exude a variety of compounds which are often unique to that type of trichome.

Specific metabolic pathways associated with glandular trichomes (GTs) can impart an additional layer of cellular specialization. Sticky residues produced by some GTs can have a negative impact on insects that encounter these residues (Vosman et al. 2018). Some residues can be so thick they form a water-impermeable layer on the leaf (Dell and McComb 1977). Some GTs store noxious compounds and then release them when disturbed. Other GTs sequester chemicals that would otherwise be harmful if left to accumulate in the other cells (Dassanayake 2017).

TRICHOME DEVELOPMENT

Arabidopsis as a model system for development of single-celled trichomes

Trichome development is best understood in the model system *Arabidopsis thaliana*. The single-celled branching trichomes of Arabidopsis develop through several distinct phases. The first phase involves protodermal cells that undergo endoreduplication and expansion in the plane of the epidermis. These cells then elongate perpendicular to the local epidermal surface. Subsequently, the newly formed trichome cell branches to produce a three- to four-pronged structure reminiscent of antlers (Marks 1994). Among the surfaces adorned with trichomes in Arabidopsis are adaxial juvenile leaves, ab- and adaxial mature leaves, inflorescence stems, and the seed coat. The entry and exit of different stages of development, as well as the placement and spacing of trichomes, is regulated by specific transcription factors, protein modifications, microRNAs, and hormones.

The development of protodermal cells into a trichome requires the activity of various transcription factors, including: the R2R3MYB paralogs GLABROUS 1 (GL1), MYB23, or MYB82; along with a member of MYC subgroup IIIf GLABROUS 3 (GL3) or ENHANCER OF GL3 (EGL3); and a member of the tryptophan aspartate repeat (WDR) family TRANSPARENT TESTA GLABROUS 1 (TTG1) (Pattanaik et al. 2014). The presence of sufficient levels of these three classes of transcription factors in the same epidermal cell allows the initiation of endoreduplication, which is required for normal development of trichomes. The MYC/R2R3MYB/WDR (MBW) regulatory complex activates other transcription factors, such as homeodomain containing transcription factor GLABROUS 2 (GL2) and the WRKY transcription factor TTG2, which affects further development of the trichome and patterning of neighboring cells. Transcription factors of the R3MYB class (CAPRICE, CPC; TRIPTYCHON, TRY; TRICHOMELESS, TCL1, and TCL2; and ENHANCER OF TRY AND CPC, ETC1, ETC2, and

ETC3) limit trichome development by disrupting the MBW complex (Kirik et al. 2004). An assembled MBW complex can recruit the mediator complex to the promoter region and induce gene expression (Çevik et al. 2012). The expression of R3MYB transcription factors such as TRY are also induced by the MBW complex and diffuse to neighboring cells, thus enforcing trichome spacing. The trihelix transcription factor GT-2-LIKE 1 (GTL1) contributes to trichome size and impacts endoreduplication. Without early stages of endoreduplication, trichome cells do not expand and development is halted. In later stages of development (e.g., following four rounds of endoreduplication), the fully formed trichomes are typically 32C (i.e., having 32 times the number of chromosomes). In GTL1 mutants the average is closer to 80C and the trichomes are significantly larger (Breuer et al. 2009).

The regulation of trichome development is also impacted by several microRNAs. The distribution of microRNA miR156 impacts trichome development by targeting the SQUAMOSA-PROMOTER BINDING PROTEIN-LIKE (SPL) transcription factors (Wu et al. 2009). SPLs induce the expression of negative regulators of trichome development, including TRY and TCL1. In this manner, low levels of miR156 result in higher levels of SPLs, which induces TRY and TCL1, and restriction of protodermal cell development into trichomes (Pattanaik et al. 2014). miR172 targets AP2-like transcription factors TARGET OF EARLY ACTIVATION TAGGED 1 (TOE1) and TOE2. Loss of transcription factors TOE1 (also named RAP2.7) and TOE2 results in more juvenile looking leaves with fewer trichomes (Zhai et al. 2015). These miRNA effects are linked by SPL-9, which promotes the expression of miR172 (Wu et al. 2009). Juvenile leaves have an abundance of miR172 and low levels of miR156, which suppresses trichome development throughout the leaf via reduction in TOE1 and 2, and inhibition of trichomes by the abundance of TRY and TCL1 because of higher levels of SPLs. More mature leaves have an abundance of

miR156, thereby inhibiting SPL levels and limiting the expression of miR172 and TRY/TCL1. This causes higher levels of TOE1 and TOE2, and allows the MBW complex to form (Pattanaik et al. 2014; Wu et al. 2009).

Arabidopsis has a characteristic non-glandular branching trichome with three to four spikes having uneven lengths. Some genes that affect trichome number also impact the degree of branching (fewer trichomes and less-branching mutants: GL3, EGL3) (more trichomes and more-branching mutants: TRY). However, there are additional genes controlling branching. Mutants defective in the MIXTA-like MYB transcription factor NOECK (NOK) have trichomes with extra branches and do not develop papillae (Jakoby et al. 2008). This latter process of forking and cuticular development implies directed cell wall remodeling. Targeting of vesicles for cell wall remodeling and cellulose synthesis requires construction and stable attachment of tubulin to the plasma membrane. The tubulin double mutant LEFTY1/LEFTY2 has trichomes with fewer branches including sometimes no branches at all (Abe et al. 2004).

As the names of many trichome regulatory genes imply, mutations affecting trichome development also affect other phenotypes. One of the best examples of phenotypic pleiotropy is transparent-testa-glabrous 1 and 2. Not only do mutations in these genes confer a defect in trichome development, they also result in reduced accumulation of anthocyanins in the seed testa. Paralogs and orthologs of several of the regulatory genes are also implicated in anthocyanin production. Arabidopsis TRANSPARENT TESTA 8 (TT8) is a close paralog of GL3 and EGL3. Maize R genes, which are major regulatory factors for anthocyanin production, are orthologs of Arabidopsis GL3, EGL3, and MYC1. There are also multiple links between cuticle and trichome development. The Shine genes (SHN1, 2 and, 3) are AP2 type transcription factors that help regulate cell wall and cuticle production. Overexpression of SHN1,2, or 3 causes a reduction in trichome density

(Aharoni et al. 2004). SHN3 is normally expressed in the trichome-support cells, and SHN2 is expressed in trichomes (Oshima et al. 2013). The cuticle wax content of trichomes is distinct from other epidermal cells, further strengthening a link between trichome developmental regulation and metabolism of the cuticle (Hegebarth et al. 2016).

Glandular trichomes

Trichome morphology across the plant kingdom varies greatly and includes diverse multicellular trichomes and GTs. Among the major morphological classes of trichomes are stellate, peltate, capitate, and colleter (Payne 1978). The ability to accumulate or secrete specialized metabolites also adds to the complexity and functional diversity of GTs. Stellate trichomes have a star-shaped, uniform branching pattern, exemplified by cotton leaf trichomes (Inamdar and Rao 1981). In peltate trichomes, cells are arranged in a single plane at the top of the structure; examples include flattened cells on trichomes of pineapple leaves or globular structures within the mint family (Maffei et al. 1986; Sakai and Sanford 1980). Capitate trichomes have a single enlarged cell at the top of a stalk, such as the type VI trichome of tomato. Colleter trichomes contain both a multicellular glandular head, and a stalk that is multicellular in cross section, which is common in medicinal plants such as *Cannabis sativa* and *Artemisia annua* (Dayanandan and Kaufman 1976; Duke and Paul 2016).

Our current understanding of multicellular GT development lags significantly behind the extensive knowledge of single-celled trichome development in Arabidopsis. Nevertheless, several recent discoveries of regulatory factors governing multicellular trichome development are worth noting. GT density and cuticle production in leaves of *Artemisia annua* is regulated by homeo-domain 1 type transcription factors; namely, AaHD1, AaHD8, and by the MYB-type transcription factor AaMIXTA1 (Yan et al. 2018). The biosynthesis of specialized metabolites in *A. annua* GTs

is regulated by Trichome and Artemisinin Regulator 1 (TAR1), a transcription factor homologous to AtSHN1/2/3 (Tan et al. 2015). Production of terpenoid and phenylpropanoid metabolites in GTs of Mentha spicata is under negative regulation by the transcription factor MsYABBY5 (Wang et al. 2016). There are also non-transcription factor genes that seem to be important for controlling essential trichome functions such as the ABC transporter PDR2 in *Petunia hybrida*. Reduced expression of phPDR2 led to a decrease in the petuniasterone and petuniolide levels in trichomes, and also resulted in increased susceptibility to herbivory (Sasse et al. 2016).

TRICHOMES OF CULTIVATED AND WILD TOMATO

Description of trichome types

Plant species within the Solanaceae clade display a variety of trichome types. The rich genetic resources available for cultivated *Solanum lycopersicum* and various wild tomato species provides an opportunity to explore the genetic basis of trichome diversity. The various trichome types in Solanaceae have been described and classified (Luckwill 1943; Snyder and Carter 1985). According to the nomenclature of Luckwill (1943), type II, III, and V are multicellular, non-glandular structures of varying lengths. Type I and IV are glandular capitate hairs, whereas type VI and VII are glandular trichomes consisting of a multicellular head (Luckwill 1943). Type VI is also considered a peltate structure. The various trichome types of cultivated and wild tomato are distributed on nearly all above-ground surfaces of the plant, with species-specific and environmentally influenced differences in trichome distribution often observed. Generally, type I trichomes occur infrequently, but being the largest (~3mm) of the tomato trichome types, is readily apparent on stems (Chang et al. 2018). By contrast, type VII trichomes are small structures with bent stalk cells associated with vasculature regions on leaves. Type IV trichomes develop on juvenile leaves and are replaced by type V as the plant ages (Vendemiatti et al. 2017). Type V and

VI trichomes are highly abundant on adult leaves, whereas the stems and petioles are dominated by type VI trichomes (Snyder and Carter 1985).

The type VI glandular trichome

Type VI trichomes are structurally and biochemically unique. These peltate trichomes consists of four glandular head cells, a neck or intermediate cell, a stalk cell, and a base cell (**Figure 1-1**). Mature type VI trichomes often have a small, clear fluid-filled cavity surrounded by the four yellow-green pigmented head cells and have a head width of 50-80 μm (Xu et al. 2018). The neck cell is small and connects the four head cells to the stem cell. The overall height of type VI trichomes is about 250 μm (Bergau et al. 2015). These trichomes contain significant amounts of flavonoids and terpenoids, the most abundant of which is rutin (70 ng per gland, or ~25% by volume) and β-phellandrene (0.5 ng, or ~0.4% by volume), respectively (Kang et al. 2010a).

Mutations affecting tomato glandular trichome development and function

Several mutations affecting trichome development in tomato have been identified and characterized. The dominant *woolly* (*wo*) mutation affects the activity of an HD-ZIP transcription factor that is homologous to Arabidopsis GL2 (Yang et al. 2011). RNAi-based silencing of *Wo* resulted in plants lacking type I trichomes. Conversely, over-expression of Wo resulted in stunted plants with curly leaves and profuse type I trichomes. Analysis of these mutants indicated that although other trichome types were not affected by RNAi-*Wo*, other trichome types were converted to type I structures in *wo* heterozygous lines (Yang et al. 2011). Another mutation, named *hairs absent* (*h*), affects the function of a C2H2 zinc-finger transcription factor. Overexpression of H led to proliferation of type I trichomes, whereas RNAi-based silencing of H caused an absence of trichomes (Chang et al. 2018). Homologs of H in Arabidopsis called GLABROUS INFLORESCENCE STEMS (GIS) promote trichome initiation but can also repress trichome branching (Wang et al. 2019). The recessive *hairless* (*hl*) mutation of tomato impairs the function of a subunit (called SRA1) of the WAVE complex, which is involved in the control of actin filament nucleation (Kang et al. 2016). All trichome types on *hl* mutant plants are misshapen, smaller, and often

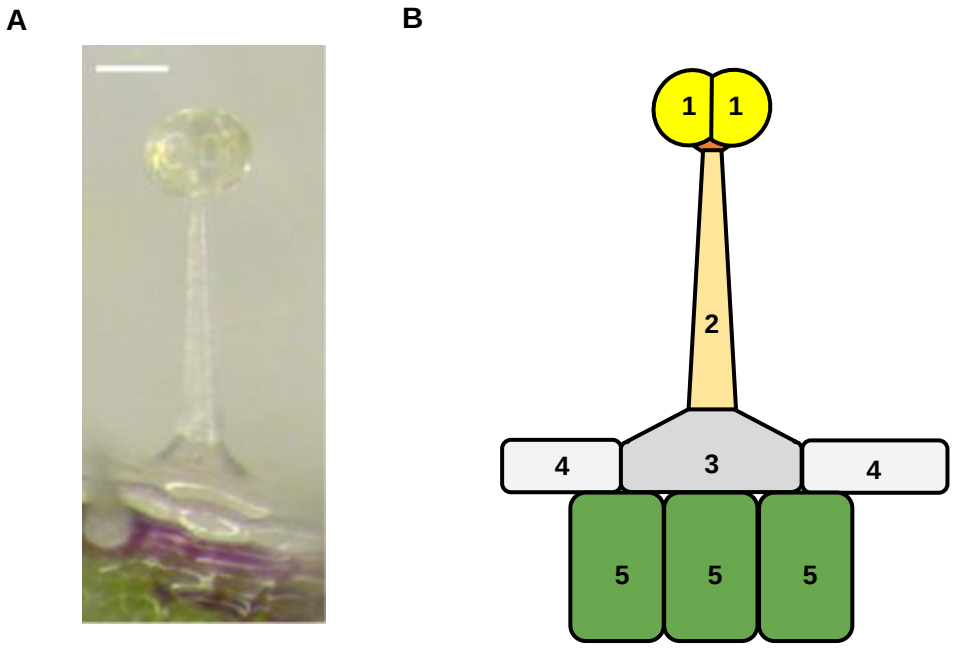

Figure 1-1: The *S. lycopersicum* type VI trichome. (A) Image of type VI trichome. Scale bar is 50 μm (B) Schematic of type VI trichome. Cell-type by number: 1 Glandular head, 2 stalk, 3 base, 4 pavement, 5 mesophyll, unnumbered intermediate (neck).

crooked compared to trichomes on wild-type plants (Kang et al. 2010b). Another recessive mutation called *anthocyanin free* (*af*) does not obviously impair trichome morphology but rather reduces the size of the glandular head cells on type VI trichomes and causes a lack the characteristic terpenoid and flavonoid metabolites (Kang et al. 2014). Kang et al. (2014) showed that the *Af* gene encodes Chalcone Isomerase 1 (CHI1) which catalyzes second step in the production of flavonoids in tomato. The *odorless-2* (*od-2*) mutant is also associated with defective trichome development and metabolic output in tomato but the corresponding gene has yet to be identified. The reported phenotypes of *od-2* plants include reduced trichome density, low abundance of flavonoids and terpenoids, defective trichome morphology, and small leaflets (Kang et al. 2010a).

GLANDULAR TRICHOME METABOLISM

Flavonoid biosynthesis

Flavonoids comprise a major class of polyphenolic compounds produced by all plants (**Figure 1-2**). The chemical diversity of flavonoids in the plant kingdom reflects species-specific modifications to the core flavonoid backbone (**Figure 1-2**), as well as differences in cell-type specificity, and cellular compartmentation (Agati et al. 2012). There are, however, a core set of flavonoid biosynthetic enzymes present in most if not all higher plants. This core flavonoid biosynthetic pathway is initiated by Chalcone synthase (CHS), which uses para-coumaroyl-CoA, produced from phenylalanine, to form the B ring of naringenin and three subsequent malonyl-CoAs in a polyketide-like reaction that generates the two-ring structure of naringenin chalcone (Rahman et al. 2012). This reaction is slow and is often a rate limiting step in this process. Chalcone isomerase (CHI) catalyzes ring closure (ring C) of naringenin chalcone to produce naringenin (Jez and Noel 2002). Flavanone 3-hydroxylase (F3H), the next enzyme in the pathway, catalyzes the production of dihydrokaempferol (Maloney et al. 2014; Spribille and Forkmann 1982). In some plants, ring A is hydroxylated by flavonol 3’(5’)-hydroxylase and/or reduced by

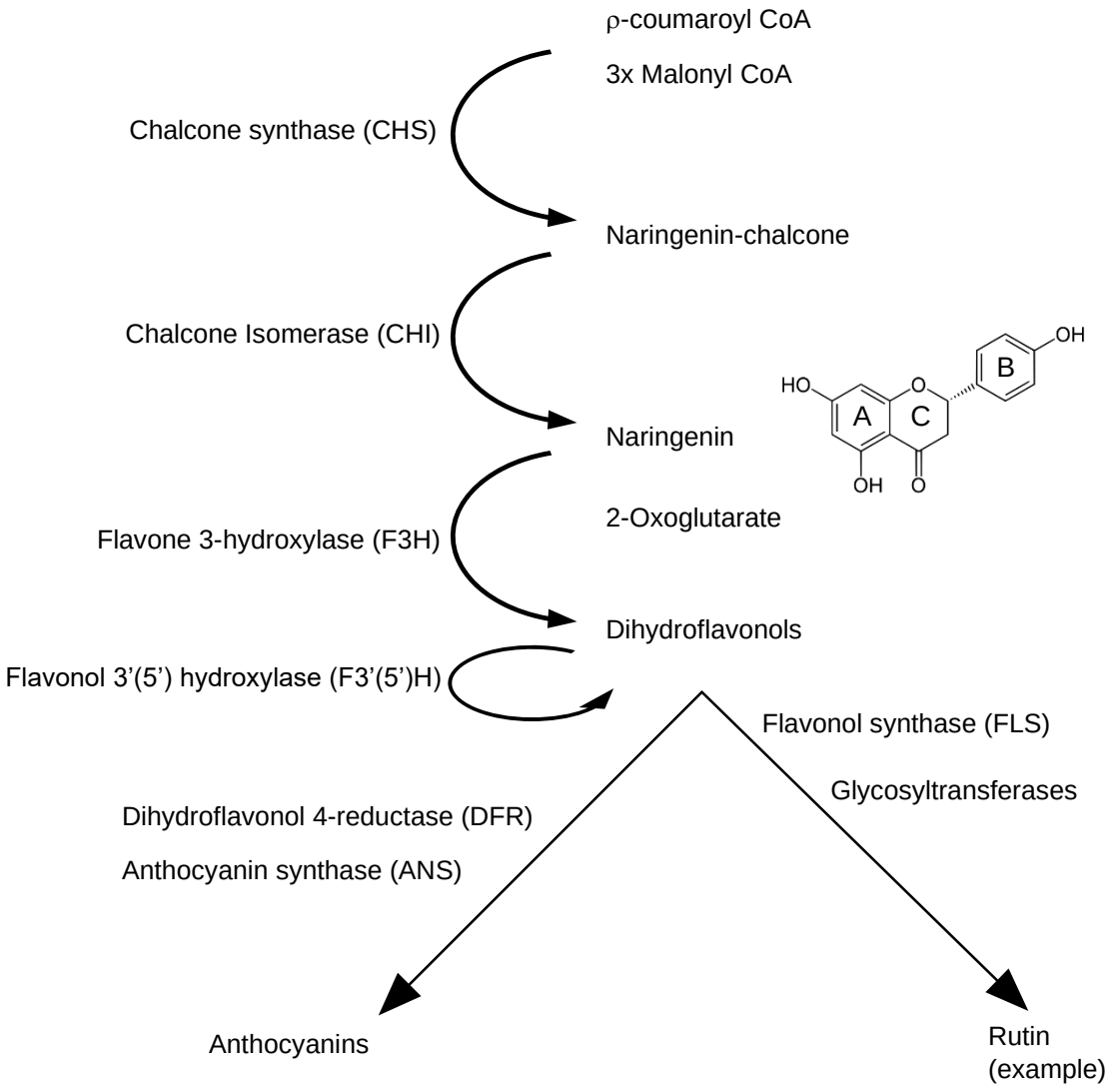

Figure 1-2. Flavonoid biosynthetic pathway. Inset shows the chemical structure of naringenin and the ring naming scheme (A, B, C).

Flavanol Synthase (FLS) (Holton et al. 1993a, 1993b). Alternatively, dihydroxyflavonol 4-reductase (DFR) and anthocyanin synthase (ANS) work in combination to produce anthocyanins from flavonols (Goldsbrough, Belzile, and Yoder 1994). Many flavonoids are glycosylated or methylated, and some plants have earlier branch points into flavones or isoflavones (Markham et al. 1978). Most genes involved with the synthesis of flavonoids have been identified in tomato.

Terpenoid biosynthesis

Terpenoids are synthesized from the isoprenoid units isopentenyl diphosphate and dimethylallyl diphosphate which, in plants, are synthesized via two distinct pathways (**Figure 1-3**). Enzymes located in the cytosol and peroxisome produce isoprenoids through the mevalonate (MVA) pathway. The second pathway resides in the chloroplast and produces isoprenoids through the methylerythritol phosphate (MEP) pathway (Schwender et al. 1996). A wide variety of terpenoid compounds are made in plants, including hormones, pigments, and defensive compounds (Tarkowská and Strnad 2018). Isoprenoid units are also attached to proteins and other metabolites via enzymes that catalyze prenylation reactions (Disch et al. 1998; Rodriguez-Concepcion et al. 1999). Monoterpenoids made from two isoprenoid units, and sesquiterpenes made from three isoprenoid units, are typically synthesized through a two enzymatic step process. Initial polymerization is conducted in a head to tail manner with the retention of only one diphosphate group, such as by neryl diphosphate synthase (NDPS) (Schilmiller et al. 2009). The next typical step is a free radical cyclization by a terpene synthase, such as β-phellandrene synthase (PHS) (Schilmiller et al. 2009). There are multiple genes encoding these enzymes in Solanaceae, with cultivated tomato having six cis-prenyltransferases other than NDPS and potentially 28 functional terpene synthases other than PHS (Akhtar et al. 2013; Falara et al. 2011). In many plants, volatile mono- and sesquiterpenes impart characteristic odors and have been implicated in various

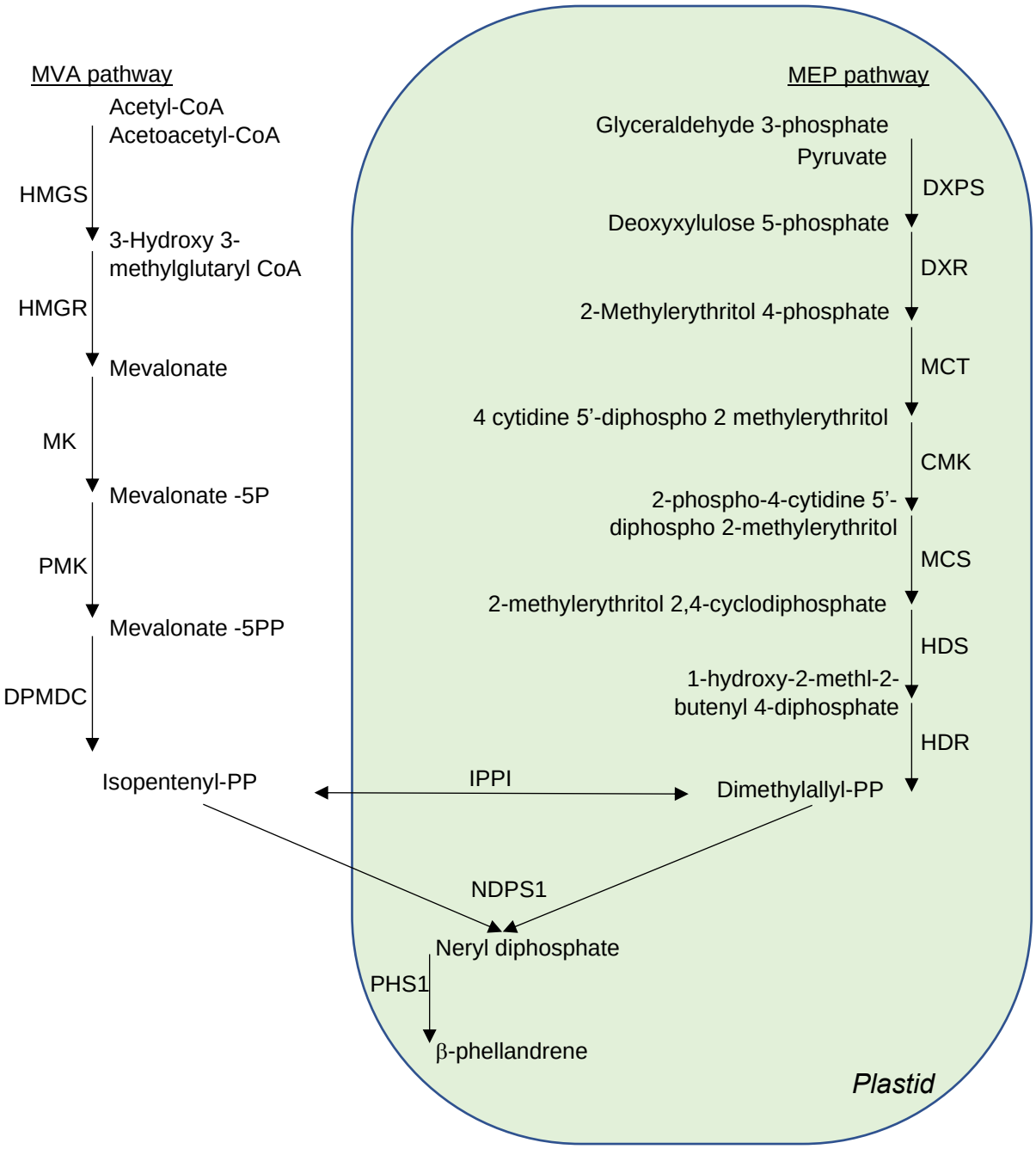

Figure 1-3: Terpenoid biosynthetic pathway. Synthesis via the cytoplasm/peroxisomal MVA pathway and via the plastidal MEP pathway. CoA Coenzyme-A, P phosphate, MVA mevalonate, HMGS hydroxy methylglutaryl synthase, HMGR hydroxy methylglutaryl reductase, MK mevalonate kinase, PMK phospho-mevalonate kinase, DPMDC diphospho-mevalonate decaboxylase, DXPS deoxyxylulosephosphate synthase, DXR deoxyxylulose reductoisomerase, MCT methylerythritolphosphate cytidylyltransferase, CMK cytidinediphosphomethyldrytritol kinase, MCS methylerythritolcyclodiphosphate synthase, HDS hydroxymethylbutenyldiphosphate synthase, HDR hydroxymethylbutenyldiphosphate reductase, IPPI isoprene diphosphate isomerase, NDPS neryl diphosphate synthase, PHS beta-phellandrene synthase.

defense processes (Langenheim 1994; Sánchez-Hernández et al. 2006). Volatile terpenoids have been found to negatively impact herbivore feeding preference of flea beetles *Epitrix hirtipennis*; and presence, feeding, and egg deposition of whitefly *Bemisia tabaci* (Bleeker et al. 2012; Du et al. 2016; Rick et al. 1976). Increased presence of plant derived terpenoids can also attracted enemies of herbivores the carnivorous mite *Phytoseiulus persimilis* and the parasitic wasp *Cotesia marginiventris* (Dicke et al. 1999; Turlings, Tumlinson, and Lewis 1990). The production of high concentrations of terpenoids is often restricted to specific cell types and the chloroplast pathway (Bleeker et al. 2012; Lange et al. 2000). The biosynthesis of terpenoids via the MEP pathway requires both ATP and NADPH, and is likely supported by a realignment of metabolism and photosynthesis inside the glandular trichome (Balcke et al. 2017; Banerjee and Sharkey 2014).

Other specialized metabolic pathways in Solanum glandular trichomes

In addition to flavonoid and terpenoid pathways, some GTs in Solanum species contain pathways for the biosynthesis of other specialized compounds, including acylsugars and methyl ketones. Acylsugars typically consist of a sugar unit (e.g. sucrose or glucose) esterified to aliphatic acyl groups. The high degree of chemical diversity among acyl sugars reflects differences in the sugar component, as well as the chain length and branching pattern of the attached acyl groups. In the Solanaceae, esterification is catalyzed by a family of BAHD acyltransferases (Schilmiller et al. 2012). There have been several duplications of the BAHDs and this has allowed the diversification of activities, with the closest sequence similarity between genes of different species coding for proteins that use different acyl sugar substrates or attach acyl groups to different locations (Moghe et al. 2017). This example of BAHDs illustrates the potential diversity of compounds that can be derived from a single set of enzymes and metabolic precursors. This chemical diversity is further compounded by differential expression and activities of acyl sugar

acylhydrolases, in the different *Solanum* species, which selectively remove acyl groups from acyl sugars (Schilmiller et al. 2016). Another class of compounds, methyl-ketones are toxic compounds found in trichomes of a subset of the Solanaceae despite the wider presence of the genes (Yu and Pichersky 2014). This presence of genes but expressional suppression of the metabolism they catalyze in some species can further increase diversity and shows the great range of potential metabolism in trichomes.

Regulation of specialized metabolism in glandular trichomes

Investigations into the regulation of specialized metabolism in tomato type VI trichomes has resulted in the identification of two transcription factors that coordinate the expression of associated biosynthetic genes. The recent characterization of tomato MYC1 demonstrates a major role for the transcription factor in the regulation of type VI trichome development (Xu et al. 2018). Loss of MYC1 resulted in an absence of type VI GTs and reduction in MYC1 expression was associated with smaller and less dense type VI trichomes. Xu et al. (2018) detected lower expression of several terpene synthases and lower production of monoterpenes in the leaves and trichomes of plants in which MYC1 was subject to RNAi-based silencing and in the heterozygous MYC1 loss of function plants. Interestingly, the levels of sesquiterpenes and expression levels of TPS12 were higher in the knockdown plant stem trichomes. This could imply that MYC1 is regulating the sesquiterpene synthases in an opposite manner, or suppression of mono-terpene synthesis results in higher levels of sesquiterpenes. Tomato MYC2 is a JA-responsive transcription factor that is homologous to Arabidopsis MYC2. Silencing of MYC2, however, does not appear to affect trichomes (Du et al. 2017). Interestingly, tomato MYC1 and MYC2 are two paralogs that share significant sequence similarity to Arabidopsis MYC2, MYC3, MYC4 in clade IIIe bHLHs. The role of clade IIIe bHLHs in regulating GT development and function contrasts the situation in

Arabidopsis, where development of non-glandular trichomes is dependent on the clade IIIf bHLHs GL3, EGL3, and MYC1 (Zhao et al. 2012). The ability of MYCs to induce transcription in response to JA requires JA and COI1-dependent degradation of JAZ repressors (Howe et al. 2018; Li et al. 2004). Because application of JA causes a proliferation of type VI GTs and increased accumulation of specialized metabolites inside of them on newly developing tomato leaves (Boughton, Hoover, and Felton 2005; Chen et al. 2018; Li et al. 2004), it seems likely that the JA-COI1-JAZ signaling module participates in development of this epidermal structure. It remains unclear, however, whether MYC1 activity is directly controlled by JAZ repressors.

MYC1 does not act alone in controlling the development and metabolic activity of type VI GTs. A zinc-finger transcription factor Expression of terpenoids 1 (EOT1) was shown to induce expression of the linalool synthase gene, named terpene synthase 5 (TPS5), in type VI trichomes through direct binding to the TPS promoter (Spyropoulou et al. 2014). A HD-ZIP mutant named *cutin deficient 2* (*cd-2*) has significantly reduced levels of anthocyanins in the epidermis, a lower density of type VI trichomes, and lower abundance of volatile terpenoids (Nadakuduti et al. 2012). In summary, trichome development in tomato is known to be controlled by multiple transcription factors, including MYC1, CD-2, WO, H and EOT1. Several other proteins acting outside the nucleus, including CHI1/Af; and SRA/Hl, also modulate the development of these structures. Despite this progress, much remains to be learned about the genetic basis of type VI trichome development and function.

AIMS OF THE THESIS RESEARCH

Many genes and metabolic pathways are likely to be critical for proper development of glandular trichomes. Identifying additional trichome mutants of tomato, and characterizing their role in trichome development, will add to our understanding of this complex structure. At a

practical level, this knowledge may facilitate biotechnological efforts aimed at improving crop resilience and the production of valuable plant-based compounds. At the start of this research, the gene defined by the *odorless-2* (*od-2*) mutant in tomato had yet to be identified; given the unique development and metabolic phenotypes of this mutant (Kang et al. 2010a), a major aim of this thesis research was to identify the *Od-2* gene and characterize its role in trichome development. Toward this goal, RNA-seq was used to determine how the *od-2* mutation affects gene expression and thus other metabolic pathways. The location of the recessive mutation was previously mapped to a position on chromosome 11 (Kang et al. 2010a). Whole-genome sequencing of the mutant and the progenitor allowed alignment of reads to the newly published genome (The Tomato Genome Consortium 2012) for SNP analysis and identification the causal mutation. Molecular identification of the *Od-2* gene was then validated with the wild-type gene. This work is described in Chapter 2.

The *anthocyanin free* (*af*) mutant of tomato displays a unique pleiotropic phenotype that links flavonoid production to the development and metabolic activity of type VI trichomes. Specifically, loss of function CHI1 in the *af* mutant results not only in a flavonoid deficiency but also in loss of terpenoid accumulation in type VI trichomes (Kang et al. 2014). Given the unique nature of this phenotype, a more thorough investigation of the function of CHI1 and associated flavonoids was warranted. Accordingly, the second major aim of this thesis was to investigate the tissue- and cell-type specific function of flavonoids through the construction and characterization of transgenic tomato lines in which CHI1 is expressed under the control of various promoters. Prior to this work, it was unclear if flavonoid production in the trichome was linked to terpenoid biosynthesis, or whether flavonoids in the leaf were responsible for a signal impacting terpenoid accumulation in the trichome. Chapter 3 describes the investigation of this question.

CHAPTER 2 THE TOMATO *ODORLESS-2* GENE LINKS TRICHOME-BORNE SPECIALIZED METABOLISM AND LEAF DEVELOPMENT TO SPHINGOLIPID BIOSYNTHESIS

ABSTRACT

Glandular trichomes are hair-like epidermal structures that produce volatile terpenoids and other specialized metabolites implicated in plant anti-herbivore defense. The *odorless-2* (*od-2*) mutant of cultivated tomato (*Solanum lycopersicum*) is severely impaired in the accumulation of terpenoids in type VI glandular trichomes and exhibits defects in leaf development. The mechanism by which *od-2* confers these pleiotropic effects remains unknown. Here, we used whole-genome sequencing to screen for nucleotide polymorphisms associated with the *od-2* locus. We identified a single nucleotide deletion in Solyc11g019950, which is predicted to encode LCB1A, a subunit of the serine palmitoyltransferase complex, involved in the biosynthesis of long-chain base precursors of sphingolipids. Consistent with this finding, the sphingolipid profile of *od-2* leaves was indicative of a biosynthetic defect in long-chain sphingoid bases. Transgenic expression of the wild-type *LCB1A* cDNA driven by the *Cauliflower Mosaic Virus* 35S promoter complemented both the leaf developmental and the bulk sphingolipid phenotypes of the mutant but failed to rescue the terpenoid deficiency. Conversely, expression of *LCB1A* from a trichome-specific promoter restored terpenoid production in type VI trichomes of *od-2* but did not complement the foliar sphingolipid profile of other developmental defects. These results provide new insights into the tissue- and cell type-specific function of sphingolipid biosynthesis in tomato.

INTRODUCTION

Terpenoids are a diverse class of biologically active compounds originating from the five-carbon subunits isoprene pyrophosphate and dimethylallyl pyrophosphate (Paduch et al. 2007; Schwender et al. 1996). Because of their volatile nature, many terpenoids (e.g. monoterpenes) contribute to the characteristic scents and flavor of plants, such as lemon, mint, and pine. Terpenoids have many practical uses in human societies. Terpenoid accumulation in plants is

regulated at multiple levels. Two recurring themes of terpenoid biology in plants is their production in specific tissues, cell types, or anatomical structures (Yazaki et al. 2017), and their biosynthesis in response to herbivory or other types of biotic stress (Turlings et al. 1990). Given the ecological and biotechnological importance of terpenoids, it would be useful to identify regulatory mechanisms that increase or otherwise modulate terpenoid production. To date there has been limited success in achieving this goal (Shen et al. 2016; Spyropoulou et al. 2014); therefore, efforts to better understand the fundamental cellular and biochemical processes required for terpenoid biosynthesis and storage are warranted.

In cultivated tomato (*Solanum lycopersicum*), the production of terpenoids and other secondary metabolites in glandular trichomes (GTs) is part of a multi-layered defense strategy for protection against insect herbivores. The major terpenoid produced in type VI GTs is β-phellandrene. Genetic defects resulting in decreased production of β-phellandrene are associated with increased susceptibility to various insect pests (Bleeker et al. 2012; Kang et al. 2014; Kang et al. 2010a; Rick et al. 1976). Exogenous application of terpenoid enhances defenses against persistent pests, such as whitefly (Du et al. 2016) confirming the role of these compounds in herbivore defense.

Genetic analysis in tomato have shown that genes required for normal development of GTs are also needed for synthesis and accumulation of various secondary metabolites suggesting that investigating the molecular basis of these mutants could lead to a better understanding of how GTs and secondary metabolites are regulated. Previous advances in understanding tomato trichome formation have found increased production of type I glandular trichomes by the dominant mutation *woolly* (*wo*) (Young and MacArthur 1947). The *wo* mutation, in a HD-bZIP transcription factor, is lethal when homozygous indicating a function outside of trichome development, and RNAi-

based silencing of the WT allele results in plants with no trichomes (Yang et al. 2011). The *hairless* (*hl*) tomato mutant, with profuse but highly deformed trichomes, provides an example of the additional structural support required for normal trichome development compared to many other cell types. The genetic identity of the *hl* mutation is a deletion of the last exon of SRA1 a member of the WAVE complex responsible for regulating and stabilizing actin dynamics (Kang et al. 2016). Mutations affecting the WAVE complex in Arabidopsis have also been shown to result in deformities of trichomes (Brembu et al. 2004). These actin dynamics are important for vesicle trafficking and structural connections to the plasma membrane (Takenawa and Suetsugu 2007).

The *odorless-2* (*od-2*) mutant was originally identified based on an altered leaf aroma phenotype, and subsequently shown to have structurally defective trichomes that fail to produce significant quantities of rutin and β-phellandrene. Type VI GT development in the *od-2* mutant is severely impaired and recognizable GTs are sparse on *od-2* leaves (Kang et al. 2010a). In testing the type VI GT from *od-2* Kang et al, (2010a) found no detectable terpenoids, which leads to the hypothesis that there is some regulatory restriction on the production of terpenoids in *od-2* even if the cells reach typical type VI GT shape (Kang et al. 2010a). Importantly, growth of *od-2* in field experiments showed that this mutation compromises resistance to natural populations of insect herbivores, such as flea beetle (*Epitrix cucumeris*), and Colorado potato beetle larvae (*Leptinotarsa decemlienata*) (Kang et al. 2010a). Another distinguishing characteristic of *od-2* was the small leaflets but otherwise normal leaf lengths (Kang et al. 2010a). Silver damage from Western flower thrips (*Frankliniella occidentalis*) was found to be much higher on *od-2* along with higher levels of JA-Ile and lower levels of ABA (Escobar-Bravo et al. 2018). The *od-2* mutant has become a useful tool for testing trichome mediated herbivore and pathogen responses due to its otherwise normal seeming induction of other defense compounds (Escobar-Bravo et al. 2018;

Escobar-Bravo et al. 2019a, 2019b; Kang et al. 2010a). The *od-2* locus was mapped to chromosome 11 (Kang et al. 2010a) but the molecular identity of this gene remained unknown.

In this study, we employed whole-genome sequencing to identify candidate mutations responsible for the pleiotropic phenotypes of *od-2*. We identified a small deletion in a gene (Solyc11g019950) predicted to encode an enzyme (termed LCB1A) involved in the biosynthesis of long-chain base precursors of sphingolipids. Sphingolipid profiling of *od-2* leaves validated a biosynthetic defect in long-chain sphingoid bases. Transgenic expression of the wild-type *LCB1A* cDNA from the Cauliflower Mosaic Virus 35S promoter complemented the leaf developmental and bulk sphingolipid phenotypes of the mutant but, interestingly, failed to rescue the terpenoid deficiency. Expression of LCB1A from a trichome-specific promoter restored terpenoid production in type VI trichomes of *od-2* but did not complement the foliar sphingolipid profile or other leaf developmental defects. These data provide new insights into the tissue- and cell type-specific function of sphingolipid biosynthesis in tomato.

MATERIALS AND METHODS

Plant materials and growth conditions

We grew our plants in growth chambers with 16 hr, 250 μE, 28°C day and 18°C, 8 hr night cycles. Wild-type tomato seeds originated from A.L. Castle Inc. (variety Castlemart II). The seed source for *od-2* was previously described (Kang et al. 2010a). The seeds were bleach sterilized for 20 minutes with 20% bleach (2.5% sodium hypochlorite) prior to use, germinated in J7 Jiffy peat pellets, and transferred to 6 cm x 6 cm x 8 cm pots containing soil at three weeks.

Photosynthetic parameters

Five-week-old plants were assessed with a LI-Cor 6800 (Lantz et al. 2019). A leaflet from the fourth leaf of each plant was monitored for CO_2 response at 400 μmol m^{-2} s^{-1} and 2000 μmol

m^{-2} s^{-1} of light. Inlet air temperature was maintained at 28° C. VPD was kept between 0.8 and 1.

Chlorophyll levels were measured using a separate leaflet from the same set of plants used for gas exchange measurements. An 8 mm diameter hole-punch was used to obtain four leaf disks from each leaf. The leaf disks were weighed and then extracted with 1 mL methanol by briefly beating in a TissueLyser II (Quiagen) with two 3 mm stainless beads and then incubating at 4°C with gentle shaking for four hours. Debris was removed by centrifugation for 1 min at 13,000 x *g* and transferred to new tubes. All extractions were diluted to 1:10 with methanol and analyzed for absorption at 652 nm, 665 nm, and 750 nm (Porra et al. 1989).

Isotopic discrimination

A single leaflet from the fourth leaf was lyophilized and analyzed for ^{13}C discrimination and carbon and nitrogen content at the Stable Isotope Ratio Facility for Environmental Research, University of Utah (Farquhar et al. 1989; Guo et al. 2018).

RNA sequencing

RNA was purified from leaflets of five-week-old Castlemart and *od-2* plants. Each sequenced sample consisted of pooled cDNA from three plants with three replicated samples for each genotype. Illumina TruSeq sequencing was performed on a single lane to obtain 125 bp paired-end reads from the six libraries. Library construction and sequencing was performed in the MSU Genomics core Research Technology Support Facility. The unprocessed sequencing data was deposited in the National Center for Biotechnology Information Short Read Archive (ncbi.nlm.nih.gov/sra/PRJNA580508). Sequencing reads were mapped to ITAG2.4 and SL2.50 available through solgenomics.net. Analysis of differential gene expression was conducted with the Bioconductor.org package EdgeR, using a threshold value of 0.05 from common dispersion false discovery rate (FDR), and greater than one $\log_2$ fold change (LFC, positive for up regulation,

or negative for down regulation). All genes with greater than one LFC had an FDR less than 0.02. Gene Ontology terms were obtained from pantherdb.org (Mi et al. 2017) and searched for statistically overrepresented terms using the list of differentially expressed genes. For Gene Ontology listing, the Panther14.1 program includes a Fisher's exact test with Benjamini–Hochberg FDR correction for multiple testing. The string diagram was generated using a list of genes that are differentially expressed in *od-2* to string-db.org.

Whole genome sequencing

Illumina sequencing was used to obtain 100 bp paired-end reads which were aligned to the SL2.5 genome and annotation ITAG2.4 developed by the International Tomato Annotation Group (Fernandez-Pozo et al. 2015). Nucleotide polymorphisms between CM and *od-2* were investigated by scanning for non-synonymous SNPs in the Integrated Genome Viewer, broadinstitute.org (Thorvaldsdóttiret al. 2013).

Sanger sequencing

Primers 1R 2L (Appendix, **Table A-1**) were used to PCR amplify a region of LCB1A from genomic DNA from wildtype and *od-2*. The thermocycled PCR reaction was verified to contain a single band on agarose gel and submitted to the Michigan State University Research Technology Support Facility Genomics Core for sanger Sequencing.

Plasmid construction

A fragment containing the *Solanum habrochaites* MKS1 promoter was PCR amplified with primers 70L and 71R (Appendix, **Table A-1**) from the MKS1-GFP expression vector (Akhtar et al. 2013) and digested with HindIII and XbaI. The 35S promoter in pGWB-402 was digested using HindIII and XbaI. The 1644 bp PCR product containing the MKS1 promoter was ligated in the place of the 35S promoter, resulting in pGWB-40x_MKS1. A cDNA obtained from *S.*

lycopersicum cv. CastleMart was amplified with primers 26L 105L (Appendix, **Table A-1**). The resulting 1522 bp fragment was used in an LR reaction with either pGWB-402 or pGWB-40x_MKS1 resulting in expression vectors *35S::LCB1A* and *MKS::LCB1A*, respectively. The steps taken in the LR reaction were performed with LR ClonaseTM II (ThermoFischer) as described by the manufacturer.

Plant and Agrobacterium transformation

The *MKS::LCB1A* and *35S::LCB1A* plasmids were introduced into *Agrobacterium tumefaciens* strain AGL0 using the heat shock method (Weigel and Glazebrook 2002). Transformation of *od-2* was conducted in the Plant Biotechnology Resource and Outreach Center of Michigan State University (http://www.ptc.msu.edu/index.html). Resulting plants were transferred to soil for seed propagation in the greenhouse.

Sphingolipid analysis

Leaflets from leaves three, four, and five were harvested from five-week-old plants and lyophilized. One plant was used per sample and five samples were obtained per genotype. One sample of *od-2* was lost during processing. Measurement of sphingolipids was performed as previously described (Markham et al. 2006).

Leaf surface chemistry extraction

Extracted leaf surface metabolites following a similar protocol to that used by Kang et al (2010a). One leaflet from leaf seven of each five-week-old plant was weighed and washed with 1 mL of methanol including 10 ng μL^{-1} tetradecane and 1 μM propyl-4-hydroxybenzoate internal standards for 2 minutes with gentle shaking. A 100% methanol extraction was used to prevent non-enzymatic isomerization of naringenin-chalcone to naringenin despite 100% methanol being a

non-ideal extraction buffer for flavonoids and terpenoids. Wash effluent as stored in individual sealed 1.5 mL glass vials at -20°C until analysis.

Mass spectrometry

Volatile terpenoids were quantified by injecting one μL into a GC 6890N/5975B quadrupole (Agilent) by a CombiPAL (CTC Analytics). The column used was a 40m VF5MS, 30 m with 10 m EZGuard, 0.25 μm film and 0.25 mm inner diameter (Agilent). Operating conditions were as follows: 280°C inlet temperature, 88.35 psi inlet pressure, 1:10 split ratio, 45-350 mass scan starting at 3.5 min. Ramp temperatures used initial 40° C for one min, to 90°C at 40°C min^{-1}, to 110°C at 15°C min^{-1}, to 250°C at 25°C min^{-1}, to 320°C at 40°C min^{-1}, then hold 320°C for 2 minutes. Total run time was 12.93 minutes.

Flavonoid abundance was measured by LC-MS. One μL of the samples were injected into an Acquity Binary Solvent Manager and Column Manager (Waters) by a 2777C Sample manager (Waters). A Xevo G2-XS QTof (Waters) mass spectrometer was operated under the following conditions: capillary voltage, 2 kV; sample cone, 40 V; source temperature, 100°C; desolvation temperature, 350°C; desolvation flow rate, 600 L hr^{-1}; and electrospray ionization, negative sensing mode. MS^e was used with several functions which split each sampling timepoint: 1. No collision energy (to gather whole molecule masses); 2. Ramp of 20-60 V collision energy (to analyze sample molecule fragmentation patterns); and 3. Ion lock spray (for calibration of exact mass). A 10 cm x 2.1 mm, 2.7 μm Ascentis® Express C-18 HPLC column (supelco) held at 40°C was used for all separations. De-ionized water containing 0.1% formic acid was used for solvent A, and methanol was used for solvent B. Using a continuous flow rate of 0.3 mL min^{-1}, the gradient profile started at 5% solvent B and ramped to 60% solvent B over 3 minutes using the curve 6 setting on the Waters solvent manager and then ramped to 100%

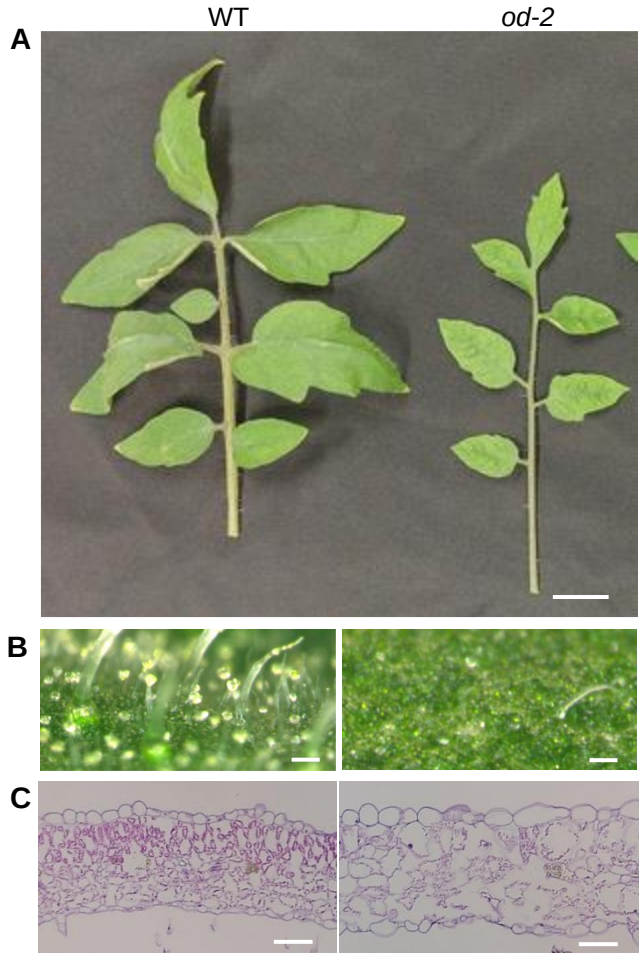

Figure 2-1: Morphological phenotypes of *od-2* leaves. (A) Representative images of 7th leaf from 6-week-old plants (WT, left; and *od-2*, right). Scale bar is 2 cm. (B) Dissecting microscope image of leaf surface (WT, left; and *od-2*, right). Scale bar is 0.1 mm. (C) Micrographs of leaf cross sections stained with hematoxylin and eosin (WT, left; and *od-2*, right). Scale bar is 100 μm.

solvent B over 4 min using curve 6, held at 100% solvent B until the 5.5 min point, dropped to 5% solvent B at 5.51 minutes, then held at 5% solvent B until 6.5 minutes.

Leaf and trichome morphology analysis

The 7th leaf of six-week-old plants was used to measure leaflet length and area. Trichomes were imaged using a Leica M16 dissecting microscope at 20x and 80x magnification.

RESULTS

The od-2 mutation impairs leaf development

Comparison of wild-type (WT) and *od-2* plants showed that the mutant has smaller compound leaves and a smaller petiole width (Figure 2-1A), as previously noted (Kang et al. 2010a). In contrast to WT leaflets, which typically exhibit varying degrees of curling, *od-2* leaflets are relatively small and flat. The small size of *od-2* leaflets is associated with epidermal surface abnormalities, most notably a sparseness of both glandular and non-glandular leaf trichomes (Figure 2-1B). To determine whether the small size of *od-2* leaflets is associated with corresponding changes in cell size, we used light microscopy to visualize the cellular organization in leaf cross sections. WT leaflets showed regularly spaced epidermal cells, rows of palisade cells, and uniform size of mesophyll cells (**Figure 2-1C**). By contrast, the epidermal cell layer of *od-2* leaflets contained very large cells having a high degree of size and shape irregularity (**Figure 2-1C**). These defects in the size and general organization of epidermal cells in the mutant extended to other cell types in the leaf, including palisade and mesophyll cells. Measurements of total leaf thickness derived from the cross-sectioned images showed that the thickness of *od-2* leaflets is significantly greater than that of WT (**Figure 2-1C**, **2-6**).

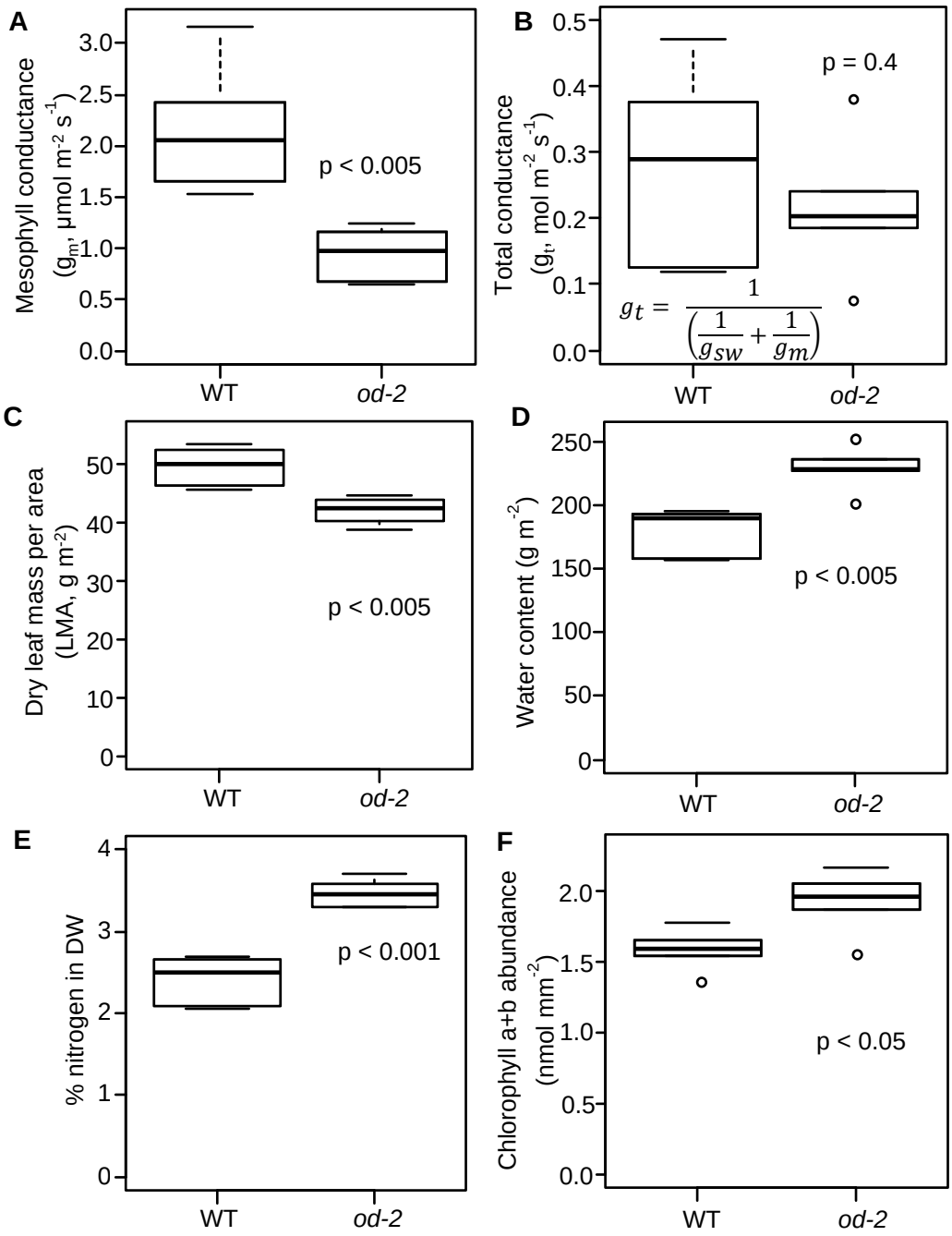

Figure 2-2: Photosynthetic parameters in WT and *od-2* leaves. Comparison of parameters related to photosynthesis in 5-week-old WT and *od-2* plants. (A) Mesophyll conductance from low irradiance measurements, n > 6 plants per genotype. (B) Total conductance from low irradiance measurements, n > 6 plants per genotype. (C) LMA, n = 10 plants per genotype. (D) Water content in leaflets, n = 10 plants per genotype. (E) Percent nitrogen by dry weight, n = 5 plants per genotype. (F) Total chlorophyll abundance, n = 10 plants per genotype. P-values derived from student's t-test. Boxplots show the median (thick center line), values in the 25th through 75th percentile (box height), and whiskers extend 1.5 times the interquartile range beyond the given quartile. Dots outside of the box and whiskers denote outlier data points.

Impact of od-2 on photosynthetic performance

The increased thickness and level of cell disorganization (e.g., larger cells) in *od-2* leaves raised the possibility that the mutant is altered in photosynthetic performance (Ren, Weraduwage, and Sharkey 2019). To address this question, we compared various photosynthetic parameters in WT and *od-2* leaves (Lantz et al. 2019). Gas exchange performed at high (2000 μmol m^{-2} s^{-1}) and low (400 μmol m^{-2} s^{-1}) light intensity revealed that *od-2* leaves have lower mesophyll conductance (**Figure 2-2A**). The rates of stomatal conductance and total conductance, however, were not significantly affected in *od-2* (**Figure 2-2B**, Appendix, **Figure A-1E**). Independent measurements of conductance by analysis of $^{12}CO_2/^{13}CO_2$ discrimination at ribulose-1,5-bisphosphate carboxylase (rubisco) showed that the overall rates of conductance were similar in *od-2* and WT leaves (Appendix, **Figure A-1K**).

The increased leaf thickness in *od-2* prompted us to investigate other physiological parameters of the leaf. Dry mass per area (LMA) is widely used as a key indicator of a variety of leaf traits that influence plant performance in, and adaptation to, variable environments (Poorter et al. 2009). We found that, despite increased thickness of *od-2* leaves, the LMA of the mutant was significantly less than WT (**Figure 2-2C**). Consistent with leaf traits that correlate with LMA (Poorter et al. 2009), *od-2* also had a higher water content and increased total leaf nitrogen in comparison to WT (**Figure 2-2D**). We also found that chlorophyll abundance on a per leaf area basis, was higher in *od-2*. The thicker leaves of *od-2* contain more water as may be expected (**Figure 2-2C**), however there was a lower dry leaf mass per area (LMA) in *od-2* (**Figure 2-2D**).

The od-2 leaf transcriptome is indicative of elevated stress and low terpenoid production

To better understand the impact of *od-2* on genome-wide processes in the leaf we used mRNA sequencing (RNA-seq) to compare the transcript profile of WT and *od-2* leaves. Analysis

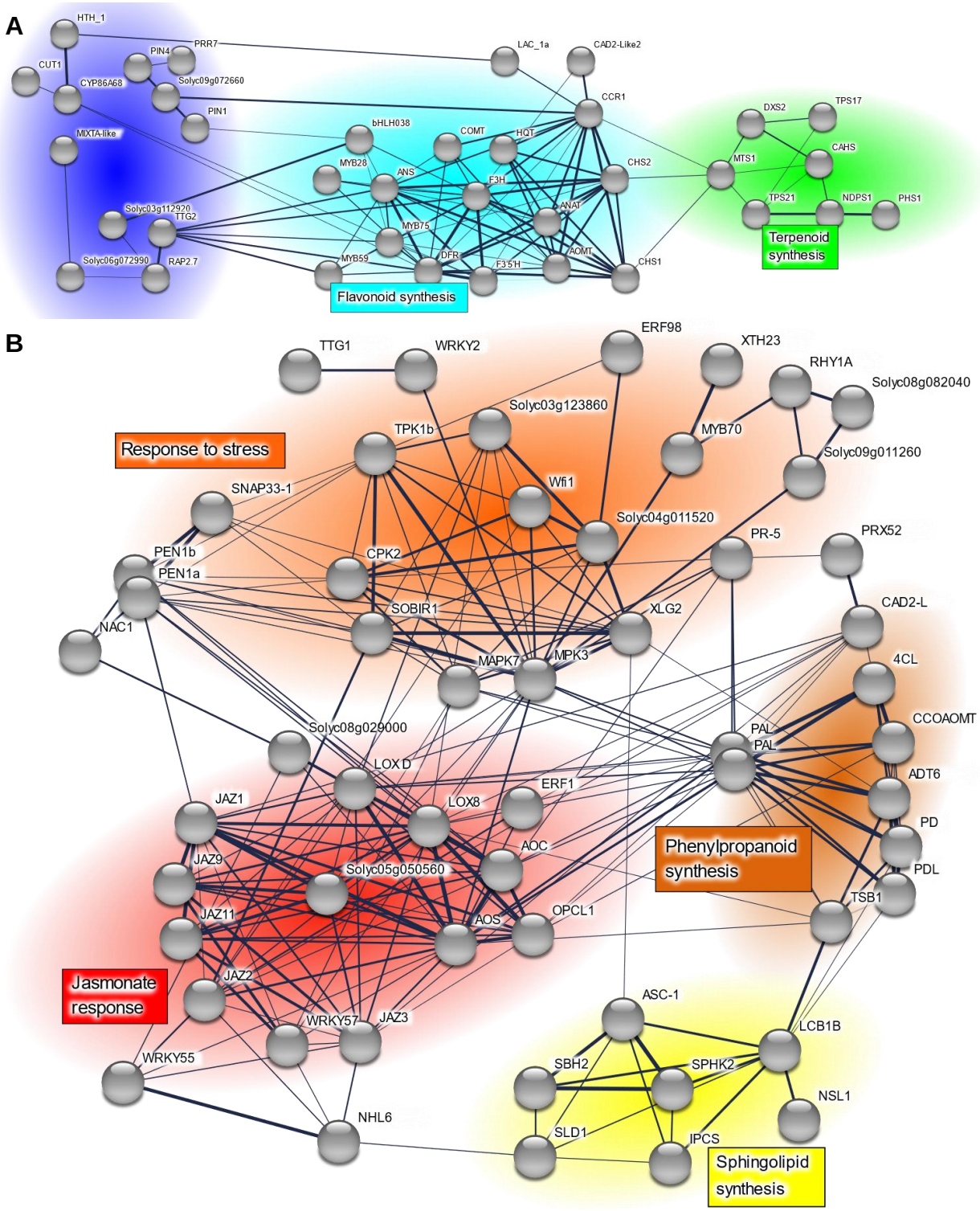

Figure 2-3: Potential interactions between genes that are differentially expressed in *od-2*. (A) Down-regulated genes in *od-2* leaves. (B) Up-regulated genes in *od-2* leaves. Image made by entering differentially expressed genes in *od-2* (threshold: FDR < 0.05, logFC > 1 or < -1 for (A) and (B) respectively) to string-db.org. Line thickness indicates confidence level of the interaction. See Supplemental table 2-1 and 2-2 for gene identifiers and expression differences.

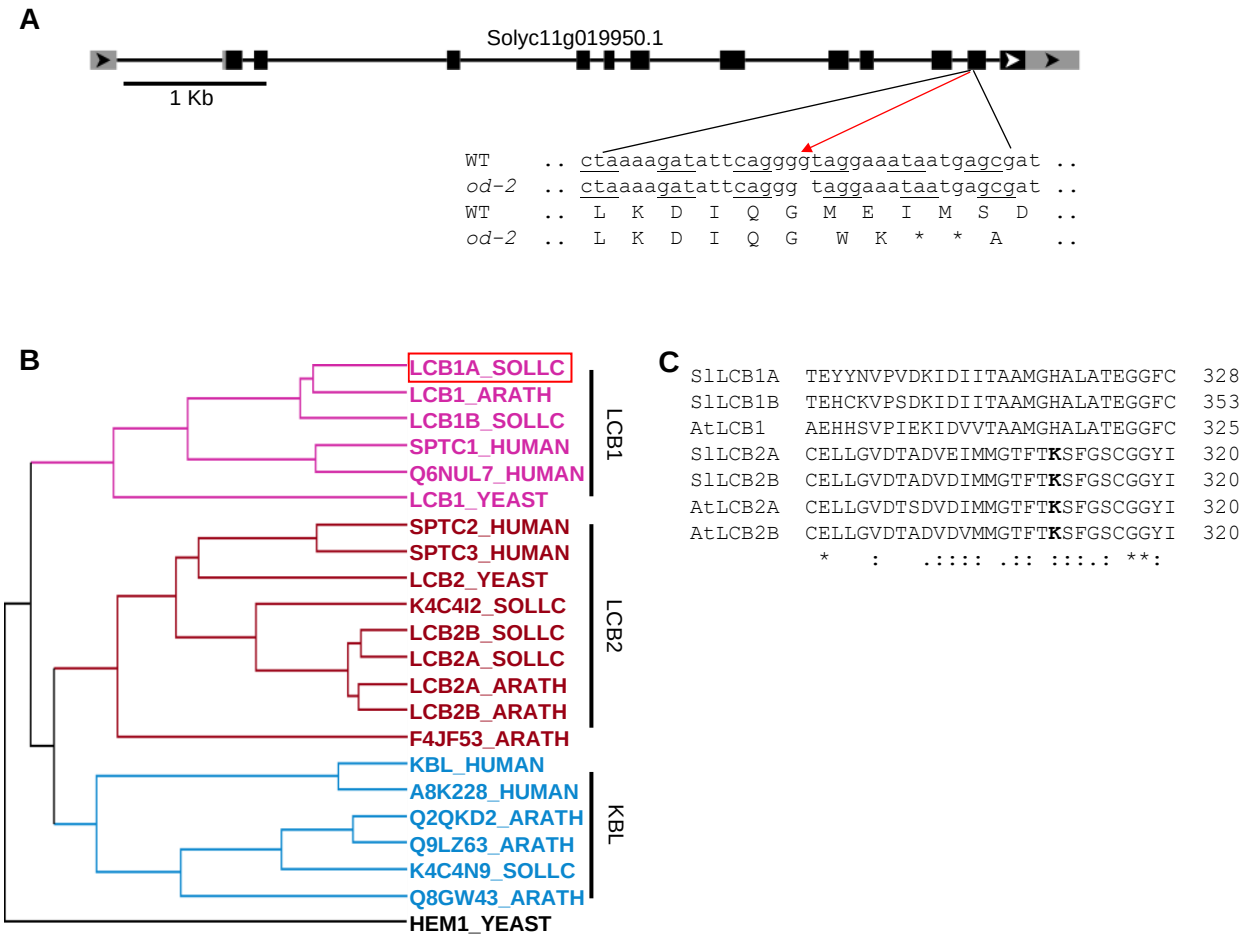

Figure 2-4: Molecular identification of *od-2* as *LCB1A*. (A) Schematic diagram of *LCB1A* gene and location of the *od-2* mutation. Exons are black boxes, untranslated regions are grey boxes, introns are black lines, and arrows indicate transcriptional read direction. Aligned wild-type (WT) and *od-2* nucleotide (top) and amino acid (bottom) sequences derived from the 11th exon of Solyc11g019950.1. Asterisks denote stop codons. (B) Phylogenetic tree showing LCB homologs with Solyc11g019959.1 as LCB1A_SOLLC (red box) clustering with the Arabidopsis LCB1, Human SPTC1, and yeast LCB1. 2-amino-3-ketobuterate CoA ligase (KBL) group included for tree completeness. HEM1_YEAST is included as an outgroup. (C) Partial alignment of LCB protein sequences from *S. lycopersicum* and *A. thaliana*. Bold K (lysine) indicates the residue required for binding pyridoxal phosphate in LCB2s, which is missing from LCB1s.

of the sequencing data identified a total of 18,705 expressed genes in either WT or *od-2*. In comparing gene expression levels between the two genotypes, the threshold for differential expression was defined as $\log_2$FC > 1 or < -1 with an FDR cutoff of 0.05. This analysis identified 1924 and 1059 genes that were up-regulated and down-regulated, respectively, in *od-2* relative to WT (Supplemental File Table 2-1, and 2-2). Gene ontology (GO) analysis of differentially regulated genes showed that "isoprenoid biosynthesis" and "terpenoid biosynthesis" were among the biological processes most significantly overrepresented in genes expressed to lower levels in *od-2* than WT leaves (Supplemental File Table 2-3). In the case of genes that were up-regulated in the mutant relative to WT, "response to stress" and "defense response" were among the major enriched GO categories (Supplemental File Table 2-4). We next used a recursive search (string-db.org) to identify groups of differentially expressed genes that potentially interact within a network (Crosara et al. 2018). As depicted in **Figure 2-3** results from this analysis further suggest that genes down-regulated in *od-2* and involved terpenoid and flavonoid synthesis are well connected, and genes up-regulated in *od-2* involved in various stress responses, including phenylpropanoid synthesis, jasmonate response, and sphingolipid synthesis are also well connected.

Odorless-2 encodes a tomato homolog of LCB1

Od-2 was previously mapped to a 6-centimorgan region on chromosome 11 (Kang et al. 2010a). In order to identify the causal mutation in *od-2*, we performed whole-genome sequencing of both the homozygous (*od-2*/*od-2*) mutant and its WT parental line (cv Castlemart). Comparison of the target interval for nucleotide polymorphisms identified a single base-pair deletion at position 9,815,979 bp of the short arm of chromosome 11. This mutation is located in exon 11 of Solyc11g019950 and is predicted to generate a frameshift followed by a pre-mature stop codon

(**Figure 2-4A**). The mutation was verified by sanger sequencing a fragment of Solyc11g019950 from 3 independent *od-2* plants and 2 wildtype plants. Solyc11g019950 is predicted to encode a protein called Long Chain Base 1 (LCB1). The predicted protein has a high degree of similarity to LCB1 from *Arabidopsis thaliana* (75% sequence identity), *Saccharomyces cerevisiae* (36% sequence identity), and a *Homo sapiens* family member called SPT1 (46% sequence identity). The pre-mature stop codon from the *od-2* mutation is predicted to truncate 93 amino acids from the C-terminus of the 486-amino-acid full-length protein (**Figure 2-4A**).

LCB1 and a related protein, LCB2, have been extensively characterized as interacting subunits of the serine palmitoyl transferase complex involved in the biosynthesis of sphingolipids (Chen et al. 2006; Gable et al. 2010; Lynch and Fairfield 1993; Nagiec et al. 1994). Phylogenetic analysis of the LCB family placed the tomato *Od-2*/*LCB1* gene within the LCB1 subclade (**Figure 2-4B**). BLAST analysis of the tomato genome with *Od-2*/*LCB1* as a query identified a closely related paralog, Solyc08g066020. We hereafter refer to this second gene (Solyc08g066020) as LCB1B and designate Od-2/LCB1 (Solyc11g019950) as LCB1A (Figure 2-4B). A major difference between members of the LCB1 and LCB2 subclades is the ability to bind the coenzyme pyridoxal 5'-phosphate (vitamin B6) within the LCB1-LCB2 heterodimeric complex (Chen et al. 2006). Specifically, LCB2s have a characteristic lysine that is required for binding the co-factor, whereas LCB1 proteins lack lysine at this position. The absence of this signature residue in tomato LCB1A is consistent with its identity as a member of the LCB1 subclade (Figure 2-4C).

To test whether the identified mutation in *LCB1A* affects sphingolipid synthesis, we measured the sphingolipid content in lyophilized leaves from 4-week-old WT and *od-2* plants. The most abundant sphingolipid in WT leaves was d18:2 glucosyl ceramide (**Figure 2-5A**), consistent with previous studies (Markham et al. 2006). In *od-2* leaves, both the total level of glucosyl

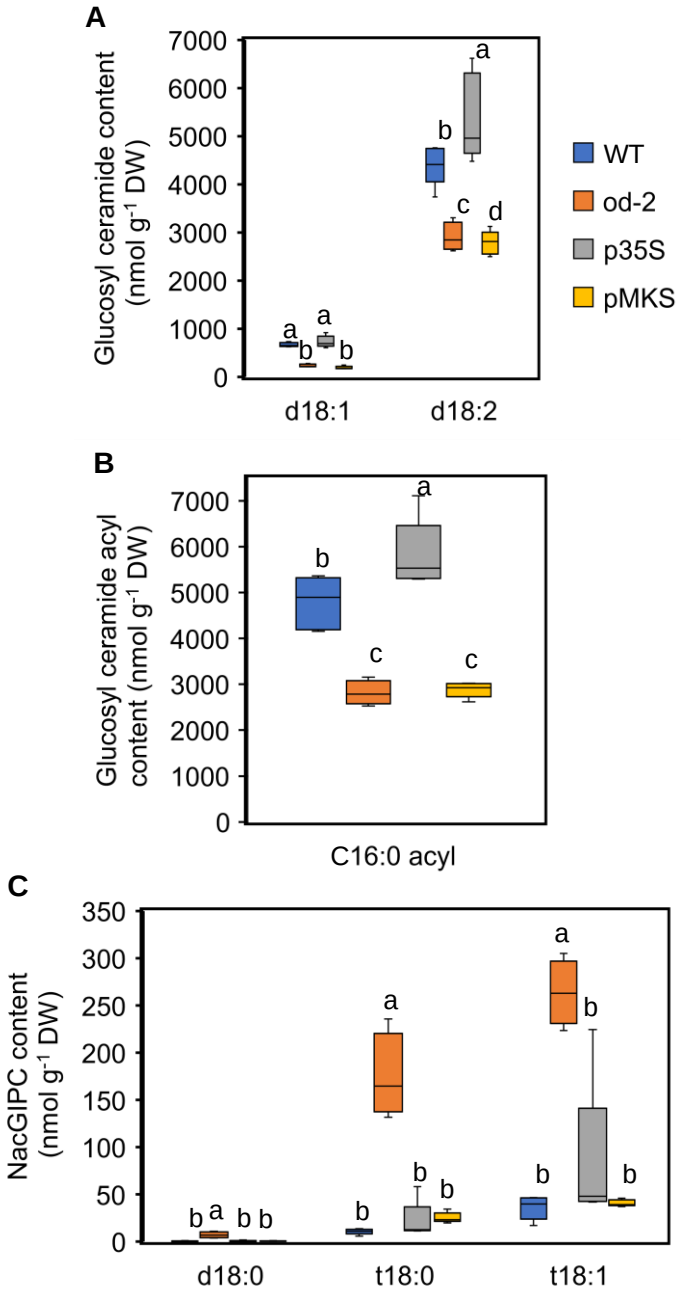

Figure 2-5: Changes in sphingolipid composition of *od-2* leaves are complemented by a *35S::LCB1A* transgene. Sphingolipid profiling was performed with leaves from WT, *od-2*, *p35S*, and *pMKS* plants. (A) Content of glucosyl ceramides containing di-hydroxylated 18:1(d18:1) or 18:2(d18:2) sphingoid bases. (B) Quantification of glucosyl ceramides containing a C16:0 acyl group. (C) N-acetyl glucosyl-inositol-phosphate ceramide (NacGIPC) content. *p35S*, *35S::LCB1A*; *pMKS*, *MKS::LCB1A*. Boxplots show the median (thick center line), values in the 25th through 75th percentile (box height), and whiskers extend 1.5 times the interquartile range beyond the given quartile. Dots outside of the box and whiskers denote outlier data points. Data were obtained from five plants for WT, *p35S, and pMKS*, or four plants for *od-2*. Different letters indicate significant differences based on ANOVA and Tukey HSD test $p < 0.05$.

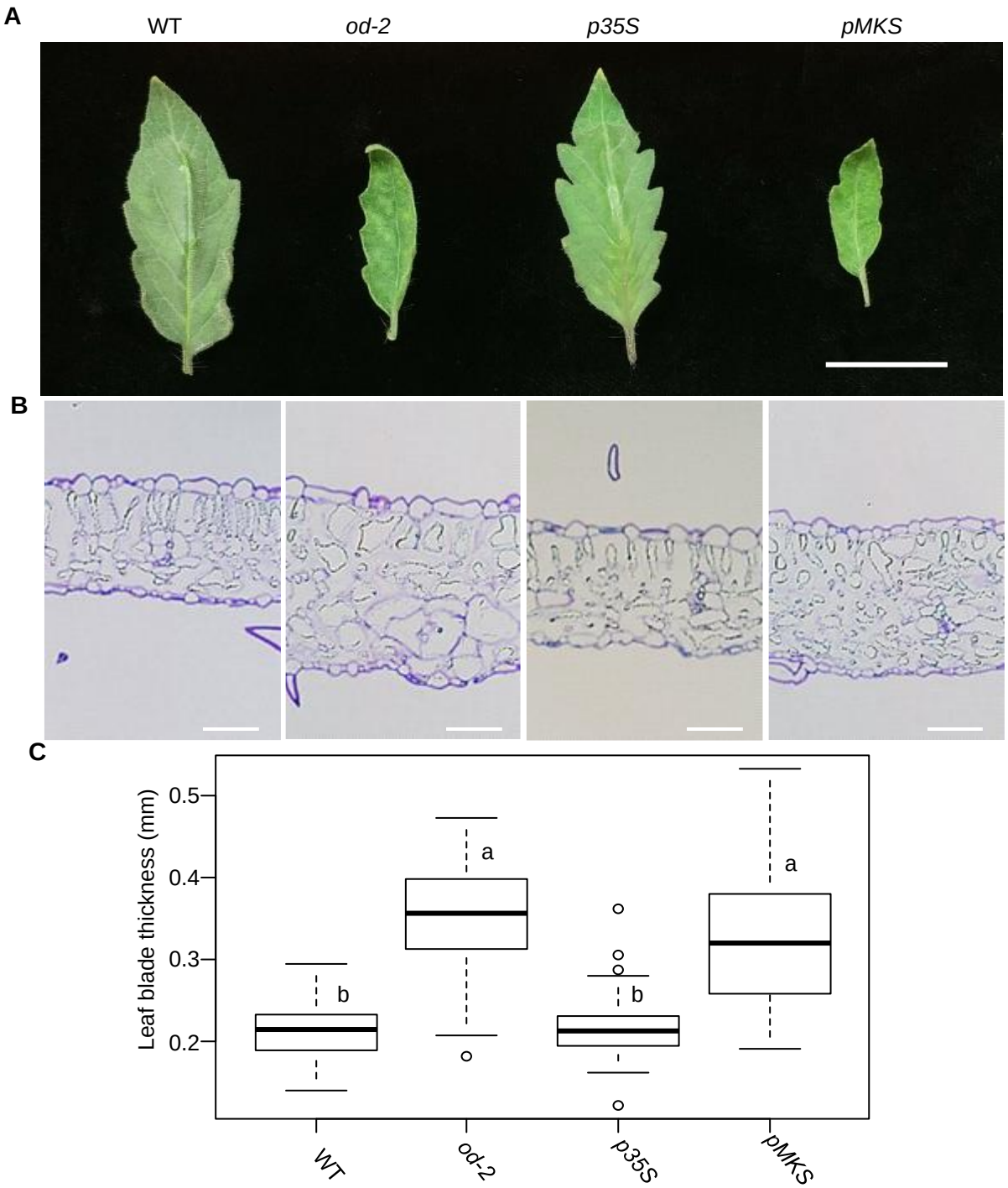

Figure 2-6: Leaf morphology of *LCB1A* complementation lines. (A) Photograph of representative leaflets from wildtype (WT), *od-2*, and *LCB1A* complemented lines (*p35S* and *pMKS*). Scalebar is 2 cm. (B) Leaf cross sections (adaxial side up) of the four genotypes shown in panel A. Scalebars are 100 μm. (C) Leaflet blade thickness as measured from cross sections. Five plants per genotype were measured in at least 10 different locations per plant. Boxplots show the median (thick center line), values in the 25th through 75th percentile (box height), and whiskers extend 1.5 times the interquartile range beyond the given quartile. Dots outside of the box and whiskers denote outlier data points.

ceramides and the amount of the abundant C16:0 acyl species (**Figure 2-5B**) was reduced to approximately 66% and 58%, respectively, of WT levels. Leaves of *od-2*, however, were not deficient in all classes of sphingolipids. The most obvious difference was an increase in the amount of N-acetyl glucosyl-inositol-phosphoryl-ceramides (NacGIPC) in the mutant relative to WT (**Figure 2-5 C**). These findings demonstrate that the *od-2* mutation is associated with changes in leaf sphingolipid content and composition.

To determine whether the mutation identified in *LCB1A* was responsible for the altered sphingolipid composition of *od-2* leaves, we performed genetic complementation experiments in which the *od-2* mutant was transformed with the WT *LCB1A* cDNA. Repeated attempts were unsuccessful to PCR amplify and clone or have manufactured the LCB1A native promoter for use in this experiment, likely due to high AT content and many long repeats of this region. As an alternative approach, we chose to express LCB1A from the strong constitutive 35S promoter and, given the multiple trichome-related phenotypes of the mutant (Kang et al. 2010a), a type VI trichome-specific promoter from the *S. habrochaites METHYL KETONE SYNTHASE 1* (*MKS1*) gene as well (Akhtar et al. 2013). *Agrobacterium* mediated transformation was used to introduce the *35S* and *MKS* promoter driven *LCB1A* constructs into the *od-2* genetic background. Multiple independent lines were generated for each construct and, following self-pollination for two generations, T3 lines homozygous for either *35S::LCB1A* (*p35S*) or *MKS::LCB1A* (*pMKS*) were obtained. Sphingolipid profiling showed that both the glucosyl ceramide and NacGIPC content of *p35S* leaves largely resembled that of the WT (**Figure 2-5A-C**). These data demonstrate that the sphingolipid defect in *od-2* leaves results from mutation of *LCB1A*.

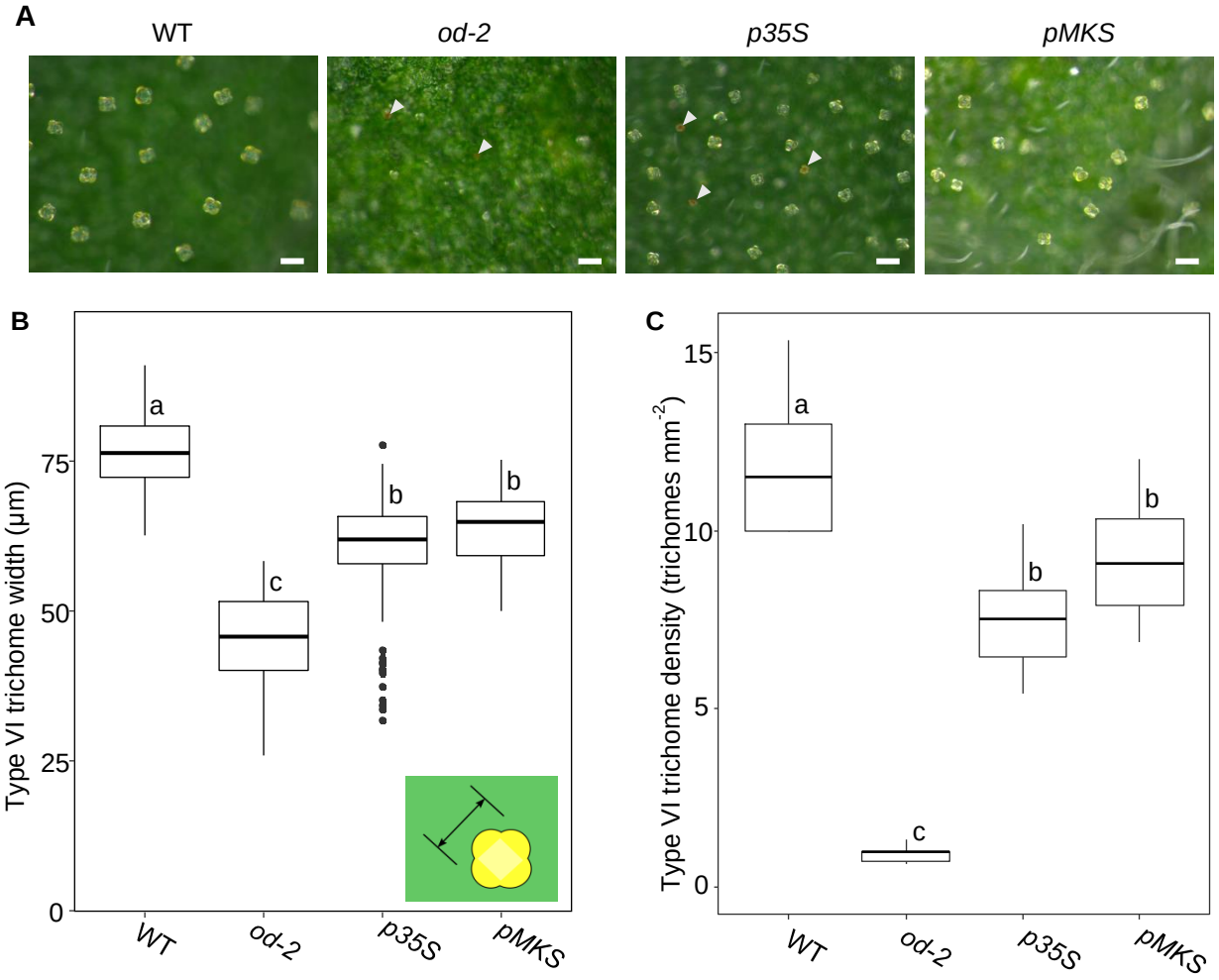

Figure 2-7: Trichome morphology of *LCB1A* complementation lines. Images of leaf seven from six-week-old plants were acquired with a dissecting microscope and used to measure the size and density of type VI trichomes. *p35S*, *35S::LCB1A*; *pMKS*, *MKS::LCB1A*. (A) Representative images used to measure trichome parameters. Scale bar is 0.1 mm. (B) Width of type VI trichome heads. Inset depicts a top-down view of the trichome as used for width measurements. Outlying data points (closed circles) observed for p35S correspond to atrophied (shrunken and brown) shown by arrows in panel A. (C) Density of type VI trichomes on adaxial leaf surface. Statistical differences denoted by ANOVA followed by Tukey HSD test are indicated by different letters. Boxplots show the median (thick center line), values in the 25th through 75th percentile (box height), and whiskers extend 1.5 times the interquartile range beyond the given quartile. Dots outside of the box and whiskers denote outlier data points.

Cell type-specific complementation of od-2 leaf traits

We next addressed the question of whether the pleiotropic phenotypes of *od-2* leaves (Kang et al. 2010a), including changes in leaf morphology and defective trichome development, are also caused by mutation of *LCB1A*. Among 6 independent *35S::LCB1A* lines tested, all displayed an overall leaflet size and thickness that was comparable to WT (**Figure 2-6**). By contrast, all *MKS::LCB1A* lines tested (n=4) had small, thick leaves that were indistinguishable from the *od-2* mutant (Figure 2-6). Thus, genetic complementation of the leaf morphology by *p35S* (but not *pMKS*) correlates with the biochemical rescue of the sphingolipid profile (**Figure 2-5**). Measurements of type VI trichome morphology (i.e., width of four-celled glandular head) showed that this trait was partially rescued in both *p35S* and *pMKS* lines (**Figure 2-7**). We noted, however, that the frequent occurrence of atrophied and discolored type VI trichomes on *od-2* leaves was occasionally observed in *p35S* lines, whereas the general appearance of type VI GTs in *pMKS* lines was indistinguishable from WT (**Figure 2-7A-B**). Measurements of type VI trichome density showed that this leaf trait was largely (but not completely) restored to that observed in WT (**Figure 2-7C**).

The *od-2* mutant was originally identified on the basis of its altered leaf aroma, which was associated with a defect in terpenoid and flavonoid accumulation in type VI trichomes (Kang et al. 2010a). To determine the extent to which these chemical phenotypes were rescued in the complemented lines, we compared the levels of the most abundant trichome-derived terpenoids from WT, *od-2*, *p35S*, and *pMKS* plants. As shown in **Figure 2-8A**, GC-MS analysis of leaf surface extracts showed that *p35S* plants fail to accumulate virtually all terpenoids identified in the WT. The terpenoid profile of extracts obtained from *pMKS* plants, by contrast, was nearly identical to WT. Quantitative data for β-phellandrene, the major terpenoid in type VI trichomes, is shown in

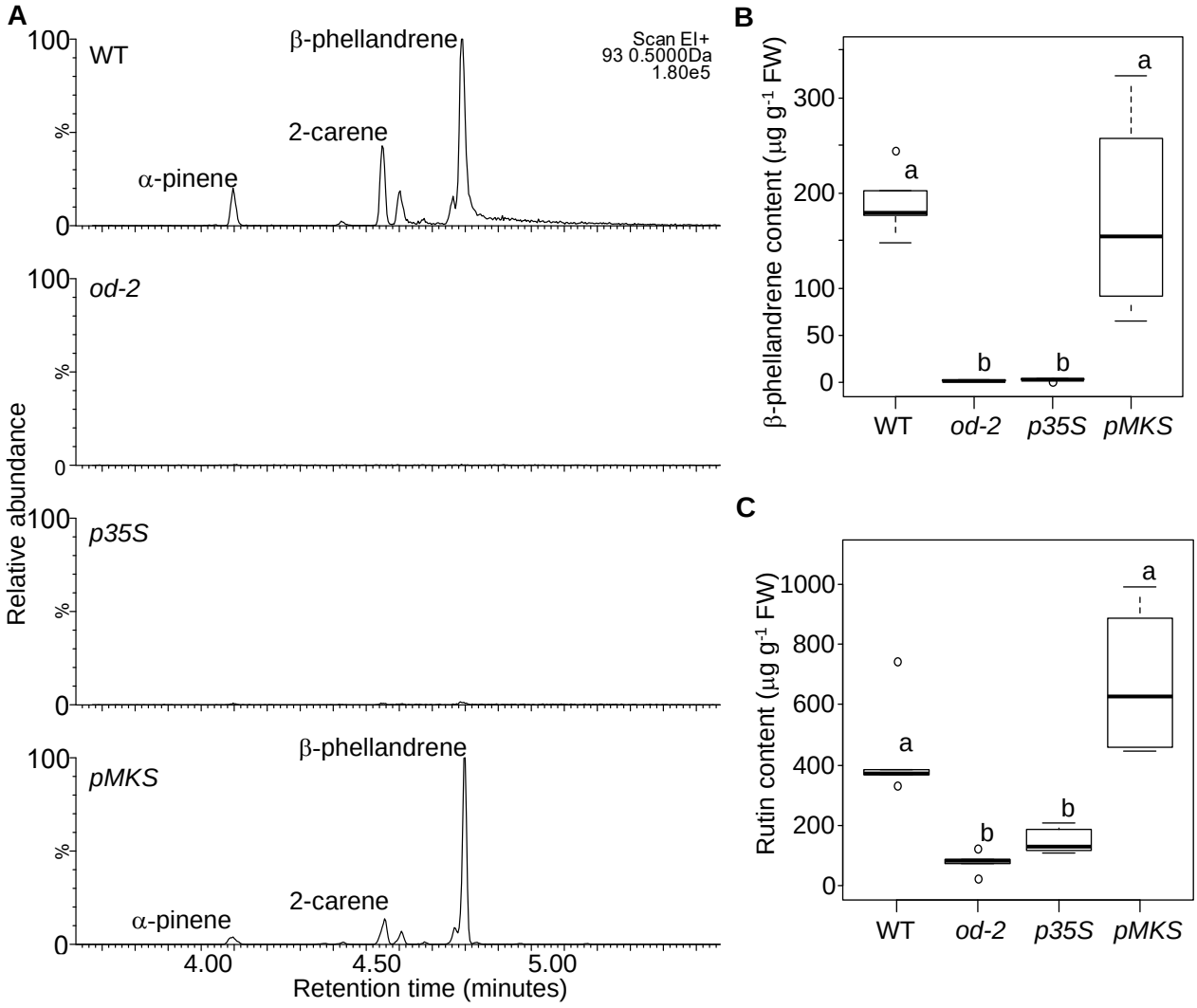

Figure 2-8: Leaf terpenoid and flavonoid content in *LCB1A* complementation lines. (A) Representative extracted-ion chromatographs for typical monoterpenoids in leaf surface extracts from the indicated genotypes. (B) Quantification of β-phellandrene, the major mono-terpenoid in type VI trichomes. (C) Quantification of rutin, the major flavonoid in type VI trichomes. Boxplots show the median (thick center line), values in the 25th through 75th percentile (box height), and whiskers extend 1.5 times the interquartile range beyond the given quartile. Dots outside of the box and whiskers denote outlier data points. Statistical differences in panels B and C are denoted lowercase letters and were obtained by ANOVA followed by Tukey HSD test ($p < 0.05$).

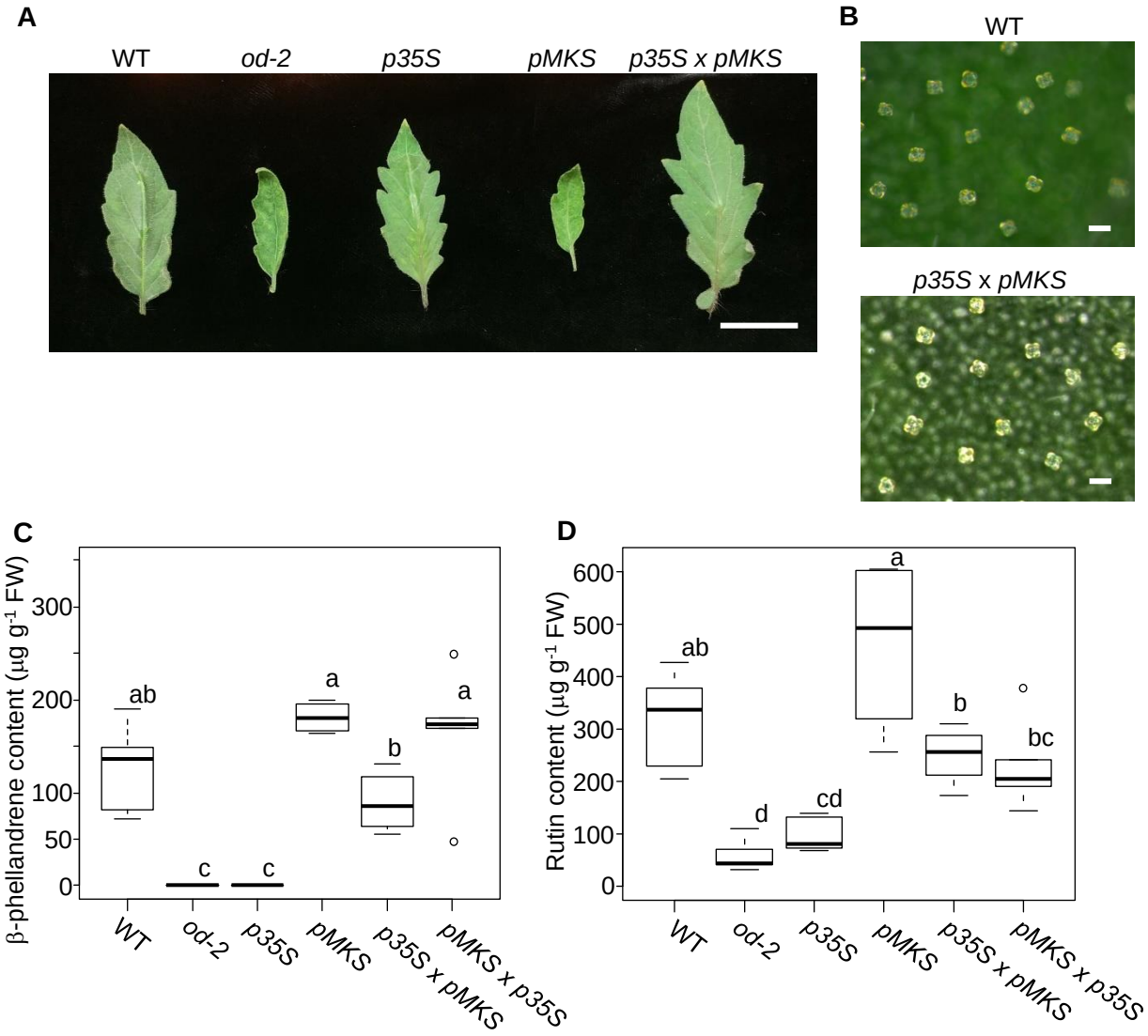

Figure 2-9: Phenotypic rescue in F_1 progeny of crosses between *p35S* and *pMKS*. (A) Photograph of representative leaflets from the indicated genotypes, including F_1 progeny from a cross between *p35S* and *pMKS* lines. Scale bar is 2 cm. (B) Photographs of type VI trichomes on adaxial surface of a WT and F_1 (from a cross between *p35S* and *pMKS*) leaf. Scale bar is 0.1 mm. (C-D) Abundance of β-phellandrene (C) and rutin (D) in leaf surface extracts from the indicated genotypes, including F_1 progeny from a cross between *p35S* and *pMKS* (genotype listed first was used as the female parent in the cross). Boxplots show the median (thick center line), values in the 25th through 75th percentile (box height), and whiskers extend 1.5 times the interquartile range beyond the given quartile. Statistical differences in panels C and D are denoted by lowercase letters and were obtained by ANOVA followed by Tukey HSD test ($p < 0.05$).

Figure 2-8B. Similar results were obtained from LC-MS analysis of rutin, which is the major flavonoid compound in type VI trichomes (**Figure 2-8C**). These data provide evidence that cell type-specific expression of LCB1A in type VI trichomes is sufficient to support the synthesis and accumulation of specialized metabolites produced in this cell type. The inability of *35S*::*LCB1A* to restore terpenoid and flavonoid production in the *od-2* genetic background further suggests that the 35S promoter is not expressed to sufficient levels in type VI trichomes. To further test whether the distinct LCB1A-complemented phenotypes of the *p35S* and *pMKS* lines results from cell type-specific expression of the respective promoters, we analyzed the leaf morphology and trichome-associated phenotypes of F_1 progeny derived from reciprocal crosses between *p35S* and *pMKS* lines, and in which the *35S::LCB1A* and *MKS::LCB1A* transgenes are hemizygous. In contrast to the partial (i.e., trait-specific) complementation phenotypes of the two parental lines, F_1 progeny from reciprocal crosses exhibited full recovery of normal leaf morphology, trichome morphology, and leaf surface chemistry (**Figure 2-9**).

DISCUSSION

Type VI GTs of tomato provide an attractive experimental system in which to study specialized metabolic pathways for terpenoid and flavonoid biosynthesis in a single cell type (Schilmiller et al. 2008; Tissier 2012). Over the past 15 years, characterization of various mutants affected in the development and chemical composition of type VI glands supports the view that these epidermal structures are an important part of a multilayered defense system for resistance to insect herbivores (Bleeker et al. 2012; Kang et al. 2014, 2016; Kang et al. 2010a, 2010b; Li et al. 2004; Xu et al. 2018). Much remains to be learned, however, about the specific cellular and biochemical processes required to coordinate the developmental and metabolic fate of glandular trichomes in tomato and other plant species. With this goal in mind, we set out to identify the

molecular basis of the defect in type VI trichome development in the tomato *od-2* mutant (Kang et al. 2010a).

The *od-2* mutation is predicted to truncate 93 amino acids (~20% of the full-length protein) from the C-terminus of LCB1A. Previous structure-function studies in yeast provide evidence that the C-terminal end of LCB1 and LCB2 are important for regulation of SPT activity or substrate specificity of the enzyme (Monaghan et al. 2002). Thus, it is possible that production of truncated LCB1A protein in the *od-2* mutant alters, but does not eliminate, the activity of the SPT complex. This, as well as the observation that null mutations in *LCB1* are lethal in Arabidopsis and yeast (*Saccharomyces cerevisiae*) (Buede et al. 1991; Chen et al. 2006; Shi et al. 2007), provides a unique opportunity to investigate the importance of sphingolipid synthesis in plants and eukaryotes in general. It is also possible that the *LCB1B* paralog of *LCB1A* contributes to sphingolipid synthesis in the *od-2* mutant by compensating for the loss of LCB1A. This hypothesis is supported by our RNA-seq data showing that *LCB1A* is expressed to about 8-fold higher levels than *LCB1B* in WT leaves, and that the absolute level of *LCB1B* mRNA abundance in *od-2* leaves increases nearly 7-fold relative to WT levels. Future studies using CRISPR-Cas9 technology to generate null mutations in tomato *LCB1A* and *LCB1B* should help to resolve this question.

Ceramides, glycosyl inositol phospho-ceramides (GIPCs), and other classes of sphingolipids perform a variety of basic cellular functions in eukaryotes, including vesicle trafficking, signaling, and modulation of membrane structure (Michaelson et al. 2016; Simons and Ikonen 1997). These functions directly impact processes such as necrosis, cell differentiation, cell cycle, and cell survival (Berkey et al. 2012). In plants, sphingolipids have been implicated in the maintenance of turgor pressure through the activation of calcium channels in guard cells and pollen tubes (Chen et al. 2015; Ng et al. 2001). Sphingolipid production is required for normal salicylic

acid (SA) production, and SA-mediated plant immunity (Rivas-San Vicente et al. 2013; Wang et al. 2008), as well as pollen development and cell adhesion (Bown et al. 2017; Msanne et al. 2015). Sphingolipid species containing very-long-chain fatty acids are required for plasma membrane stability, organization and cytoskeletal connections which, for example, impact the localization of auxin transport proteins (Markham et al. 2011). The *od-2* mutation does not eliminate sphingolipid synthesis but rather alters the composition of specific classes of these lipids. The lower abundance of d18:1 glucosyl ceramides in *od-2* is reminiscent of the altered sphingolipid composition resulting from RNAi-based suppression of *LCB1* in Arabidopsis (Chen et al. 2006). In this context, it has also been shown that pharmacological down-regulation of LCB1 activity in yeast leads to lower abundance of sphingolipids, including inositol phosphoryl ceramides (Huang et al. 2012). We also found that expression of the WT *LCB1A* cDNA from the 35S promoter rescued most of the changes in sphingolipid content in *od-2* plants, demonstrating a functional role for LCB1A in sphingolipid metabolism. These changes in sphingolipids are apparently responsible for the pleiotropic phenotypic changes seen in *od-2*.

Given the many known roles of sphingolipids in eukaryotic cells and their importance in cellular differentiation, it is perhaps not surprising that homozygous *od-2* plants exhibit a wide spectrum of abnormalities. For example, the disorganization of multiple cell layers in *od-2* leaves appears to underlie the observed changes in leaf thickness, with larger mesophyll cells potentially accounting for the decreased mesophyll conductance of the mutant. Sphingolipid involvement with control of the cell cycle and polar localization of signaling factors could impact tissue development processes such as cell-size regulation or asymmetric cell division (Cheng et al. 2001; Humphries et al. 2011). It is possible that cell size regulation through changes in ploidy contribute to cell morphological phenotypes in *od-2*, as has been seen in mutants of Arabidopsis (Breuer et al. 2009;

Sugimoto-Shirasu and Roberts 2003). It has also been reported inhibition of SPT activity in human cells results in cell cycle arrest prior to mitosis at the G2/M transition (Lee et al. 2011). Aanalysis of ploidy levels in the various cells of *od-2*, would provide a test of this hypothesis. The full recovery of normal leaf morphology, including mesophyll patterning, in *p35S* but not *pMKS* lines indicates that production of sphingolipids are critically required for normal blade expansion and photosynthetic capacity.

The full recovery of type VI trichomes in the *pMKS* lines but not the *p35S* lines further shows the importance of sphingolipids in the development of this specialized structure. The use of cell- and tissue-type promoters for these experiments highlights the cell-autonomous role of sphingolipids in trichome development and metabolic function (e.g., volatile terpenoid production) as well. It is conceivable that sphingolipid deficiency disrupts one or more processes involved in the transport and storage of terpenoids and other specialized metabolites. Unidirectional (polar) transport of metabolites in glandular cells is known to depend on targeting of proteins and vesicles to specific regions of the plasma membrane (Jasiński et al. 2001; Werker 2000). Polar localization of such components commonly involves lipid rafts, which are characterized by a high abundance of sphingolipids (Simons and Ikonen 1997). Long distance transport of other lipids has been demonstrated in species across the plant kingdom (Guelette et al. 2012; Hoffmann-Benning et al. 2002). Our data, however, suggests that sphingolipids act cell autonomously in gland cells of the type VI trichome. Future studies directed at understanding the precise effects of altered sphingolipid synthesis on the accumulation of terpenoids and other specialized metabolites in type VI trichomes is warranted.

Some trichome phenotypes of *od-2* are similar to those of another tomato mutant, *anthocyanin free* (*af*), but there are some key differences. The production of trichome-associated

terpenoids and flavonoids is severely compromised in both *od-2* and *af*. In *af* plants, low flavonoid levels are caused by a mutation that abolishes the activity of chalcone isomerase 1 (CHI1), an enzyme that is required for the biosynthesis of flavonoids (Kang et al. 2014). Although the mechanism by which flavonoids promote terpenoid accumulation in type VI trichomes remains to be determined, these findings raise the possibility that the terpenoid deficiency in *od-2* trichomes is related to low flavonoid production. This hypothesis is supported by the very low levels of rutin and other flavonoids in *od-2* glandular trichomes, even though this mutant accumulates normal anthocyanin levels in other cell types of the leaf.

Of particular relevance to the trichome chemical phenotypes of *od-2* is the low expression of terpenoid and flavonoid biosynthetic genes. The final steps of β-phellandrene biosynthesis are catalyzed by neryl-diphosphate synthase 1 (NDPS1) and phellandrene synthase (PHS) (Schilmiller et al. 2009). Interestingly, the genes encoding these two enzymes are among the most strongly down-regulated in *od-2* leaves. Reduced expression of these genes may explain the low abundance of volatile terpenoids in *od-2*. A similar correlation was observed between low expression of flavonoid biosynthetic genes and the flavonoid deficiency of *od-2* type VI trichomes. Previous studies showed over-expression of the transcription factor MYB75 (encoded by Solyc10g086250) promotes the accumulation of flavonoids (Jian et al. 2019). The low expression of this gene in *od-2* leaves relative to WT suggests that altered MYB75 activity may contribute to the metabolic phenotypes of *od-2*. Another MYB transcription factor, MYB101 (encoded by Solyc07g052300), is also down regulated in *od-2*. Increased activity of MYB101 homologs in Arabidopsis and *Solanum tuberosum* homologs via reduced miR159 expression caused an increase in trichome density (Pieczynski et al. 2013), whereas overproduction of miR159 caused a reduction of trichome abundance and enlarged mesophyll cells in Arabidopsis (Alonso-Peral et al. 2010). These

collective observations support the notion that changes in the activity of specific transcription factors may account for the pleiotropic metabolic phenotypes of the *od-2* mutant.

The developmental phenotypes of *od-2* leaves suggests that differentiation of protodermal cells into trichomes or stomata may also be influenced by changes in sphingolipid content. For example, we found that the tomato homolog (Solyc08g079980) of the Arabidopsis *STOMATA CELL DENSITY DISRUPTION 1* (*SDD1*) gene is strongly upregulated in *od-2* leaves. Previous studies showed that overexpression of *SDD1* in Arabidopsis resulted in lower stomata density and developmental arrest of stomata (Von Groll et al. 2002). Moreover, *ssd1* mutants display altered trichome branching, consistent with a role for SSD1 in trichome development (Lawson et al. 2014). Similar to the *ssd1* mutant, Arabidopsis mutants defective in MPK3 have paired stomata. We found that the tomato homolog of At*MPK3* (Solyc06g005170) is also up regulated in *od-2* leaves. Down-regulation of an Arabidopsis ERECTA-LIKE (ERL1 and ERL2) homolog of tomato (Solyc03g007050) may contribute to the large size and disorganization of cells in *od-2* leaves, which is reminiscent of the cell morphology defects observed in the corresponding loss-of-function mutants in Arabidopsis (Shpak et al. 2003). We also observed down regulation of two tomato homologs (Solyc01g104210 and Solyc07g018240) of the Arabidopsis *FATTY ACID ELONGATION 1* and *2* genes (*ELO1* and *ELO2*) in *od-2*. Leaves of the Arabidopsis *elo1* and *elo2* mutants have increased cell size, smaller blade area, and reduced numbers of palisade cells (Falcone et al. 2007; Nelissen et al. 2005). We also noted that homologs (Solyc03g096770, Solyc03g096780, and Solyc06g072990) of the Arabidopsis *LOW SULFUR* (LSU) genes are all down regulated in *od-2*; the fourth (Solyc03g096760) was not within the -1 LFC cutoff (LFC -0.978, FDR 0.0005). In Arabidopsis, *LSU* expression is induced in response to low sulfur, low iron, basic pH, excess copper, or high salt conditions (Garcia-Molina et al. 2017). It has also been

shown that elevated *LSU* expression promotes the production of H_2O_2 from O_2^- during various stress conditions by activating superoxide dismutase, whereas reduced expression of *LSU* is results in low H_2O_2 levels (Garcia-Molina et al. 2017). Another sulfur gene homolog (Solyc06g007970) of the Arabidopsis *SULFUR DEFICIENCY INDUCED 1* (SDI1) is also down regulated. SDI1 is involved in the utilization of SO_4^{2-} while under sulfur depravation, and low expression is associated with sulfur replete conditions (Howarth et al. 2009). Further investigation of sulfur metabolism will be required to verify if there is a deficiency in *od-2*. A non-targeted metabolomics study of *od-2* could additionally identify other deficiencies or metabolic imbalances in the mutant.

Restoration of type VI trichome size and density in both the *p35S*- and *pMKS*-complementation lines demonstrates the importance of sphingolipids in development of this trichome type. However, the precise spatial and temporal requirement for these lipids in development and initiation of type VI trichomes from the epidermal pavement cells remains to be determined. Assuming that sphingolipids function cell autonomously, as our data suggest, it is possible that weak expression of *LCB1A* in trichomes of *p35S* plants, as well as weak expression of *LCB1A* in epidermal cells of *pMKS* plants, is sufficient to allow normal specification and differentiation of the type VI structure. The presence of atrophied type VI trichomes in the *p35S* but not *pMKS* lines, however, suggests that later stages of trichome development (e.g., gland filling) require a certain threshold of sphingolipid synthesis for normal trichome function.

In comparing the extent to which the *35S::LCB1A* and *MKS::LCB1A* transgenes complemented the various phenotypes of *od-2*, this study provides new insight into the tissue-specific functions of sphingolipids in tomato. Whereas *35S::LCB1A* restored leaf and trichome morphology, it did not rescue flavonoid and terpenoid production in type VI GTs. Conversely, *MKS::LCB1A* did not restore leaf morphology but did fully restore all trichome-related

phenotypes. It may be possible to extend this approach to additional tissue- or cell type-specific promoters, such as mesophyll- or epidermal cell-specific promoters, to better understand the cell type-specific roles of sphingolipids in plants.

APPENDIX

Primer name	Sequence 5'→3'	Solyc ID	Target gene
1R	CCTGGTATGGTTTCAGGTCTAA	Solyc11g019950	*LCB1A*
2L	CTTCAAGACCTGCAATGACAAT	Solyc11g019950	*LCB1A*
103L	cagaaagcttCCGGTGAAGATTGTCGTTC	NA	*pMKS1*
104R	agtggtctagaTTTTGAACAACTACCACAAAG	NA	*pMKS1*
26L	ggggaccactttgtacaagaaagctgggtcctaGCTCTGATCTGTCAATAGCG	Solyc11g019950	*LCB1A*
105L	ggggacaagtttgtacaaaaaagcaggctagATGGATACAACAATATCAGTTC	Solyc11g019950	*LCB1A*

Table A-1: PCR primers used in this study. Sequence in capital letters is complementary to the target. Lower case sequence is the adapter. Solyc ID is the reference *Solanum lycopersicum* locus from solgenomics.net for the indicated target gene.

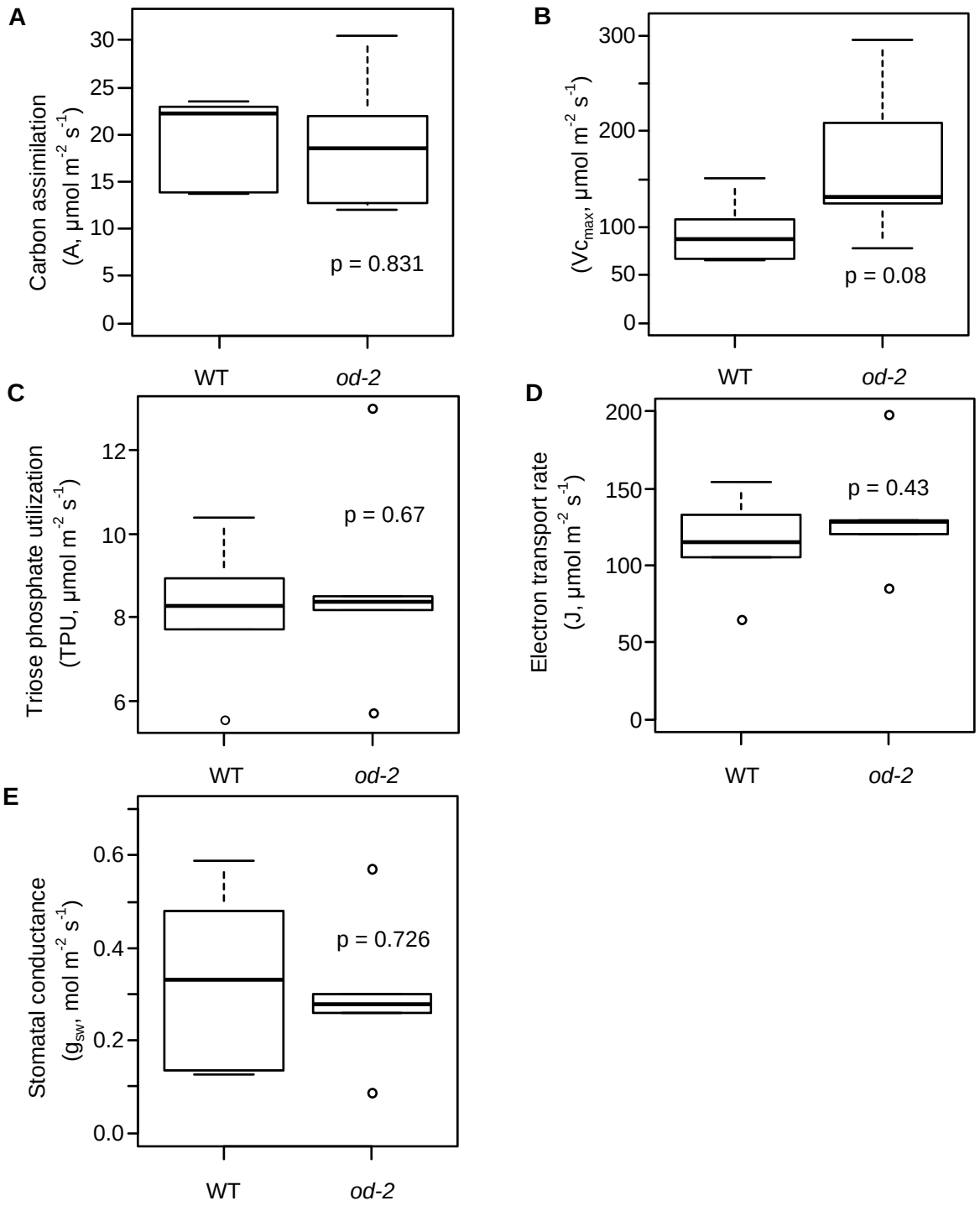

Figure A-1: Additional photosynthetic parameters in wildtype and *od-2* leaves. (A) Carbon assimilation. (B) Maximum CO_2 fixation rate. (C) Triose phosphate synthesis rate. (D) Electron transport rate. (E) Stomatal conductance. Boxplots show the median (thick center line), values in the 25th through 75th percentile (box height), and whiskers extend 1.5 times the interquartile range beyond the given quartile. Dots outside of the box and whiskers denote outlier data points.

Figure A-1 (cont'd). (F) Chlorophyll a:b ratio. (G) Percent carbon by dry weight. (H) Partial pressure of CO2 at rubisco. (I) C:N ratio, percent carbon to percent nitrogen per dry mass. (J) Percent fraction of nitrogen that is ^{15}N. (K) Percent fraction of carbon that is ^{13}C below atmospheric levels.

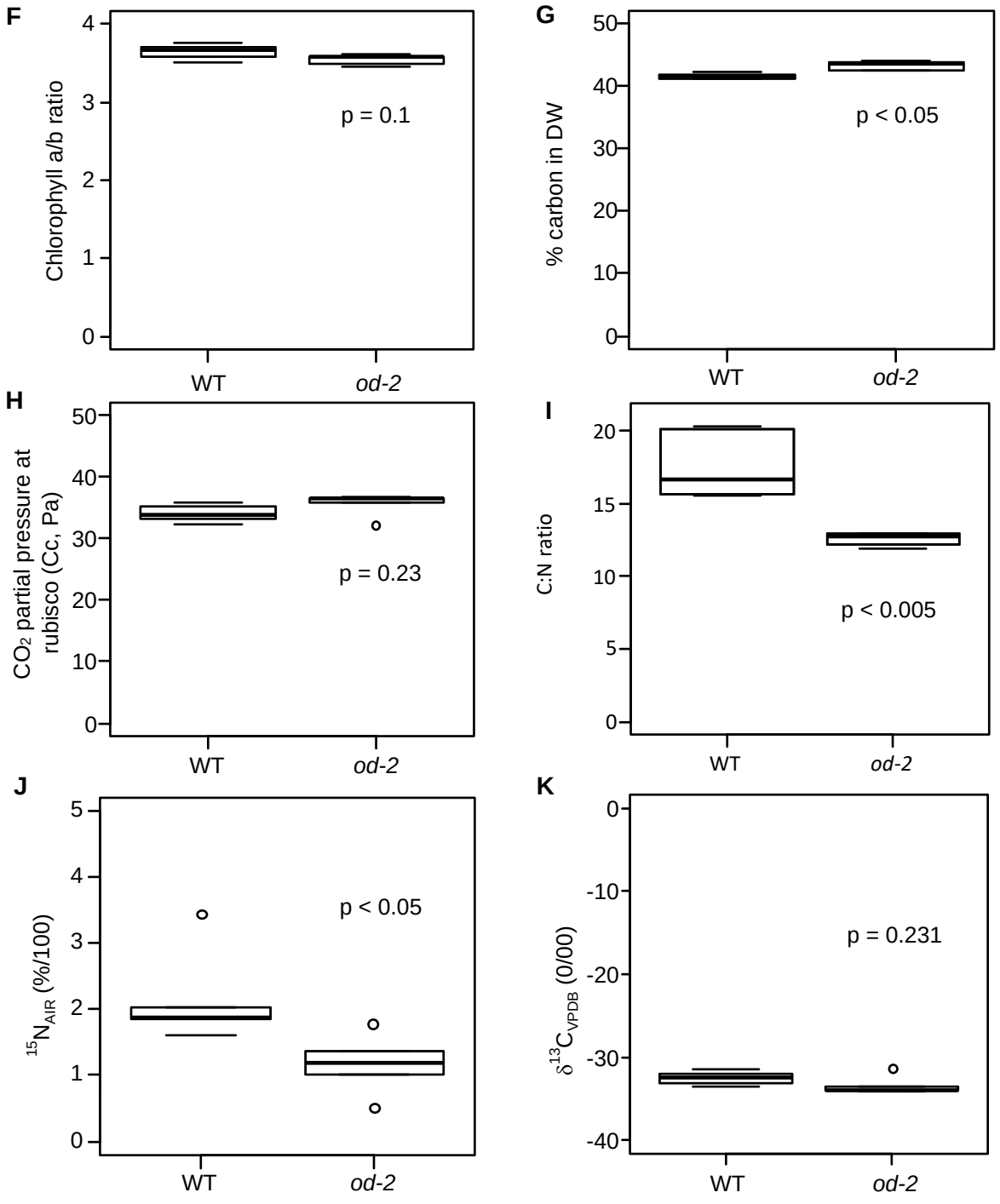

CHAPTER 3 CELL TYPE SPECIFIC COMPLEMENTATION OF CHALCONE ISOMERASE IN *S. LYCOPERSICUM*

ABSTRACT

Plants produce an array of structures and compounds that deter herbivory. Unfortunately, analysis of a mutation which affects herbivory is often confounded by pleiotropic phenotypes. Some specialized structures, such as glandular trichomes, not only physically deter herbivory but are also the source of defense compounds that deter herbivory. Complementation of the tomato mutant *anthocyanin free* (*af*) by expressing chalcone isomerase 1 (CHI1) with the *Solanum habrochaites* methyl ketone synthase 1 promoter resulted in expression of CHI1 specifically in type VI glandular trichomes, restored type VI trichome flavonoid and terpenoid levels, increased resistance to herbivory by the two-spotted spider mite, *Tetranychus urticae*, but did not restore anthocyanin production. Complementation of the tomato mutant *af* by expressing CHI1 with the Cauliflower Mosaic virus 35S promoter resulted in expression of CHI1 in leaf tissue, restored type VI trichome flavonoid and leaf anthocyanin levels, but did not restore type VI trichome terpenoids, and had no effect on herbivory by the two-spotted spider mite. Deterrence of spider mite-herbivory correlated with restoration of terpenoid production and expression of CHI1 in type VI trichomes.

INTRODUCTION

Investigations of plant mutants that are compromised in resistance to herbivore deterrence have identified many genes that control plant development and responses to the environment. These genes are often identified through the study of mutations that have pleiotropic phenotypes. One example is the *jasmonate insensitive 1-1* (*jai1-1*) mutant in tomato, which disrupts the gene CORONATINE INSENSITIVE 1 (COI1). COI1 codes for an F-box subunit that is responsible for targeting transcriptional repressors for degradation in the presence of jasmonate (Chini et al. 2007; Thines et al. 2007). The *jai1-1* mutant has fewer type VI glandular trichomes (GTs), reduced levels of volatile terpenoids, lower levels of anti-insect proteins such as protease inhibitors, reduced

sensitivity to jasmonate, reduced fertility, and minimal amounts of anthocyanin (Li et al, 2004). Other plant defense genes have been identified through profiling various tissues and treatments for induction of genes and those are then assigned a function based on in-vivo activity, such as polyphenol oxidase (Haruta et al, 2001). These and other investigations laid the groundwork for understanding the genes and molecular phenomena that impact plant-herbivore interactions. What is not clear from these findings is for which cell types these genes hold importance, and what specific metabolites or structures confer the herbivore deterrence seen. For example, Li et al (2004) associate increased spider mite feeding on *jai1-1* with reduced abundance of GTs and volatile-terpenoids, however there are also lower levels of protease inhibitor II and polyphenol oxidase. Without separating each of these pleotropic mutant phenotypes into different plants that share a common genetic background, theories about the loss of herbivore deterrence due to a specific compound or structure cannot be tested.

An example of separating out pleotropic phenotypes was given by Jewell and Browse (2016) where they used a variety of promoters to attempt to restore infertility to the mutant of the COI1 homolog in Arabidopsis. In Arabidopsis the *coi1-1* mutant is male sterile; the stamens do not reach their wildtype length, the pollen is non-viable, and the pollen does not dehisce (Feys et al. 1994). Restoration of COI1 activity in the tapetal layer of *coi1-1* by using the A9 promoter resulted in no recovery of fertility phenotypes (Jewell and Browse 2016). Use of the cell specific promoters for the filament by the DEFECTIVE ANTHER DEHISCENCE 1 promoter, or the anther epidermis by the WUSHEL promoter resulted in partial recovery of the *coi1-1* fertility phenotypes (Jewell and Browse 2016). However, use of the epidermal specific LIPID TRANSFER PROTEIN 1 promoter to express COI1 in the *coi1-1* mutant restored all fertility deficiencies normally seen in *coi1-1* (Jewell and Browse 2016). This series of experiments clearly showed that

sensing of jasmonate is required in the epidermis of filaments and anthers to provide normal male fertility and identified the cell types that require COI1 protein for proper development of stamen and pollen (Ishiguro et al. 2001; Sanders et al. 2000).

The *S. lycopersicum* mutant *anthocyanin free* (*af*) contains a frameshift mutation in the gene encoding chalcone isomerase 1 (CHI1). As a consequence, CHI1 protein does not accumulate in the mutant (Kang et al. 2014). CHI1 catalyzes the second step in flavonoid production by isomerizing naringenin chalcone to naringenin. In addition to expected mutant phenotypes such as decreased anthocyanin and other flavonoid levels, the *af* mutant displays several pleiotropic phenotypes that are more difficult to interpret based on a defect in CHI1. Of particular interest is the impaired production of type VI trichome volatile terpenoids and the increased susceptibility to insect herbivores (Kang et al. 2014; Rick et al. 1976). The difficulty in interpreting this phenotype is related to the fact that terpenoids and flavonoids are derived from largely independent pathways that operate in distinct subcellular compartments: anthocyanin and flavonoid synthesis occur in the cytoplasm and ER, whereas isoprenoid synthesis via the methyl-erythritol phosphate (MEP) pathway occurs in the chloroplast, which is the source of most volatile terpenoids (Balcke et al. 2017; Banerjee and Sharkey 2014). The flavonoid biosynthesis substrates are malonyl-CoA and ρ-coumaroyl-CoA, while biosynthesis of terpenoids via the MEP pathway utilizes glyceraldehyde-3-phosphate and pyruvate. The different substrates utilized for the flavonoid and terpenoid pathways makes metabolic feedback an unlikely source of regulation in type VI trichomes. Yet restoration of all phenotypes, including terpenoid accumulation, was achieved by expressing wild-type CHI1 from the native promoter (*pCHI*) in the *af* mutant (Kang et al. 2014).

Synthesis of mono-terpenoids in type VI trichomes originates in the plastids through the MEP pathway. The pathway culminates in the production of isopentenyl pyrophosphate (IPP) and

dimethylallyl pyrophosphate (DMAP). As an example, neryl diphosphate synthase 1 (NDPS1) combines two isoprenoid units to form neryl diphosphate (NPP), then phellandrene synthase 1 (PHS1) cyclizes NPP to form β-phellandrene. Plants also produce isoprenoid units from the mevalonic acid (MVA) pathway in the cytosol and ER. The MVA pathway is not considered the major source of substrates for volatile terpenoid production in tomato, but may be a source of sesquiterpenes (Sallaud et al. 2009; Schilmiller et al. 2009).

Many genes have highly specific expression patterns that reflect their function (Hause et al. 2000; Mohan, Vijayan, and Kolattukudy 1993; Pattison et al. 2015). Publicly available expression data, however, indicates that CHI1 (Solyc05g010320) has a broad expression pattern excluding ripe fruit (bar.utoronto.ca/eplant_tomato) (The Tomato Genome Consortium 2012). This pattern correlates well with visual accumulation of anthocyanins in most above ground tissues, and the low levels of flavonoids in fruits except naringenin chalcone in fruit skin due to a lack of chalcone-isomerase activity (España et al. 2014; Muir et al. 2001). The broad expression pattern of CHI1 makes it difficult to attribute specific phenotypes in *af* to deficiency of CHI1 expression in specific cell types, such as trichomes.

To better understand the function of CHI1 in particular cell types of tomato, I adopted an experimental approach in which general and tissue specific promoters were used to drive the expression of CHI1 in the *af* mutant background. The native CHI1 promoter was used to drive expression of CHI1 (*pCHI1*) to verify phenotypes associated with a normal CHI1 expression pattern (Kang et al. 2014). The *cauliflower mosaic virus* 35S promoter was used to induce expression of CHI1 (*p35S*) throughout much of the plant. The 35S promoter has been used extensively to promote over-expression in a number of species, especially in leaves (Sanders et al. 1987). The 35S promoter is specific to particular cell types within the tissues it is expressed

(Benfey and Chua 1990; Zhang et al. 1995). The *S. lycopersicum* type VI trichome specific methyl ketone synthase 1 (MKS1) promoter from *Solanum habrochaites* was used to drive expression of CHI1 (*pMKS*) (Akhtar et al. 2013). Transgenic lines in which CHI1 is expressed in specific tissues were used to study the pleiotropic phenotypes of the *af* mutation separately, and to better define the connection between the loss of flavonoid production and the loss of terpenoid production in type VI trichomes.

MATERIALS AND METHODS

Plant material and growth conditions

Plants were grown in a single growth chamber operated at 28° C/18° C and 16 hr / 8 hr, 250 μE light/dark. Seed for *anthocyanin free* (*af*) (LA1049) and the *pCHI1* line (line CHI4) were previously described (Kang et al. 2014). Seed from the homozygous *p35S* line (line D3) was used throughout and seed from a hemizygous (line H4) plant was used in Appendix **Figure B-1**. Seed from the *pMKS* line (line 50) was used for all experiments. Seeds were bleach sterilized for 20 minutes with 20% bleach (2.5% Sodium hypochlorite) prior to use, germinated in Jiffy 7 Peat Pellets 42 mm, and transferred to 6 cm x 6 cm x 8 cm pots with soil prior to week three.

Plasmid construction

35S::CHI1 expression vector (pBI-35S::CHI1) was previously published (Kang et al. 2014). A fragment containing the *S. habrochaites* methyl ketone synthase 1 (MKS1) promoter (see GenBank: GU987105.1) (Akhtar et al. 2013) was PCR amplified with primers 103L and 104R (Appendix, **Table B-1**) using the MKS1-GFP expression vector as a template. The 1644 bp product was digested with HindIII and XbaI. The 35S promoter in pGWB-402 was released by digestion with HindIII and XbaI, and the pMKS1 fragment was inserted in its place resulting in pGWB-40x_MKS1. A CHI1 cDNA from *S. lycopersicum* cv. Castlemart was amplified with

primers 34R and 102L (Appendix, **Table B-1**). The resulting 906 bp fragment was used in an LR reaction with pGWB-40x_MKS1, resulting in expression vector *MKS1::CHI1*. LR reactions were performed with LR Clonase^{TM} II (ThermoFischer) as described by the manufacturer.

Plant and Agrobacterium transformation

The *35S::CHI1* and *MKS1::CHI1* expression vectors were introduced into *Agrobacterium tumefaciens* strain AGL0 using the heat shock method from Weigel and Glazebrook (2002). Transformation of the *af* mutant was conducted in the Plant Biotechnology Resource and Outreach Center of Michigan State University (http://www.ptc.msu.edu/index.html). For each expression vector, cotyledons from 100-150 one-week old *af* seedlings were excised and placed into minimal growth medium. Two days later, the explants were infected with *A. tumefaciens* harboring *35S::CHI1* or *MKS1::CHI1* plasmids. Explants were transferred to agar plates containing 100 mg L^{-1} kanamycin to select for resistant plant cells containing on of the plasmids. Resulting calli were regenerated into plants and transferred to soil for seed propagation in the greenhouse.

Anthocyanin quantification

Anthocyanins were extracted from weighed leaflets with 480 μL methanol:HCl (99:1) for about eight hours with slow shaking at 4° C in the dark. The following day, 320 μL deionized water and 320 μL chloroform:isoamyl-alcohol (24:1) was added to each sample. The extracts were vortexed and centrifuged at 10,000 x *g* for 10 min at 4°C. The aqueous layer (top) containing anthocyanin pigments was used to determine the absorption at 530 nm on a Spectramax M2e plate reader (Molecular Devices) and adjusted for chlorophyll interference based on (Spitzer-Rimon et al. 2010). Absorbance readings were normalized to leaflet fresh weight.

Metabolite analysis

Extraction of trichome metabolites was conducted with 1 μL methanol with 1 μM tetradecane and 1 μg L^{-1} propyl-4-hydroxybenzoate as internal standards was used to extract each pre-measured leaflet (Kang et al. 2010a). After two minutes of extraction with gentle shaking the solvent was transferred to 1.5 mL sealed glass containers for analysis by gas chromatography-mass spectroscopy (GC-MS) and liquid chromatography-mass spectroscopy (LC-MS).

Mass spectrometry

Volatile terpenoids were quantified by injecting one μL into a GC 6890N/5975B quadrupole (Agilent) by a CombiPAL (CTC Analytics). The column used is a 40m VF5MS, 30 m with 10 m EZGuard, 0.25 μm film and 0.25 mm inner diameter (Agilent). Operating conditions were as follows: 280° C inlet temperature, 88.35 psi inlet pressure, 1:10 split ratio, and 45-350 mass scan starting at 3.5 min. Ramp temperatures used initial 40° C for one min, 90° C at 40° C min^{-1}, 110° C at 15° C min^{-1}, 250° C at 25° C min^{-1}, 320° C at 40° C min^{-1}, and finally held at 320° C for 2 minutes. Total run time was 12.93 minutes.

Flavonoids were analyzed by injecting one μL of the samples were injected into an Acquity Binary Solvent Manager and Column Manager (Waters) by a 2777C Sample manager (Waters). A Xevo G2-XS QTof (Waters) mass spectrometer was operated under the following conditions: capillary voltage, 2 kV; sample cone, 40 V; source temperature, 100° C; desolvation temperature, 350° C; desolvation flow rate, 600 L hr^{-1}; electrospray ionization in negative sensing mode. MS^e was used with several functions which split each sampling timepoint: 1. No collision energy (to gather whole molecule masses); 2. Ramp of 20-60 V collision energy (to analyze sample molecule fragmentation patterns); and 3. Ion lock spray (for calibration of exact mass). A 10 cm x 2.1 mm, 2.7 μm Ascentis® Express C-18 HPLC column (supelco) held at 40° C was used for all

separations. De-ionized water containing 0.1% formic acid was used for solvent A, and methanol was used for solvent B. Using a continuous flow rate of 0.3 mL min^{-1}, the gradient profile was started at 5% solvent B and ramped to 60% solvent B over 3 minutes using curve 6 setting on the Waters solvent manager and then ramped to 100% solvent B over 4 min using curve 6, held at 100% solvent B until the 5.5 min point, dropped to 5% solvent B at 5.51 minutes, then held at 5% solvent B until 6.5 minutes.

Isolation of glandular trichomes

Type VI glandular trichomes were picked by hand using a pulled glass Pasteur pipet (Kang et al. 2014), or washed from leaflets (McDowell et al. 2011). For chemical analysis of picked trichomes, 200 trichomes were placed into 100 μL 100% methanol and the resulting samples were analyzed by either GCMS or LCMS. Approximately 50 mg washed trichomes were used for protein extraction.

Western blot analysis

Protein was extracted from leaf tissue (50 mg) or isolated trichomes as previously described (Schilmiller et al. 2010). Protein concentration was quantified by Bradford assay using Bio-Rad reagents and manufacturer's protocol. Western blot analysis of CHI1 protein levels was performed as previously described (Kang et al. 2014) using 13 μg of total protein for SDS-PAGE.

Spider mite feeding assays

Tetranychus urticae (two-spotted spider mites) were used in both choice and no-choice assays. Spider mites were obtained from tomato and alfalfa plants growing in the greenhouse and reared on *af* leaflets at room temperature for longer than 10 days prior to use in the assays. The choice assay used a toothpick bridge and a 10-minute time course in which five adult females were placed in the center of a toothpick that was balanced between two leaflets of either the same host

genotype or two different genotypes. The number of spider mites on each leaflet was scored after 10 minutes. Several replicates were conducted with different leaflets from different plants and with different sets of spider mites. The mites typically settled on a leaflet within the 10-minute time frame of the assay, and mites were rarely observed to move once a leaf was reached. For the no-choice assay, mites were placed onto leaflets (three leaflets per genotype per plate) incubated on a petri plate containing a moist filter paper. Each genotype was tested multiple times in independent plates. Each leaflet was challenged with three adult female spider mites. Leaf damage caused by mite feeding was assessed as previously described (Santamaria et al. 2012). Leaf images were obtained with a photocopier after 7 days for feeding, and area determined using Inkscape (inkscape.org).

RESULTS

CHI1 protein expression localization

To better understand the function of chalcone isomerase in respect to type VI trichomes of tomato (**Figure 3-1A**), we used three different promoters to express the *CHI1* cDNA in the *af* mutant, which lacks CHI1 protein in all tissues (Kang et al. 2014). We reasoned that each promoter, namely the native *CHI1* promoter, the *CaMV* 35S promoter, and the type VI-specific *MKS* promoter, would generate distinct CHI1 expression domains in the resulting *CHI1::CHI1* (*pCHI*), *35S::CHI1* (*p35S*), and *MKS::CHI1* (*pMKS*) transgenic lines respectively. To test this, we used Immunoblot analysis to determine the level of CHI1 protein in whole leaves, purified trichomes, and leaves in which trichomes were removed by shaving from each of the three tissue-specific transgenic lines, as well as the *af* mutant (null control). In *pCHI* plants, which are evaluated as the phenotypic equivalent to the WT control, accumulated CHI1 in total leaves, trichomes, and shaved leaves lacking trichomes (**Figure 3-1B**). In *pMKS* plants, CHI1 was detected in trichomes but not

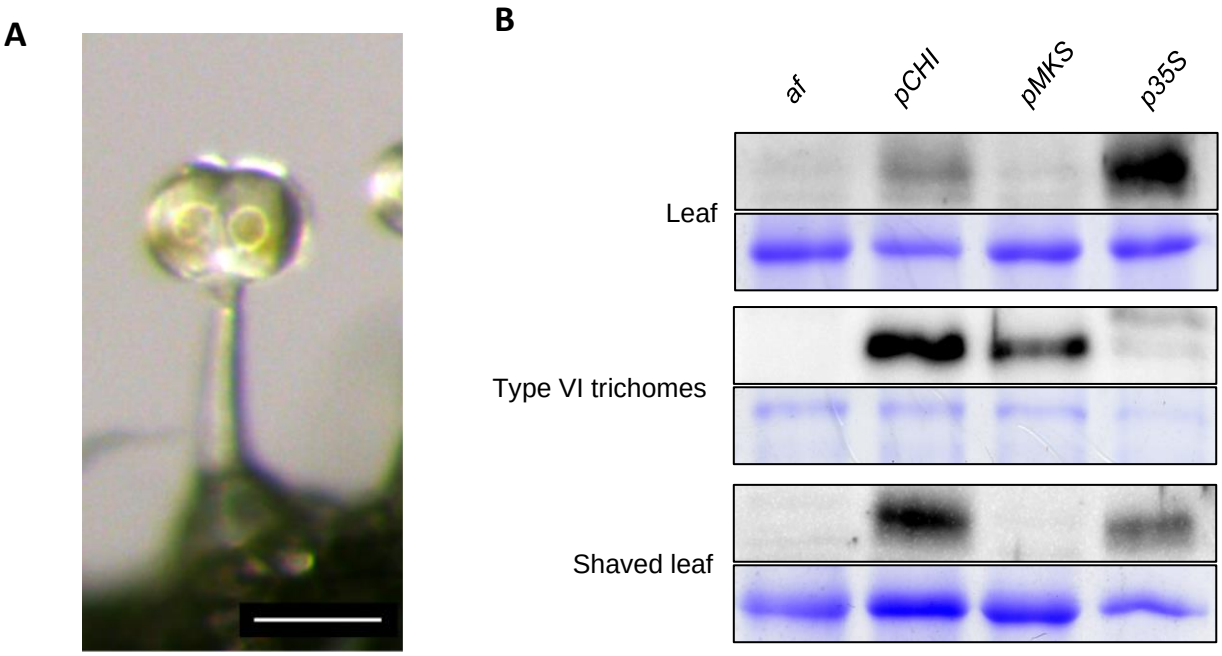

Figure 3-1: CHI1 protein levels in leaves and trichomes of tomato genotypes used in this study. (A) Light micrograph of a tomato leaf type VI trichome. Scale bar = 50 μm. (B) Western blot analysis of CHI1 protein levels in various leaf tissues from *af* mutant and transgenic lines expressing CHI1 from the *CHI1*, *MKS1* and *CaMV 35S* promoters. For each genotype, total protein was isolated from whole leaves (upper panel), purified type VI trichomes (middle panel), or leaves in which trichomes were physically removed by shaving (lower panel). Coomassie blue staining shows rubisco large subunit as loading control.

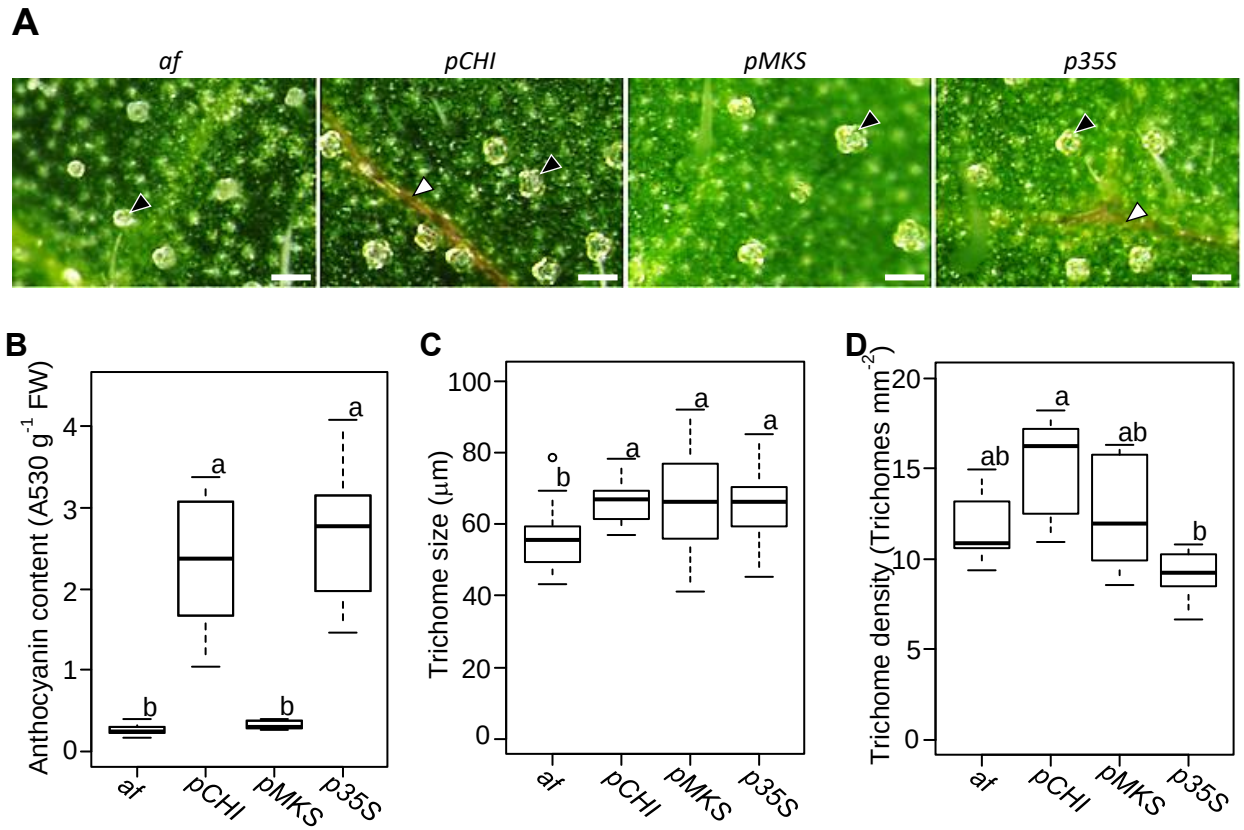

Figure 3-2: Tissue-specific expression of CHI1 modulates anthocyanin accumulation and trichome morphology. (A) Light micrographs of the leaf surface of the indicated genotypes. Type VI GTs (black arrows) and anthocyanin accumulation (white arrows) in minor veins. Scale bar = 100 µm. (B) Leaf anthocyanin levels in indicated genotypes. Boxplots show the median (thick center line), values in the 25th through 75th percentile (box height), and whiskers extending 1.5 times the interquartile range beyond the given quartile. Dots outside of the box and whiskers denote outlier data points. n = 10 samples per genotype. Each sample was from a single plant. (C) Width of the four-celled glandular head of type VI trichomes in the indicated genotypes. n ≥ 50 trichomes per genotype. (D) Density of type VI trichomes in the indicated genotypes. n = 5 plants per genotype. Different letters within each analysis indicate significant differences based on the results of an ANOVA and Tukey HSD test, $p < 0.05$.

in total leaf or shaved leaf samples. *p35S* plants accumulated CHI1 in both the total and shaved leaf samples, with very low levels of protein detected in isolated trichomes. These findings indicate that *p35S* and *pMKS* plants express CHI1 primarily in foliar (i.e. non-trichome) and trichome cells, respectively, and demonstrate the feasibility of using different gene promoters to manipulate the tissue-specific expression of CHI1 in tomato leaves.

Tissue-specific expression of CHI1 modulates leaf anthocyanin levels

Cultivated tomato plants grown under normal conditions accumulate anthocyanins which can be visualized in the major veins and the abaxial surface of leaves (Von Wettstein-Knowles 1968). The *af* mutant fails to accumulate anthocyanins in all parts of the leaf (Rick et al. 1976). This deficiency is completely restored in *pCHI1* plants, which expresses CHI1 from the native CHI1 promoter (Kang et al. 2014) (**Figure 3-2**). Leaf anthocyanin levels were also fully restored in *p35S* plants, whereas *pMKS* plants displayed an anthocyanin-deficient phenotype similar to that of the *af* mutant (**Figure 3-2A B**). These findings are consistent with the CHI1 protein expression pattern in these lines, and further validate the utility of this approach for producing flavonoids in a tissue-specific manner.

Effects of tissue-specific CHI1 expression on type VI trichome size and density

The size of the four-celled glandular head of type VI trichomes in the *af* mutant was slightly but significantly smaller than that of trichomes produced by the *pCHI* complemented line (**Figure 3-2C**), consistent with previous reports (Kang et al. 2014). A similar increase in trichome size was observed in the p35S and pMKS lines (Figure 3-2C). Measurements of the type VI trichome density on the adaxial leaf surface in each genotype showed no consistent differences between the lines (**Figure 3-2D**).

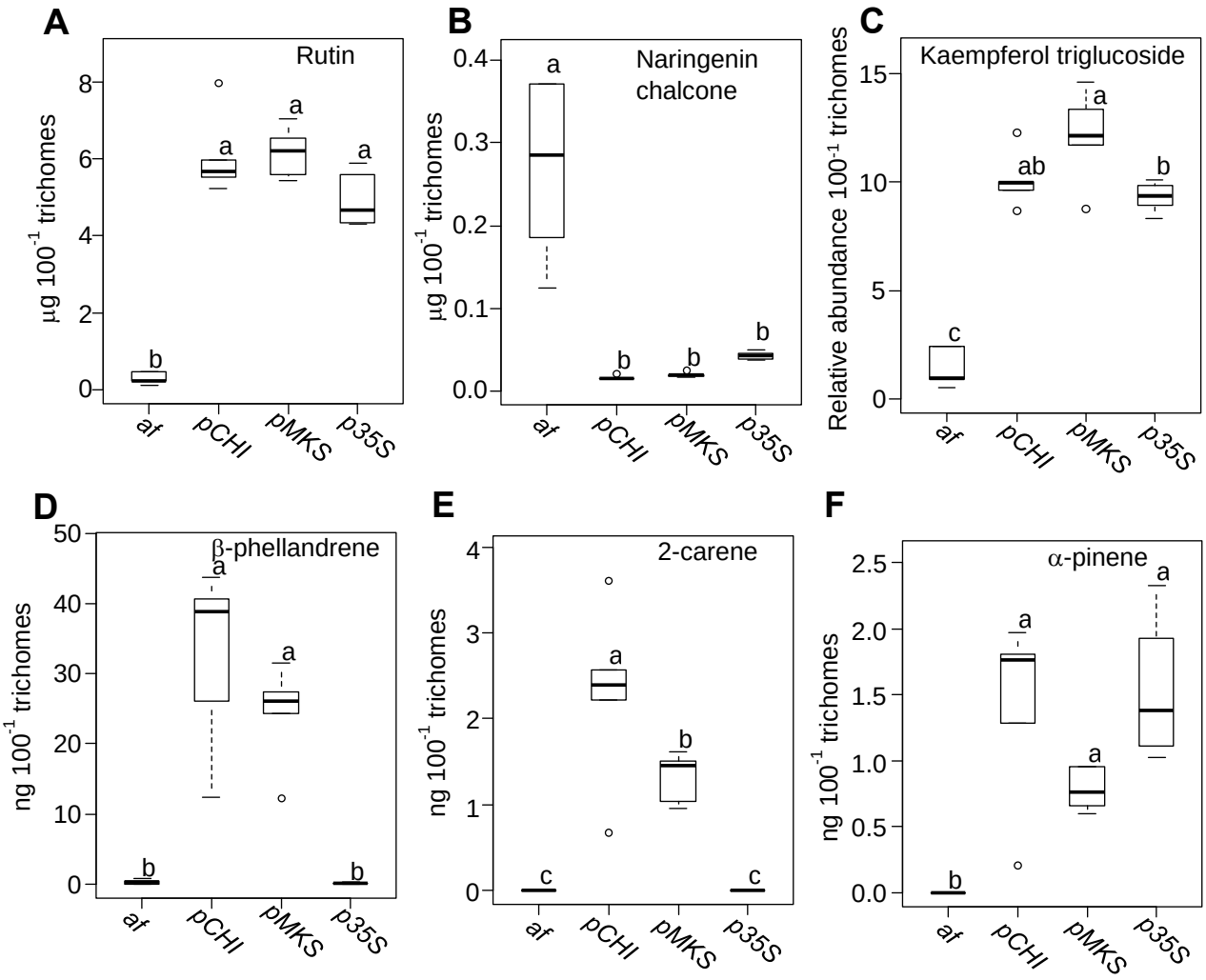

Figure 3-3: Flavonoid and terpenoid levels in type VI trichomes of CHI1-complemented lines. Various flavonoids (A-C) and terpenoids (D-F) were measured from type VI glands isolated (hand-picked) from the indicated genotypes. Different letters within each analysis indicate significant differences based on the results of an ANOVA and Tukey HSD test, $p < 0.05$. Boxplots show the median (thick center line), values in the 25th through 75th percentile (box height), and whiskers extending 1.5 times the interquartile range beyond the given quartile. Dots outside of the box and whiskers denote outlier data points. n = at least 5 plants per genotype.

Trichome metabolite abundance in CHI1-complemented lines

We performed targeted metabolite analysis to determine how the restriction of CHI1 expression to specific leaf tissues affects flavonoid and terpenoid production in the type VI trichomes. For these studies, the glandular head of type VI trichomes was isolated using a fine glass needle (Kang et al. 2010a) to minimize potential contamination by other cell types of the leaf. As previously observed (Kang et al. 2014), type VI trichomes from *af* plants accumulated relatively high levels of naringenin chalcone (the substrate for CHI1) but had very low levels of both rutin, the major flavonoid product of CHI1 in this trichome, and terpenoids (**Figure 3-3**). Expression of CHI1 from the *MKS* promoter in *pMKS* plants largely restored the flavonoid and terpenoid content to that observed in *pCHI* plants. In the *p35S* plants flavonoids are recovered as evidenced by levels of rutin and other prevalent flavonoids (**Figure 3-3,** Appendix, **Figure B-1**). The *p35S* line did not recover the major terpenoids like β-phellandrene and 2-carene (**Figure 3-3D, E**), however, some of the low abundance monoterpenes such as α-pinene were found at levels comparable to those found in the pCHI line (**Figure 3-3F**).

Restricted expression of CHI1 to type VI trichomes confers resistance to the two-spotted spider mite

During the growth of *af* and *pCHI* plants in the greenhouse, we consistently observed that leaves of *af* plants were infested with two-spotted spider mites (*Tetranychus urticae*), whereas leaves of neighboring *pCHI* plants were not (Sugimoto and Howe, unpublished results). This observation suggested that CHI1 is an important factor in tomato leaf resistance to two-spotted spider mites, and also raised the possibility that resistance results from CHI1 expression in a specific tissue type. To test this hypothesis, we performed no-choice feeding assays in which detached *af*, *pCHI*, *pMKS*, *p35S* leaves were infested with spider mites and leaf damage was

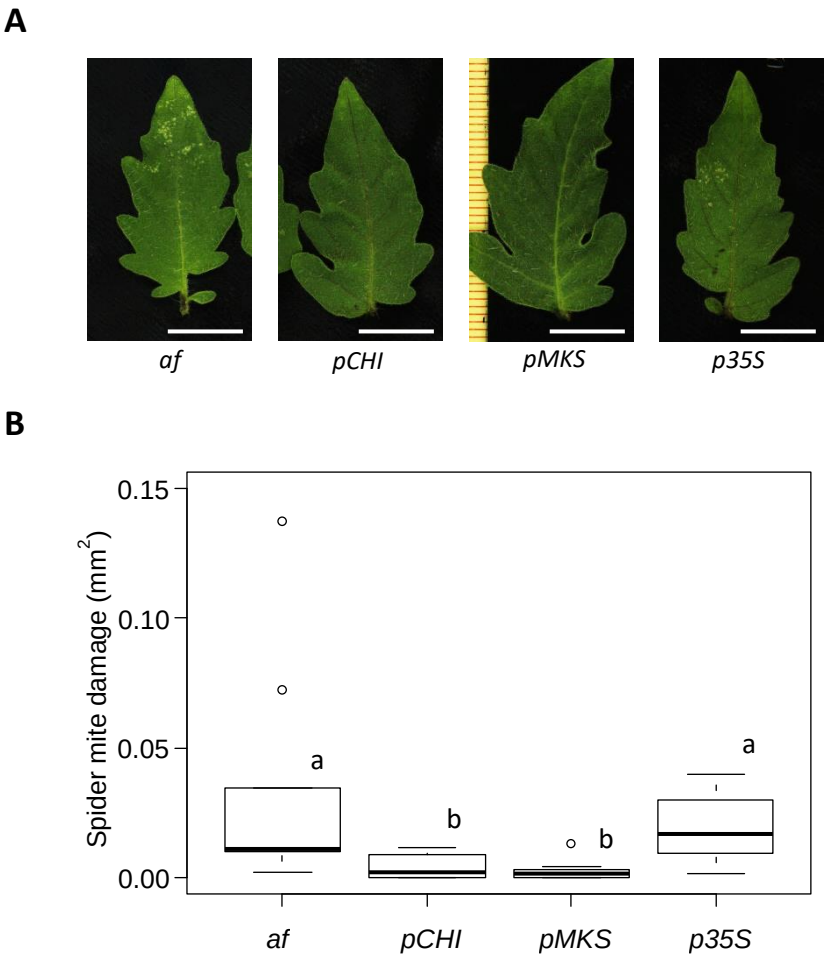

Figure 3-4: Trichome-specific expression of CHI1 confers resistance to the two-spotted spider mite (*Tetranychus urticae*). Three adult female spider mites were placed on the adaxial surface of detached leaflets of the indicated genotype. Following 7 days of infestation, leaf damage was assessed by quantifying the amount of leaf surface area devoid of chlorophyll. (A) Photograph of representative leaves showing feeding damage at the end of the feeding trial. Scale bars correspond to 1 cm. (B) Quantification of leaf area damaged by feeding. Lower case letters indicate significant differences based on Kruskal-Wallis followed by Nemenyi test ($p < 0.05$). n = 10 leaflets per genotype. Boxplots show the median (thick center line), values in the 25th through 75th percentile (box height), and whiskers extending 1.5 times the interquartile range beyond the given quartile. Dots outside of the box and whiskers denote outlier data points.

assessed seven days after challenge. Spider mites caused significant damage to *af* leaves but did little or no damage to *pCHI* leaves during the feeding assay (Figure 3-4), consistent with the preliminary observations in the green house. Interestingly, the level of damage inflicted to infested *pMKS* leaves was similar to *pCHI* leaves, whereas the amount of damage to *p35S* leaves was similar to the *af* control (**Figure 3-4**). Close monitoring of spider mite behavior further showed that mites were either immobilized on *pCHI* or *pMKS* leaves or had moved off the leaf completely during the feeding trial. In contrast, spider mites placed onto *af* and *p35S* leaves often laid eggs and contained newly hatched juvenile mites (**Figure 3-4A**). These findings establish an important role for CHI1 in resistance of tomato to the two-spotted spider mite, and further demonstrate that expression of CHI1 in type VI trichomes is sufficient for resistance.

DISCUSSION

Separation of pleiotropic phenotypes by cell-type-specific expression allows proper attribution of mutant phenotypes to deficiencies in specific cell types and testing the hypothesis that there is a transmittable signal responsible for a phenotype. This approach has previously been used to address the question of whether genes act in a cell autonomous or non-autonomous manner. Differential development of chloroplasts in C4 plants exhibiting Kranz anatomy was demonstrated through cell-type specific expression of the *Golden2-like* gene (Waters et al. 2008). Complementation of Arabidopsis *bri1* mutants with cell-type specific promoters showed significant morphological differences due to recovery of brassinosteroid sensitivity in specific cell types (Hategan et al. 2014). In the case of jasmonate signaling for male fertility, this approach was used to show that COI1 activity in the epidermis is necessary for jasmonate sensing and proper development of the stamen and pollen (Jewell and Browse 2016). Likewise, cell type specific production of bilin chromophores was used to show that mesophyll cells play a critical role in

certain responses to high light (Oh and Montgomery 2019). Flavonoids have been implicated as signals for a variety of processes, including pollen development, pollen germination, bending of roots during development, and development of root hairs and lateral roots (Brown et al. 2001; Maloney et al. 2014; Mo et al. 1992). A potential role for flavonoids as a signal in trichome development and metabolism has been proposed but remains to be demonstrated (Kang et al. 2014).

In this study, we dissected the various pleiotropic phenotypes of the *af* mutant by expressing the wildtype *CHI1* gene from tissue-specific promoters in the *af* background. As previously reported by Kang et al. (2014), *af* contains no detectable CHI1 protein in leaves and no detectable anthocyanins, indicating that this single member of the tomato CHI gene family plays a major, if not sole, role in anthocyanin production. The *af* mutant thus provides a genetic background in which to restore CHI1 activity in any tissue or cell type for which a suitable promoter is available. As proof of concept, we compared *af* and *pCHI1* plants to transgenic lines that express CHI1 from either the 35S or trichome-specific MKS promoter. Anthocyanin recovery in leaves by both the *pCHI1* and *p35S* lines, but not the *pMKS* line, lends support to the idea that CHI1 is expressed in the leaf lamina of the *pCHI* and *p35S* lines but not in the *pMKS* lines.

CHI1 protein was readily detectable in type VI trichomes of the *pMKS* but not the *p35S* lines. In the *p35S* lines, CHI1 accumulated to high levels in the leaf lamina, consistent with the general pattern of 35S expression. Unexpectedly, however, rutin (the major type VI trichome flavonoid) production was restored in *p35S* whereas β-phellandrene (the major terpenoid) was not. The most straightforward interpretation of this finding is that the level of CHI1 in trichomes of *p35S* plants is sufficient to support the biosynthesis of rutin from naringenin but is not sufficient to support terpenoid biosynthesis. In *p35S* lines, there was some accumulation of minor terpenoids

such as α-pinene and limonene, but no recovery of the major terpenoids including β-phellandrene and 2-carene. Although we detected low levels of CHI1 protein in type VI GTs in the *p35S* line, the plants are likely able to recover flavonoid levels due to the high activity of the CHI protein (Jez and Noel 2002). Species within the mint family also accumulate both flavonoids and volatile terpenoids in glandular trichomes, although the levels of flavonoids in this case is much lower than that seen in tomato (Lange et al. 2000; Voirin et al. 1993). In the closely related *Solanum habrochaites*, high-level production of terpenoids does not strictly depend on the production of large quantities of flavonoids (Balcke et al. 2017). These examples indicate that the production of volatile terpenoids in tomato trichomes may also not depend on the production of large quantities of flavonoids. One potential explanation for the unequal restoration of terpene synthesis in the *p35S* line trichomes is that the activity of a subset of terpene synthases is sensitive to metabolic changes resulting from the loss of CHI1 in *af* trichomes. Additional studies are needed to clarify the connection between CHI1 and terpenoid biosynthesis in glandular trichomes of tomato and other plants. With the abundance of flavonoid biosynthesis mutants and the identification of damage-induced volatile terpenoids (Kroes et al. 2017), Arabidopsis could potentially provide an experimental system in which to investigate the metabolic linkage between flavonoids and terpenoids.

Several factors may contribute to the low expression by the 35S promoter in type VI trichomes. One possibility is that glandular cells of the type VI trichome lack the activity of factors that initiate transcription from the 35S promoter. In support of this hypothesis, previous studies have shown that the 35S promoter is expressed in stalk cells of tobacco floral trichomes but not in the glandular secreting cells (Benfey and Chua 1990). Members of the bZIP TGA-like transcription factor family have been implicated as positive regulators of the 35S promoter (Benfey

and Chua 1990), but whether these factors are active in type VI trichomes remains to be determined. It is also possible that gland cells of the trichome express transcription factors that negatively regulate the 35S promoter in the glandular cells (Lee and Seo 2018). Analysis of epigenetic marks in type VI trichomes could help clarify regulatory processes governing transcriptional control in the type VI trichomes.

Metabolic flux through the phenylpropanoid pathway impacts the production of multiple classes of compounds, amino acids, quinones, flavonoids, anthocyanins, and lignin subunits (Soubeyrand et al. 2018; Suzuki et al. 2005; Wang and Maeda 2018). In addition to specific transcription factors that bind to the promoter regions of genes encoding phenylpropanoid biosynthetic enzymes, recent studies have shown that the transcription co-activator complex, Mediator, also plays an important role in controlling metabolic flux through the phenylpropanoid pathway (Dolan et al. 2017). In general, the multi-subunit Mediator complex is thought to integrate external signals such as light, temperature, and biotic stress with transcription factors that coordinate the balance between primary and specialized metabolism (Çevik et al. 2012; Kazan 2017). Given the likely role of the Mediator complex in controlling metabolic processes in specific cell-types (Kagey et al. 2010), it will be interesting to determine the extent to which Mediator controls specialized metabolism in glandular trichomes.

Crop damage caused by the two-spotted spider mite is a significant problem in greenhouses and other high intensity crop-production systems. Spider mite infestation of cotton and strawberry, for example, resulted in 84% and 40% losses, respectively (Walsh et al. 2002; Wilson et al. 1991). Greenhouse grown tomato is also susceptible to spider mites and can result in yield losses of up to 50% (Stacey et al. 1985). Several defense-related compounds have been implicated in tomato resistance to spider mites, including proteinase inhibitors, acylsugars, and sesquiterpenes (Bleeker

et al. 2012; Leckie et al. 2016; Santamaria et al. 2012). Considerable genetic evidence has further established an important role for jasmonate in promoting tomato resistance to this pest (Li et al. 2002, 2004). However, because jasmonate promotes the expression of a wide range of chemical (e.g., proteinase inhibitors) and physical (e.g., trichomes) defense traits, it remains to be determined which specific jasmonate-mediated defense traits are most effective for resistance to spider mites. Observations by a previous lab member (Koichi Sugimoto) that the *af* mutant is compromised in resistance to two-spotted spider mites provides new insight into this question. Previous work showed that the *af* mutation does not impair the production of several tomato defensive compounds, including the glycoalkaloid tomatine, acylsugars, and proteinase inhibitors (Kang et al. 2014). The low level of spider mite feeding on *pCHI* and *pMKS* lines (relative to the af mutant) correlated with high levels of trichome-borne β-phellandrene and other volatile terpenoids. By contrast, *p35S* lines that produced low levels of β-phellandrene remained susceptible to spider mite feeding. These data suggest that CHI1-mediated production of terpenoids in type VI trichomes contributes to the resistance of tomato to the two-spotted spider mite.

In summary, data presented in the Chapter show that CHI1 expression in glandular trichomes comprises one component of a multi-layered defense system employed by cultivated tomato for defense against arthropod herbivores. In addition to its canonical role in flavonoid biosynthesis, CHI1 appears to exert broad effects on trichomes development and metabolism, which is consistent with the proposed function of flavonoids in other aspects of plant growth and development (Brown et al. 2001; Maloney et al. 2014; Muir et al. 2001). The use of tissue- and cell-type-specific promoters as described here offers an attractive approach to further dissect the complex roles of flavonoids in the plant life cycle.

APPENDIX

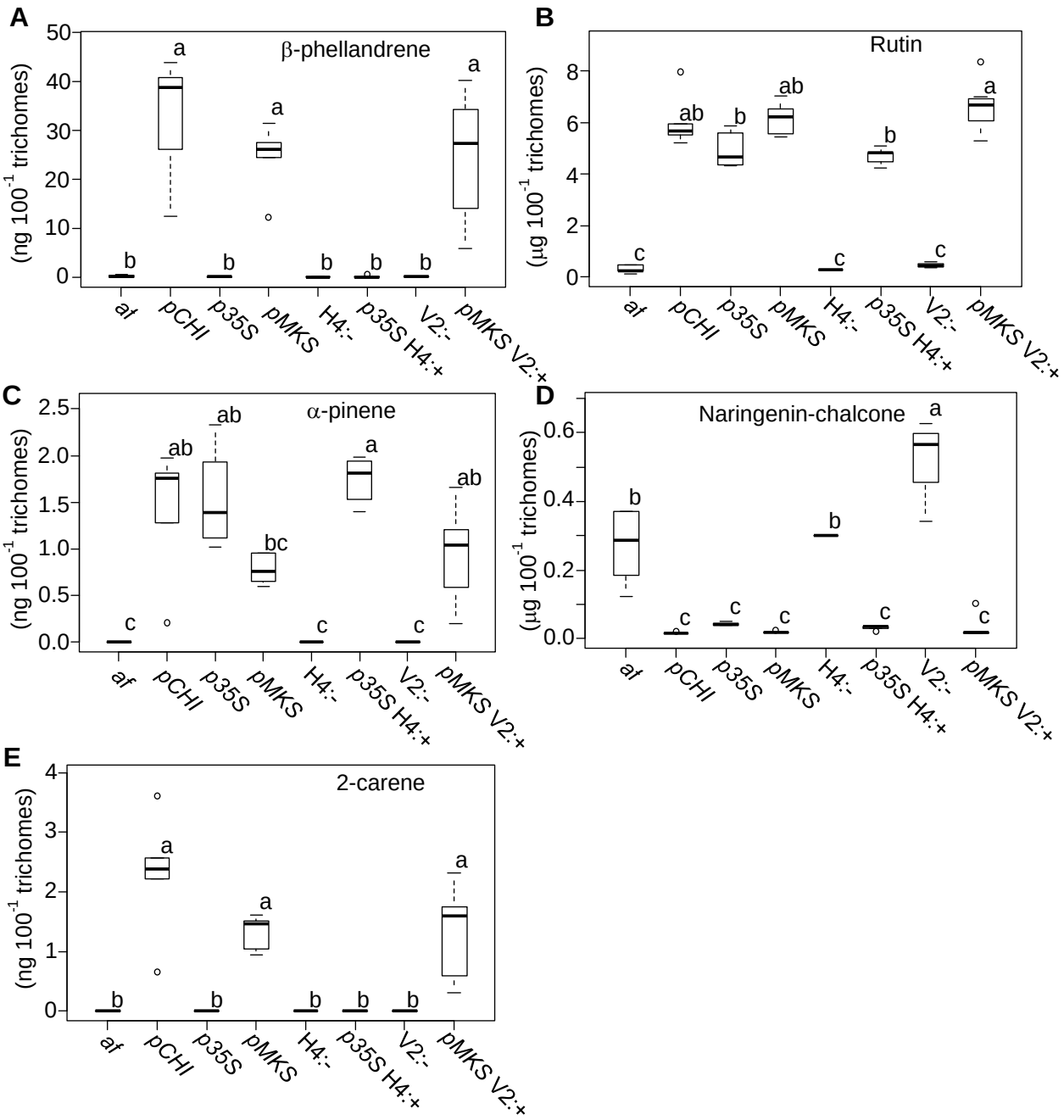

Figure B-1: Additional data of terpenoid and flavonoid levels in trichomes of CHI1-complemented tomato lines. Various flavonoids (B, D) and terpenoids (A,C,E) were measured type VI glands isolated (hand-picked) from the indicated four genotypes. Lines H4 and V2 are hemizygous and the progeny are segregating for the *35S::CHI1* and *MKS::CHI1* transgene, respectively. "+" and "-" denote segregating progeny either containing or lacking the transgene, respectively, as determined by PCR. *pCHI* corresponds to *CHI1:CHI1* line CHI4 (Kang et al. 2014), *p35S* corresponds to *35S::CHI1* line D3, and *pMKS* corresponds to *MKS::CHI1* line 50. Boxplots, Thick center line is the median, box covers the 25th through 75th percentile, whiskers extend 1.5 times the interquartile range beyond the given quartile, dots outside of the box and whiskers are outliers.

Primer name	Sequence 5'→3'	Solyc ID	Target gene
103L	cagaaagcttCCGGTGAAGATTGTCGTTC	NA	pMKS1
104R	agtggtctagaTTTTGAACAACTACCACAAAG	NA	pMKS1
34R	ggggaccactttgtacaagaaagctgggtcctaGTGGGACCTTATTGCACACT	Solyc05g010320	CHI1
102L	ggggacaagtttgtacaaaaaagcaggcttcACTAATAGATCTTAAATGG	Solyc05g010320	CHI1

Table B-1: PCR primers used in this study. Sequence in capital letters is complementary to the target. Lower case sequence is the adapter. Solyc is the reference *Solanum lycopersicum* locus from solgenomics.net for the indicated target gene.

REFERENCES

REFERENCES

Abe, T., Thitamadee, S., and Hashimoto, T. 2004. “Microtubule defects and cell morphogenesis in the Lefty1Lefty2 hibulin mutant of *Arabidopsis thaliana*.” *Plant and Cell Physiology* 45:211–20.

Agati, G., Azzarello, E., Pollastri, S., and Tattini, M. 2012. “Flavonoids as antioxidants in plants: location and functional significance.” *Plant Science* 196:67–76.

Agrawal, A.A. 1999. “Induced responses to herbivory in wild radish: effects on several herbivores and plant fitness.” *Ecology* 80:1713–23.

Agren, J., and Schemske, D.W. 1993. “The cost of defense against herbivores : an experimental study of trichome production in *Brassica rapa*.” *The American Naturalist* 141:338–50.

Aharoni, A., Dixit, S., Jetter, R., Thoenes, E., van Arkel, G., and Pereira, A. 2004. “The SHINE clade of AP2 domain transcription factors activates wax biosynthesis, alters cuticle properties, and confers drought tolerance when overexpressed in Arabidopsis.” *The Plant Cell* 16:2463–80.

Akhtar, T.A., Matsuba, Y., Schauvinhold, I., Yu, G., Lees, H.A., Klein, S.E., and Pichersky, E. 2013. “The tomato cis-prenyltransferase gene family.” *Plant Journal* 73:640–52.

Alonso-Peral, M.M., Li, J., Li, Y., Allen, R.S., Schnippenkoetter, W., Ohms, S., White, R.G., and Millar, A.A. 2010. “The microRNA159-regulated GaMYB-like genes inhibit growth and promote programmed cell death in Arabidopsis.” *Plant Physiology* 154:757–71.

Balcke, G.U., Bennewitz, S., Bergau, N., Athmer, B., Henning, A., Majovsky, P., Jiménez-Gómez, J.M., Hoehenwarter, W., and Tissier, A. 2017. “Multi-omics of tomato glandular trichomes reveals distinct features of central carbon metabolism supporting high productivity of specialized metabolites.” *The Plant Cell* 29:960–83.

Banerjee, A., and Sharkey, T.D. 2014. “Methylerythritol 4-phosphate (MEP) pathway metabolic regulation.” *Natural Product Reports* 31:1043–55.

Barthlott, W., Wiersch, S., Čolić, Z., and Koch, K. 2009. “Classification of trichome types within species of the water fern *Salvinia*, and ontogeny of the eggbeater trichomes.” *Botany* 87:830–36.

Benfey, P.N., and Chua, N. 1990. “The cauliflower mosaic virus 35S promoter : combinatorial regulation of transcription in plants.” *Science* 250:959–66.

Bergau, N., Bennewitz, S., Syrowatka, F., Hause, G., and Tissier, A. 2015. “The development of type VI glandular trichomes in the cultivated tomato *Solanum lycopersicum* and a related wild species *S. habrochaites*.” *BMC Plant Biology* 15:1–15.

Berkey, R., Bendigeri, D., and Xiao, S. 2012. “Sphingolipids and plant defense/disease: the

'death' connection and beyond." *Frontiers in Plant Science* 3:68.

Bleeker, P.M., Mirabella, R., Diergaarde, P.J., VanDoorn, A., Tissier, A., Kant, M.R., Prins, M., De Vos, M., Haring, M.A., and Schuurink, R.C. 2012. "Improved herbivore resistance in cultivated tomato with the sesquiterpene biosynthetic pathway from a wild relative." *Proceedings of the National Academy of Sciences of the United States of America* 109:20124–29.

Boughton, A.J., Hoover, K., and Felton, G.W. 2005. "Methyl jasmonate application induces increased densities of glandular trichomes on tomato, *Lycopersicon esculentum*." *Journal of Chemical Ecology* 31:2211–16.

Bown, L., Kusaba, S., Goubet, F., Codrai, L., Dale, A.G., Zhang, Z., Yu, X., Morris, K., Ishii, T., Evered, C., Dupree, P., and Jackson, S. 2017. "The ectopically parting cells 1-2 (Epc1-2) mutant exhibits an exaggerated response to abscisic acid." *Journal of Experimental Botany* 58:1813–23.

Brembu, T., Winge, P., Seem, M., and Bones, A.M. 2004. "NAPP and PIRP encode subunits of a putative WAVE regulatory protein complex involved in plant cell morphogenesis." *Plant Cell* 16:2335–49.

Breuer, C., Kawamura, A., Ichikawa, T., Tominaga-Wada, R., Wada, T., Kondou, Y., Muto, S., Matsui, M., and Sugimoto, K. 2009. " The trihelix transcription factor GTL1 regulates ploidy-dependent cell growth in the Arabidopsis trichome ." *The Plant Cell* 21:2307–22.

Brown, D.E., Rashotte, A.M., Murphy, A.S., Normanly, J., Tague, B.W., Peer, W.A., Taiz, L., Muday, G.K. 2001. "Flavonoids act as negative regulators of auxin transport in vivo in Arabidopsis." *Plant Physiology* 126:524–35.

Buede, R., Rinker-Schaffer, C., Pinto, W.J., Lester, R.L., and Dickson, R.C. 1991. "Cloning and characterization of LCB1, a Saccharomyces gene required for biosynthesis of the long-chain base component of sphingolipids." *Journal of Bacteriology* 173:4325–32.

Çevik, V., Kidd, B.N., Zhang, P., Hill, C., Kiddle, S., Denby, K.J., Holub, E.B., Cahill, D.M., Manners, J.M., Schenk, P.M., Beynon, J., and Kazan, K. 2012. "MEDIATOR25 acts as an integrative hub for the regulation of jasmonate-responsive gene expression in Arabidopsis." *Plant Physiology* 160:541–55.

Chang, J., Yu, T., Yang, Q., Li, C., Xiong, C., Gao, S., Xie, Q., Zheng, F., Li, H., Tian, Z., Yang, C., and Ye, Z. 2018. "Hair, encoding a single C2H2 zinc-finger protein, regulates multicellular trichome formation in tomato." *Plant Journal* 96:90–102.

Chen, G., Klinkhamer, P.G.L., Escobar-Bravo, R., and Leiss, K.A. 2018. "Type VI glandular trichome density and their derived volatiles are differently induced by jasmonic acid in developing and fully developed tomato leaves: implications for thrips resistance." *Plant Science* 276:87–98.

Chen, M., Han, G., Dietrich, C.R., Dunn, T.M., and Cahoon, E.B. 2006. "The essential nature of

sphingolipids in plants as revealed by the functional identification and characterization of the Arabidopsis LCB1 subunit of serine palmitoyltransferase." *The Plant Cell Online* 18:3576–93.

Cheng, J., Park, T.S., Fischl, A.S., and Ye, X.S. 2001. "Cell cycle progression and cell polarity require sphingolipid biosynthesis in *Aspergillus nidulans*." *Molecular and Cellular Biology* 21:6198–6209.

Chini, A., Fonseca, S., Fernández, G., Adie, B., Chico, J.M., Lorenzo, O., García-Casado, G., López-Vidriero, I., Lozano, F.M., Ponce, M.R., Micol, J.L., and Solano, R. 2007. "The JAZ family of repressors is the missing link in jasmonate signalling." *Nature* 448:666–71.

Crosara, K.T.B., Moffa, E.B., Xiao, Y., and Siqueira, W.L. 2018. "Merging in-silico and in vitro salivary protein complex partners using the STRING database: a tutorial." *Journal of Proteomics* 171:87–94.

Dassanayake, M. 2017. "Corrigendum: making plants break a sweat: the structure, function, and evolution of plant salt glands." *Frontiers in Plant Science* 8:1–20.

Dayanandan, P., and Kaufman, P.B. 1976. "Trichomes of *Cannabis sativa* L. (Cannabaceae)." *American Journal of Botany* 63:578.

Dell, B., and McComb, A.J. 1977. "Glandular hair formation and resin secretion in *Eremophila fraseri* F. Meull (Myoporaceae)." *Protoplasma* 92:71–86.

Dicke, M., Gols, R., Ludeking, D., and Posthumus, M.A. 1999. "Jasmonic acid and herbivory differentially induce carnivore-attracting plant volatiles in lima bean plants." *Journal of Chemical Ecology* 25:1907–22.

Disch, A., Hemmerlin, A., Bach, T.J., and Rohmer, M.. 1998. "Mevalonate-derived isopentenyl diphosphate is the biosynthetic precursor of ubiquinone prenyl side chain in tobacco BY-2 cells." *Biochemical Journal* 331:615–21.

Dolan, W.L., Dilkes, B.P., Stout, J.M., Bonawitz, N.D., and Chapple, C. 2017. "Mediator complex subunits MED2, MED5, MED16, and MED23 genetically interact in the regulation of phenylpropanoid biosynthesis." *Plant Cell* 29:3269–85.

Du, M., Zhao, J., Tzeng, D.T.W., Liu, Y., Deng, L., Yang, T., Zhai, Q., Wu, F., Huang, Z., Zhou, M., Wang, Q., Chen, Q., Zhong, S., Li, C.B., and Li, C. 2017. "MYC2 orchestrates a hierarchical transcriptional cascade that regulates jasmonate-mediated plant immunity in tomato." *Plant Cell* 29:1883–1906.

Du, W., Han, X., Wang, Y., and Qin, Y. 2016. "A primary screening and applying of plant volatiles as repellents to control whitefly *Bemisia tabaci* (Gennadius) on tomato." *Scientific Reports* 6:22140.

Duke, S.O., and Paul, R.N. 2016. "Development and fine structure of the glandular trichomes of *Artemisia annua L*." *International Journal of Plant Sciences* 154:107–18.

El-Assal, S.E.D., Le, J., Basu, D., Mallery, E.L., and Szymanski, D.B. 2004. “Distorted2 encodes an ARPC2 subunit of the putative Arabidopsis ARP2/3 complex.” *Plant Journal* 38:526–38.

Escobar-Bravo, R., Chen, G., Grosser, K., Van Dam, N.M., Leiss, K.A., and Klinkhamer, P.G.L. 2019a. “Ultraviolet radiation enhances salicylic acid-mediated defense signaling and resistance to pseudomonas syringae DC3000 in a jasmonic acid-deficient tomato mutant.” *Plant Signaling & Behavior* 14:e1581560.

Escobar-Bravo, R., Chen, G., Kim, H.K., Grosser, K., Van Dam, N.M., Leiss, K.A., and Klinkhamer, P.G.L. 2019b. “Ultraviolet radiation exposure time and intensity modulate tomato resistance to herbivory through activation of jasmonic acid signaling.” *Journal of Experimental Botany* 70:315–27.

Escobar-Bravo, R., Ruijgrok, J., Kim, H.K., Grosser, K., Van Dam, N.M., Klinkhamer, P.G.L., and Leiss, K.A. 2018. “Light intensity-mediated induction of trichome-associated allelochemicals increases resistance against thrips in tomato.” *Plant & Cell Physiology* 59:2462–75.

España, L., Heredia-Guerrero, J.A., Reina-Pinto, J.J., Fernández-Muñoz, R., Heredia, A., and Domínguez, E. 2014. “Transient silencing of CHALCONE SYNTHASE during fruit ripening modifies tomato epidermal cells and cuticle properties.” *Plant Physiology* 166:1371–86.

Falara, V., Akhtar, T.A., Nguyen, T.T.H., Spyropoulou, E.A., Bleeker, P.M., Schauvinhold, I., Matsuba, Y., Bonini, M.E., Schilmiller, A.L., Last, R.L., Schuurink, R.C., and Pichersky, E. 2011. “The tomato terpene synthase gene family.” *Plant Physiology* 157:770–89.

Falcone, A., Nelissen, H., Fleury, D., Van Lijsebettens, M., and Bitonti, M.B. 2007. “Cytological investigations of the *Arabidopsis thaliana* ELO1 mutant give new insights into leaf lateral growth and elongator function.” *Annals of Botany* 100:261–70.

Feys, B.J.F., Benedetti, C.E., Penfold, C.N., and Turner, J.G. 1994. “Arabidopsis mutants selected for resistance to the phytotoxin coronatine are male sterile, insensitive to methyl jasmonate, and resistant to a bacterial pathogen.” *Plant Cell* 6:751–59.

Folkers, U., Kirik, V., Schobinger, U., Falk, S., Krishnakumar, S., Pollock, M.A., Oppenheimer, G.D., Day, I., Reddy, A.R., Jurgens, G., and Hulskamp, M. 2002. “The cell morphogenesis gene ANGUSTIFOLIA encodes a CtBP/BARS-like protein and is involved in the control of the microtubule cytoskeleton.” *EMBO Journal* 21:1280–88.

Gable, K., Gupta, S.D., Han, G., Niranjanakumari, S., Harmon, J.M., and Dunn, T.M. 2010. “A disease-causing mutation in the active site of serine palmitoyltransferase causes catalytic promiscuity.” *Journal of Biological Chemistry* 285:22846–52.

Garcia-Molina, A., Altmann, M., Alkofer, A., Epple, P.M., Dangl, J.L., and Falter-Braun, P. 2017. “LSU network hubs integrate abiotic and biotic stress responses via interaction with the superoxide dismutase FSD2.” *Journal of Experimental Botany* 68:1185–97.

Glas, J.J., Schimmel, B.C.J., Alba, J.M., Escobar-Bravo, R., Schuurink, R.C., and Kant, M.R. 2012. “Plant glandular trichomes as targets for breeding or engineering of resistance to herbivores.” *International Journal of Molecular Sciences* 13:17077–103.

Goldsbrough, A., Belzile, F., and Yoder, J.I. 1994. “Complementation of the tomato anthocyanin without (Aw) mutant using the dihydroflavonol 4-reductase gene.” *Plant Physiology* 105:491–96.

Von Groll, U., Berger, D., and Altmann, T. 2002. “The subtilisin-like serine protease SDD1 mediates cell-to-cell signaling during Arabidopsis stomatal development.” *The Plant Cell* 14:1527–39.

Guelette, B.S., Benning, U.F., and Hoffmann-Benning, S. 2012. “Identification of lipids and lipid-binding proteins in phloem exudates from *Arabidopsis thaliana*.” *Journal of Experimental Botany* 63:3603–16.

Hategan, L., Godza, B., Kozma-Bognar, L., Bishop, G.J., and Szekeres, M. 2014. “Differential expression of the brassinosteroid receptor-encoding BRI1 gene in Arabidopsis.” *Planta* 239:989–1001.

Hause, B., Stenzel, I., Miersch, O., Maucher, H., Kramell, R., Ziegler, J., and Wasternack, C. 2000. “Tissue-specific oxylipin signature of tomato flowers: allene oxide cyclase Is highly expressed in distinct flower organs and vascular bundles.” *Plant Journal* 24:113–26.

Hegebarth, D., Buschhaus, C., Wu, M., Bird, D., and Jetter, R. 2016. “The composition of surface wax on trichomes of *Arabidopsis thaliana* differs from wax on other epidermal cells.” *Plant Journal* 88:762–74.

Hoffmann-Benning, S., Gage, D.A., McIntosh, L., Kende, H., and Zeevaart, J.A.D. 2002. “Comparison of peptides in the phloem sap of flowering and non-flowering perilla and lupine plants using microbore HPLC followed by matrix-assisted laser desorption/ionization time-of-flight mass spectrometry.” *Planta* 216:140–47.

Holton, T.A., Brugliera, F., Lester, D.R., Tanaka, Y., Hyland, C,D., Menting, J.G.T., Lu, C.Y., Farcy, E., Stevenson, T.W., and Cornish, E.C. 1993a. “Cloning and expression of cytochrome P450 genes controlling flower colour.” *Nature* 366:276–79.

Holton, T.A., Brugliera, F., and Tanaka, Y. 1993b. “cloning and expression of flavonol synthase from petunia hybrida.” *The Plant Journal* 4:1003–10.

Howarth, J.R., Parmar, S., Barraclough, P.B., and Hawkesford, M.J. 2009. “A sulphur deficiency-induced gene, SDI1, involved in the utilization of stored sulphate pools under sulphur-limiting conditions has potential as a diagnostic indicator of sulphur nutritional status.” *Plant Biotechnology Journal* 7:200–209.

Howe, G.A., Major, I.T., and Koo, A.J. 2018. “Modularity in jasmonate signaling for multistress resilience.” *Annual Review of Plant Biology* 69:387–415.

Huang, X., Liu, J., and Dickson, R.C. 2012. “Down-regulating sphingolipid synthesis increases yeast lifespan.” *PLoS Genetics* 8:16.

Humphries, J.A., Vejlupkova, Z., Luo, A., Meeley, R.B., Sylvester, A.W., Fowler, J.E., and Smith, L.G. 2011. “ROP GTPases act with the receptor-like protein PAN1 to polarize asymmetric cell division in maize.” *Plant Cell* 23:2273–84.

Inamdar, J.A., and Rao, V.S. 1981. “Structure, ontogeny, classification, taxonomic significance of trichomes and extra-floral nectaries in cultivars of cotton.” *Feddes Repertorium* 92:551–56.

Ingram, G., and Nawrath, C. 2017. “The roles of the cuticle in plant development: organ adhesions and beyond.” *Journal of Experimental Botany* 68:5307–21.

Ishiguro, S., Kawai-Oda, A., Ueda, J., Nishida, I., and Okada, K. 2001. “The defective in anther dehiscence1 gene encodes a novel phospholipase A1 catalyzing the initial step of jasmonic acid biosynthesis, which synchronizes pollen maturation, anther dehiscence, and flower opening in Arabidopsis.” *Plant Cell* 13:2191–2209.

Jakoby, M.J., Falkenhan, D., Mader, M.T., Brininstool, G., Wischnitzki, E., Platz, N., Hudson, A., Hülskamp, M., Larkin, J., and Schnittger, A. 2008. “Transcriptional profiling of mature Arabidopsis trichomes reveals that NOECK encodes the MIXTA-Like transcriptional regulator MYB106.” *Plant Physiology* 148:1583–1602.

Jasiński, M., Stukkens, Y., Degand, H., Purnelle, B., Marchand-Brynaert, J., and Boutry, M. 2001. “A plant plasma membrane ATP binding cassette-type transporter is involved in antifungal terpenoid secretion.” *The Plant Cell* 13:1095–1107.

Jewell, J.B., and Browse, J. 2016. “Epidermal jasmonate perception is sufficient for all aspects of jasmonate-mediated male fertility in arabidopsis.” *The Plant Journal* 85:634–47.

Jez, J.M., and Noel, J.P. 2002. “Reaction mechanism of chalcone isomerase: Ph dependence, diffusion control, and product binding differences.” *Journal of Biological Chemistry* 277:1361–69.

Jian, W., Cao, H., Yuan, S., Liu, Y., Lu, J., Lu, W., Li, N., Wang, J., Zou, J., Tang, N., Xu, C., Cheng, Y., Gao, Y., Xi, W., Bouzayen, M., and Li, Z. 2019. “SlMYB75, an MYB-type transcription factor, promotes anthocyanin accumulation and enhances volatile aroma production in tomato fruits.” *Horticulture Research* 6:15.

Kagey, M.H., Newman, J.J., Bilodeau, S., Zhan, Y., Orlando, D.A., van Berkum, N.L., Ebmeier, C.C., Goossens, J., Rahl, P.B., Levine. S.S., Taatjes, D.J., Dekker, J., and Young, R.A. 2010. “Mediator and cohesin connect gene expression and chromatin architecture.” *Nature* 467:430–35.

Kang, J., McRoberts, J., Shi, F., Moreno, J.E., Jones, A.D., and Howe, G.A. 2014. “The flavonoid biosynthetic enzyme chalcone isomerase modulates terpenoid production in glandular trichomes of tomato.” *Plant Physiol* 164:1161–74.

Kang, J., Campos, M.L., Zemelis-durfee, S., Al-haddad, J.M., Jones, A.D., Telewski, F.W., Brandizzi, F., and Howe, G.A. 2016. "Molecular cloning of the tomato hairless gene implicates actin dynamics in trichome-mediated defense and mechanical properties of stem tissue." *Journal of Experimental Botany* 67:5313–24.

Kang, J., Liu, G.H., Shi, F., Jones, A.D., Beaudry, R.M., and Howe, G.A. 2010a. "The tomato Odorless-2 mutant is defective in trichome-based production of diverse specialized metabolites and broad-spectrum resistance to insect herbivores." *Plant Physiology* 154:262–72.

Kang, J., Shi, F., Jones, A.D., Marks, M.D., and Howe, G.A. 2010b. "Distortion of trichome morphology by the hairless mutation of tomato affects leaf surface chemistry." *Journal of Experimental Botany* 61:1053–64.

Kazan, K. 2017. "The multitalented MEDIATOR25." *Frontiers in Plant Science* 8:1–11.

Kirik, V., Simon, M., Wester, K., and Schiefelbein, J. 2004. "ENHANCER of TRY and CPC2 (ETC2) reveals redundancy in the region-specific control of trichome development of Arabidopsis." *Plant Molecular Biology* 55:389–98.

Kroes, A., Weldegergis, B.T., Cappai, F., Dicke, M., and van Loon, J.J.A. 2017. "Terpenoid biosynthesis in arabidopsis attacked by caterpillars and aphids: effects of aphid density on the attraction of a caterpillar parasitoid." *Oecologia* 185:699–712.

Lange, B.M., Wildung, M.R., Stauber, E.J., Sanchez, C., Pouchnik, D., and Croteau, R. 2000. "Probing essential oil biosynthesis and secretion by functional evaluation of expressed sequence tags from mint glandular trichomes." *Proceedings of the National Academy of Sciences of the United States of America* 97:2934–39.

Langenheim, J.H. 1994. "Higher plant terpenoids: a phytocentric overview of their ecological roles." *Journal of Chemical Ecology* 20:1223–80.

Lantz, A.T., Solomon, C., Gog, L., McClain, A.M., Weraduwage, S.M., Cruz, J.A., and Sharkey, T.D. 2019. "Isoprene suppression by CO2 is not due to triose phosphate utilization (TPU) limitation." *Frontiers in Forests and Global Change* 2:1–13.

Lawson, S.S., Pijut, P.M., and Michler, C.H. 2014. "Comparison of arabidopsis stomatal density mutants indicates variation in water stress responses and potential epistatic effects." *Journal of Plant Biology* 57:162–73.

Leckie, B.M., D'Ambrosio, D.A., Chappell, T.M., Halitschke, R., De Jong, E.M., Kessler, A., Kennedy, G.G., and Mutschler, M.A. 2016. "Differential and synergistic functionality of acylsugars in suppressing oviposition by insect herbivores." *PLoS ONE* 11:1–19.

Lee, K., and Seo, P.J. 2018. "Dynamic epigenetic changes during plant regeneration." *Trends in Plant Science* 23:235–47.

Lee, Y.S., Choi, K.M., Choi, M.H., Ji, S.Y., Lee, S., Sin, D.M., Oh, K.W., Lee, Y.M., Hong,

J.T., Yun, Y.P., and Yoo, H.S. 2011. “Serine palmitoyltransferase inhibitor myriocin induces growth inhibition of B16F10 melanoma cells through G2/M phase arrest.” *Cell Proliferation* 44:320–29.

Li, C., Williams, M.M., Loh, Y.T., Gyu, I.L., and Howe, G.A. 2002. “Resistance of cultivated tomato to cell content-feeding herbivores is regulated by the octadecanoid-signaling pathway.” *Plant Physiology* 130:494–503.

Li, L., Zhao, Y., Mccaig, B.C., Wingerd, B.A., Wang, J., Whalon, M.E., Pichersky, E., and Howe, G.A. 2004. “The tomato homolog of CORONATINE-INSENSITIVE1 is required for the maternal control of seed maturation , jasmonate-signaled defense responses, and glandular trichome development.” *The Plant Cell* 16:126–43.

Liakoura, V., Stefanou, M., Manetas, Y., Cholevas, C., and Karabourniotis, G. 1997. “Trichome density and its UV-B protective potential are affected by shading and leaf position on the canopy.” *Environmental and Experimental Botany* 38:223–29.

Luckwill, L. 1943. *The genus Lycopersicon: historical, biological, and taxonomic survey of the wild and cultivated tomatoes*. Aberdeen, Scotland: Aberdeen University Press.

Lynch, D.V., and Fairfield, S.R. 1993. “Sphingolipid long-chain base synthesis in plants (characterization of serine palmitoyltransferase activity in squash fruit microsomes).” *Plant Physiology* 103:1421–29.

Maffei, M., Gallino, M., and Sacco, T. 1986. “Glandular trichomes and essential oils of developing leaves in *Mentha viridis lavanduliodora*.” *Planta Medica* 3:187–93.

Maloney, G.S., DiNapoli, K.T., and Muday, G.K. 2014. “The anthocyanin reduced tomato mutant demonstrates the role of flavonols in tomato lateral root and root hair development.” *Plant Physiology* 166:614-U254.

Markham, J.E., Li, J., Cahoon, E.B., and Jaworski, J.G. 2006. “Separation and identification of major plant sphingolipid classes from leaves.” *Journal of Biological Chemistry* 281:22684–94.

Markham, K.R., Ternai, B., Stanley, R., Geiger, H., and Mabry, T.J. 1978. “Carobon-13 NMR studies of flavonoids-III naturally occuring flavonoid glycosides and their acylated derivatives.” *Tetrahedron* 34:1389–97.

Marks, D.M. 1994. “Plant development: the making of a plant hair.” *Current Biology* 4:621–23.

McDowell, E.T., Kapteyn, J., Schmidt, A., Li, C., Kang, J., Descour, A., Shi, F., Larson, M., Schilmiller. A.L., An, L., Jones, A.D., Pichersky, E., Soderlund, C.A., and Gang, D.R. 2011. “Comparative functional genomic analysis of *Solanum* glandular trichome types.” *Plant Physiology* 155:524–39.

Michaelson, L.V., Napier, J.A., Molino, D., and Faure, J.D. 2016. “Plant sphingolipids: their importance in cellular organization and adaption.” *Biochimica et Biophysica Acta* -

Molecular and Cell Biology of Lipids 1861:1329–35.

Mo, Y., Nagel, C., and Taylor, L.P. 1992. "Biochemical complementation of chalcone synthase mutants defines a role for flavonols in functional pollen." *Proceedings of the National Academy of Sciences of the United States of America* 89:7213–17.

Moghe, G.D., Leong, B.J., Hurney, S.M., Jones, A.D., and Last, R.L. 2017. "Evolutionary routes to biochemical innovation revealed by integrative analysis of a plant-defense related specialized metabolic pathway." *ELife* 6:1–33.

Mohan, R., Vijayan, P., and Kolattukudy, P.E. 1993. "Developmental and tissue-specific expression of a tomato anionic peroxidase (Tap1) gene by a minimal promoter, with wound and pathogen induction by an additional 5′-flanking region." *Plant Molecular Biology* 22:475–90.

Monaghan, E., Gable, K., and Dunn, T. 2002. "Mutations in the Lcb2p subunit of serine palmitoyltransferase eliminate the requirement for the TSC3 gene in *Saccharomyces cerevisiae*." *Yeast* 19:659–70.

Msanne, J., Chen, M., Luttgeharm, K.D., Bradley, A.M., Mays, E.S., Paper, J.M., Boyle, D.L., Cahoon, R.E., Schrick, K., and Cahoon, E.B. 2016. "Glucosylceramide is critical for cell-type differentiation and organogenesis, but not for cell viability in Arabidopsis." *Plant Journal* 84:188–201.

Muir, S.R., Collins, G.J., Robinson, S., Hughes, S., Bovy, A., De Vos, C.H.R., van Tunen, A.J., and Verhoeyen, M.E. 2001. "Overexpression of petunia chalcone isomerase in tomato results in fruit containing increased levels of flavonols." *Nature Biotechnology* 19:470–74.

Nadakuduti, S.S., Pollard, M., Kosma, D.K., Allen, C., Ohlrogge, J.B., and Barry, C.S. 2012. "Pleiotropic phenotypes of the sticky peel mutant provide new insight into the role of CUTIN DEFICIENT2 in epidermal cell function in tomato." *Plant Physiology* 159:945–60.

Nagiec, M.M., Baltisberger, J.A., Wells, G.B., Lester, R.L., and Dickson, R.C. 1994. "The LCB2 gene of Saccharomyces and the related LCB1 gene encode subunits of serine palmitoyltransferase, the initial enzyme in sphingolipid synthesis." *Proceedings of the National Academy of Sciences of the United States of America* 91:7899–7902.

Nelissen, H., Fleury, D., Bruno, L., Robles, P., De Veylder, L., Traas, V.J., Micol, J.L., Van Montagu, M., Inze, D., and Van Lijsebettens M. 2005. "The elongata mutants identify a functional elongator complex in plants with a role in cell proliferation during organ growth." *Proceedings of the National Academy of Sciences* 102:7754–59.

Oh, S., and Montgomery, B.L. 2019. "Mesophyll-specific phytochromes impact chlorophyll light-harvesting complexes (LHCs) and non-photochemical quenching." *Plant Signaling & Behavior* 14:1609857.

Oshima, Y., Shikata, M., Koyama, T., Ohtsubo, N., Mitsuda, N., and Ohme-Takagi, M. 2013. "MIXTA-Like transcription factors and WAX INDUCER1/SHINE1 coordinately regulate

cuticle development in Arabidopsis and *Torenia fournieri*." *The Plant Cell* 25:1609–24.

Paduch, R., Kandefer-Szerszeń, M., Trytek, M., and Fiedurek, J. 2007. "Terpenes: substances useful in human healthcare." *Archivum Immunologiae et Therapiae Experimentalis* 55:315–27.

Pattanaik, S., Patra, B., Singh, S.K., and Yuan, L. 2014. "An overview of the gene regulatory network controlling trichome development in the model plant, Arabidopsis." *Frontiers in Plant Science* 5:1–8.

Pattison, R.J., Csukasi, F., Zheng, Y., Fei, Z., van der Knaap, E., and Catalá, C. 2015. "Comprehensive tissue-specific transcriptome analysis reveals distinct regulatory programs during early tomato fruit development." *Plant Physiology* 168:1684–1701.

Payne, W.W. 1978. "A glossary of plant hair terminology." *Brittonia* 30:239–55.

Pieczynski, M., Marczewski, W., Hennig, J., Dolata, J., Bielewicz, D., Piontek, P., Wyrzykowska, A., Krusiewicz, D., Strzelczyk-Zyta, D., Konopka-Postupolska, D., Krzeslowska, M., Jarmolowski, A., and Szweykowska-Kulinska, Z. 2013. "Down-regulation of CBP80 gene expression as a strategy to engineer a drought-tolerant potato." *Plant Biotechnology Journal* 11:459–69.

Poorter, H., Niinemets, Ü., Poorter, L., Wright, I.J., and Villar, R. 2009. "Causes and consequences of variation in leaf mass per area (LMA): a meta-analysis." *New Phytologist* 182:565–88.

Porra, R.J., Thompson, W.A., and Kriedemann, P.E. 1989. "Determination of accurate extinction coefficients and simultaneous equations for assaying chlorophylls a and b extracted with four different solvents: verification of the concentration of chlorophyll standards by atomic absorption spectroscopy." *Biochimica et Biophysica Acta - Bioenergetics* 975:384–94.

Rahman, R.N.Z.R.A., Zakaria, I.I., Salleh, A.B., and Basri, M. 2012. "Enzymatic properties and mutational studies of chalcone synthase from *Physcomitrella patens*." *International Journal of Molecular Sciences* 13:9673–91.

Ren, T., Weraduwage, S.M., and Sharkey, T.D. 2019. "Prospects for enhancing leaf photosynthetic capacity by manipulating mesophyll cell morphology." *Journal of Experimental Botany* 70:1153–65.

Rick, C.M., Quiros, C.F., Lange, W.H., and Stevens, M.A. 1976. "Monogenic control of resistance in the tomato to the tobacco flea beetle: probable repellance by foliage volatiles." *Euphytica* 25:521–30.

Rodriguez-Concepcion, M., Yalovsky, S., Zik, M., Fromm, H., and Gruissem, W. 1999. "The prenylation status of a novel plant calmodulin directs plasma membrane or nuclear localization of the protein." *The EMBO Journal* 18:1996–2007.

Sakai, W.S. and Sanford, W.G. 1980. "Ultrastructure of the water-absorbing trichomes of

pineapple (*Ananas comosus*, *Bromeliaceae*).” *Annals of Botany* 46:7–11.

Sallaud, C., Rontein, D., Onillon, S., Jabes, F., Duffe, P., Giacalone, C., Thoraval, S., Escoffier, C., Herbette, G., Leonhardt, N., Causse, M., and Tissier, A. 2009. “A novel pathway for sesquiterpene biosynthesis from Z,Z-farnesyl pyrophosphate in the wild tomato *Solanum habrochaites*.” *The Plant Cell* 21:301–17.

Sánchez-Hernández, C., López, M.G., and Délano-Frier, J.P. 2006. “Reduced levels of volatile emissions in jasmonate-deficient Spr2 tomato mutants favour oviposition by insect herbivores.” *Plant, Cell and Environment* 29:546–57.

Sanders, P.R., Winter, J.A., Barnason, A.R., Rogers, S.G., and Fraley, R.T. 1987. “Comparison of cauliflower mosaic virus 35S and nopaline synthase promoters in transgenic plants.” *Nucleic Acids Research* 15:1543–58.

Sanders, P.M., Lee, P.Y., Biesgen, C., Boone, J.D., Beals, T.P., Weiler, E.W., and Goldberg, R.B. 2000. “The Arabidopsis DELAYED DEHISCENCE1 gene encodes an enzyme in the jasmonic acid synthesis pathway.” *Plant Cell* 12:1041–61.

Santamaria, M.E., Cambra, I., Martinez, M., Pozancos, C., González-Melendi, P., Grbic, V., Castañera, P., Ortego, F., and Diaz, I. 2012. “Gene pyramiding of peptidase inhibitors enhances plant resistance to the spider mite *Tetranychus urticae*.” *PLoS ONE* 7:2–11.

Sasse, J., Schlegel, M., Borghi, L., Ullrich, F., Lee, M., Liu, G.W., Giner, J.L., Kayser, O., Bigler, L., Martinoia, E., and Kretzschmar, T. 2016. “Petunia hybrida PDR2 is involved in herbivore defense by controlling steroidal contents in trichomes.” *Plant Cell and Environment* 39:2725–39.

Schilmiller, A. L., Schauvinhold, I., Larson, M., Xu, R., Charbonneau, A.L., Schmidt, A., Wilkerson, C., Last, R.L., and Pichersky, E.. 2009. “Monoterpenes in the glandular trichomes of tomato are synthesized from a neryl diphosphate precursor rather than geranyl diphosphate.” *Proceedings of the National Academy of Sciences of the United States of America* 106:10865–70.

Schilmiller, A.L., Charbonneau, A.L., and Last, R.L. 2012. “Identification of a BAHD acetyltransferase that produces protective acyl sugars in tomato trichomes.” *Proceedings of the National Academy of Sciences of the United States of America* 109:16377–82.

Schilmiller, A.L., Gilgallon, K., Ghosh, B., Jones, A.D., and Last, R.L. 2016. “Acylsugar acylhydrolases: carboxylesterase-catalyzed hydrolysis of acylsugars in tomato trichomes.” *Plant Physiology* 170:1331–44.

Schilmiller, A.L., Last, R.L., and Pichersky, E.. 2008. “Harnessing plant trichome biochemistry for the production of useful compounds.” *The Plant Journal* 54:702–11.

Schilmiller, A.L., Miner, D.P., Larson, M., Mcdowell, E., Gang, D.R., Wilkerson, C., Last, R.L. 2010. “Studies of a biochemical factory : tomato trichome deep expressed sequence tag sequencing and proteomics.” *Plant Physiology* 153:1212–23.

Schwender, J., Seemann, M., Lichtenthaler, H.K., and Rohmer, M. 1996. “Biosynthesis of isoprenoids (carotenoids, sterols, prenyl side-chains of chlorophylls and plastoquinone) via a novel pyruvate/glyceraldehyde 3-phosphate non-mevalonate pathway in the green alga *Scenedesmus obliquus*.” *The Biochemical Journal* 316:73–80.

Shen, Q., Lu, X., Yan, T., Fu, X., Lv, Z., Zhang, F., Pan, Q., Wang, G., Sun, X., and Tang, K. 2016. “The jasmonate-responsive AaMYC2 transcription factor positively regulates artemisinin biosynthesis in *Artemisia annua*.” *New Phytologist* 210:1269–81.

Shi, L., Bielawski, J., Mu, J., Dong, H., Teng, C., Zhang, J., Yang, X., Tomishige, N., Hanada, K., Hannun, Y.A., and Zuo, J. 2007. “Involvement of sphingoid bases in mediating reactive oxygen intermediate production and programmed cell death in Arabidopsis.” *Cell Research* 17100:1030–40.

Shpak, E.D., Lakeman, M.B., and Torii, K.U. 2003. “Dominant-negative receptor uncovers redundancy in the Arabidopsis ERECTA leucine-rich repeat receptor–like kinase signaling pathway that regulates organ shape.” *The Plant Cell* 15:1095–1110.

Shpak, E.D., McAbee, J.M., Pillitteri, L.J., and Torii, K.U. 2005. “Plant science: stomatal patterning and differentiation by synergistic interactions of receptor kinases.” *Science* 309:290–93.

Simons, K., and Ikonen, E. 1997. “Functional rafts in cell membranes.” *Nature* 387:569–72.

Snyder, J.C., and Carter, C.D. 1985. “Trichomes on leaves of *Lycopersicon hirsutum, L. esculentum* and their hybrids.” *Euphytica* 34:53–64.

Soubeyrand, E., Johnson, T.S., Latimer, S., Block, A., Kim, J., Colquhoun, T.A., Butelli, E., Martin, C., Wilson, M.A., and Basset, G.J. 2018. “The peroxidative cleavage of kaempferol contributes to the biosynthesis of the benzenoid moiety of ubiquinone in plants.” *The Plant Cell* 30:2910–21.

Spitzer-Rimon, B., Marhevka, E., Barkai, O., Marton, I., Edelbaum, O., Masci, T., Prathapani, N.K., Shklarman, E., Ovadis, M., and Vainstein, A. 2010. “EOBII, a gene encoding a flower-specific regulator of phenylpropanoid volatiles biosynthesis in petunia.” *Plant Cell* 22:1961–76.

Spribille, R., and G. Forkmann, G. 1982. “Chalcone synthesis and hydroxylation of flavonoids in 3′-position with enzyme preparations from flowers of *Dianthus caryophyllus L.* (carnation).” *Planta* 155:176–82.

Spyropoulou, E.A., Haring, M.A., and Schuurink, R.C. 2014. “Expression of terpenoids 1, a glandular trichome-specific transcription factor from tomato that activates the terpene synthase 5 promoter.” *Plant Molecular Biology* 84:345–57.

Stacey, D.L., Wyatt, I.J., and Chambers, R.J. 1985. “The effect of glasshouse red spider mite damage on the yield of tomatoes.” *Journal of Horticultural Science* 60:517–23.

Sugimoto-Shirasu, K., and Roberts, K. 2003. "'Big it up': endoreduplication and cell-size control in plants." *Current Opinion in Plant Biology* 6:544–53.

Suzuki, T., Honda, Y., and Mukasa, Y. 2005. "Effects of UV-B radiation, cold and desiccation stress on rutin concentration and rutin glucosidase activity in tartary buckwheat (*Fagopyrum tataricum*) leaves." *Plant Science* 168:1303–7.

Takenawa, T., and Suetsugu, S. 2007. "The WASP-WAVE protein network: connecting the membrane to the cytoskeleton." *Nature Reviews Molecular Cell Biology* 8:37–48.

Tan, H., Xiao, L., Gao, S., Li, Q., Chen, J., Xiao, Y., Ji, Q., Chen, R., Chen, W., and Zhang, L. 2015. "TRICHOME and ARTEMISININ REGULATOR 1 is required for trichome development and artemisinin biosynthesis in *Artemisia annua*." *Molecular Plant* 8:1396–1411.

Tarkowská, D., and Strnad, M. 2018. "Isoprenoid-derived plant signaling molecules: biosynthesis and biological importance." *Planta* 247:1051–66.

The Tomato Genome Consortium. 2012. "The tomato genome sequence provides insights into fleshy fruit evolution." *Nature* 485:635–41.

Thines, B., Katsir, L., Melotto, M., Niu, Y., Mandaokar, A., Liu, G., Nomura, K., He, S.Y., Howe, G.A., and Browse, J. 2007. "JAZ repressor proteins are targets of the SCFCOI1 complex during jasmonate signalling." *Nature* 448:661–65.

Tissier, A. 2012. "Trichome specific expression: promoters and their applications." *InTech* 17:357–378.

Turlings, A.T.C.J., Tumlinson, J.H., and Lewis, W.J. 1990. "Exploitation of herbivore-induced plant odors by host-seeking parasitic wasps." *Science* 250:1251–53.

Vendemiatti, E., Zsögön, A., e. Silva, G.F.F., de Jesus, F.A., Cutri, L., Figueiredo, C.R.F., Tanaka, F.A.O., Nogueira, F.T.S., and Peres L.E.P. 2017. "Loss of type-IV glandular trichomes is a heterochronic trait in tomato and can be reverted by promoting juvenility." *Plant Science* 259:35–47.

Voirin, B., Bayet, C., and Colson, M. 1993. "Demonstration that flavone aglycones accumulate in the peltate glands of *Mentha* x *Piperita* leaves." *Phytochemistry* 34:85–87.

Vosman, B., Westende, W.P.C., Henken, B., van Eekelen, H.D.L.M., de Vos, R.C.H., and Voorrips, R.E. 2018. "Broad spectrum insect resistance and metabolites in close relatives of the cultivated tomato." *Euphytica* 214:14.

Walsh, D.B., Zalom, F.G., Shaw, D.V., and Larson, K.D. 2002. "Yield reduction caused by twospotted spider mite feeding in an advanced-cycle strawberry breeding population." *Journal of the American Society for Horticultural Science* 127:230–37.

Wang, M., and Maeda, H.A. 2018. "Aromatic amino acid aminotransferases in plants."

Phytochemistry Reviews 17:131–59.

Wang, Q., Reddy, V.A., Panicker, D., Mao, H.Z., Kumar, N., Rajan, C., Venkatesh, P.N., Chua, N.H., and Sarojam, R. 2016. "Metabolic engineering of terpene biosynthesis in plants using a trichome-specific transcription factor MsYABBY5 from spearmint (*Mentha spicata*)." *Plant Biotechnology Journal* 1619–32.

Wang, Z., Yang, Z., and Li F. 2019. "Updates on molecular mechanisms in the development of branched trichome in Arabidopsis and nonbranched in cotton." *Plant Biotechnology Journal* 1706–22.

Waters, Mark T., Elizabeth C. Moylan, and Langdale, J.A. 2008. "GLK transcription factors regulate chloroplast development in a cell-autonomous manner." *Plant Journal* 56:432–44.

Werker, E. 2000. "Trichome diversity and development." *Advances in Botanical Research* 31:35.

Von Wettstein-Knowles, P. 1968. "Mutations affecting anthocyanin synthesis in the tomato I. genetics, histology." *Hereditas* 60:317–46.

Wilson, L.T., Trichilo, P.J., and Gonzalez, D. 1991. "Spider mite (Acari: Tetranychidae) infestation rate and initiation: effect on cotton yield." *Journal of Economic Entomology* 84:593–600.

Wu, G., Park, M.Y., Conway, S.R., Wang, J.W., Weigel, D., and Poethig, R.S. 2009. "The sequential action of MiR156 and MiR172 regulates developmental timing in Arabidopsis." *Cell* 138:750–59.

Xu, J., Van Herwijnen, Z.O., Dräger, D.B., Sui, C., Haring, M.A., and Schuurink, R.C. 2018. "SlMYC1 regulates type VI glandular trichome formation and terpene biosynthesis in tomato glandular cells." *Plant Cell* 30:2988–3005.

Yan, T., Li, L., Xie, L., Chen, M., Shen, Q., Pan, Q., Fu, X., Shi, P., Tang, Y., Huang, H., Huang, Y., Huang, Y., and Tang, K. 2018. "A novel HD-ZIP IV/MIXTA complex promotes glandular trichome initiation and cuticle development in *Artemisia annua*." *New Phytologist* 218:567–78.

Yang, C., Li, H., Zhang, J., Luo, Z., Gong, P., Zhang, C., and Li, J. 2011. "A regulatory gene induces trichome formation and embryo lethality in tomato." *Proceedings of the National Academy of Sciences of the United States of America* 108:11836–41.

Yazaki, K., Arimura, G.I., and Ohnishi, T. 2017. "'Hidden terpenoids in plants: their biosynthesis, localization and ecological roles." *Plant and Cell Physiology* 58:1615–21.

Yi, Hojae, Yintong Chen, James Z. Wang, Puri, V.M., and Anderson, C.T. 2019. "The stomatal flexoskeleton: how the biomechanics of guard cell walls animate an elastic pressure vessel." *Journal of Experimental Botany* 70:3561–72.

Young, P. A., and MacArthur, J.W. 1947. "Horticultural characters of tomatoes." *Texas*

Agricultural Experiment Station 698:61.

Yu, G., and Pichersky, E,. 2014. “Heterologous expression of Methylketone Synthase1 and Methylketone Synthase2 leads to production of methylketones and myristic acid in transgenic plants.” *Plant Physiology* 164:612–22.

Zhai, Q., Zhang, X., Wu, F., Feng, H., Deng, L., Xu, L., Zhang, M., Wang, Q., and Li, C. 2015. “Transcriptional mechanism of jasmonate receptor COI1-mediated delay of flowering time in Arabidopsis.” *The Plant Cell* 27:1–16.

Zhang, B., Chen, W., Foley, R.C., Buttner, M., and Singh, K.B. 1995. “Interactions between distinct types of DNA binding proteins enhance binding to OCS element promoter sequences.” *The Plant Cell* 7:2241–52.

Zhao, H., Wang, X., Zhu, D., Cui, S., Li, X., Cao, Y., and Ma, L. 2012. “A single amino acid substitution in IIIf subfamily of basic helix-loop-helix transcription factor AtMYC1 leads to trichome and root hair patterning defects by abolishing its interaction with partner proteins in Arabidopsis.” *Journal of Biological Chemistry* 287:14109–21.